https://doi.org/10.59761/RCR5126

Solid-state electrolytes: a way to increase the power of lithium-ion batteries

Daria Yu. Voropaeva, Irina A. Stenina, Andrey B. Yaroslavtsev

Kurnakov Institute of General and Inorganic Chemistry, Russian Academy of Sciences, Leninsky prosp. 31, 119991 Moscow, Russian Federation

Currently, all-solid-state lithium metal batteries are considered among the most promising energy storage devices, due to their safety and high energy density. Solid-state electrolytes, the key components of the batteries, are attracting increasing attention. This review presents an analysis of important recent advances in the field of lithium conducting solid-state electrolytes, including the mechanisms of conductivity, the main approaches to increase the conductivity, optimization of interfaces and ways to improve the stability for the main types of electrolytes, *i.e.*, inorganic, polymer and composite materials. For solid inorganic electrolytes, high conductivity and stability have been achieved; however, the problems related the formation of dense thin films and formation of a reliable contact with electrode materials are still unsolved. Polymer electrolytes are characterized by lower conductivity, which is improved upon plasticization with aprotic solvents. Composite electrolytes, for which it is possible to achieve a combination of high conductivity and good mechanical properties along with stability, are considered as the most promising. The main problems in the field of solid electrolytes for all-solid-state lithium metal batteries and possible ways to solve them are outlined. The bibliography includes 661 references.

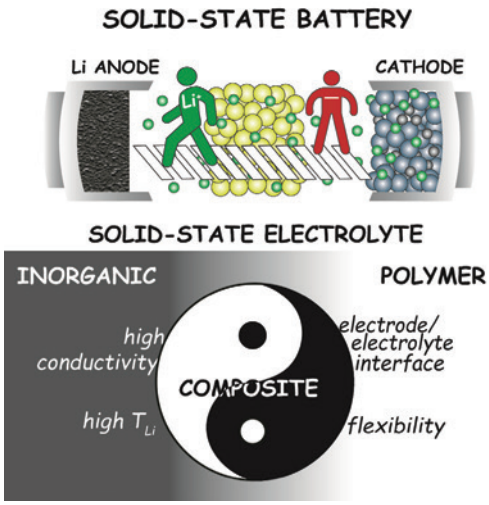

Keywords: solid-state lithium battery, inorganic electrolyte, polymer electrolyte, composite electrolyte, ionic conductivity, lithium conductivity, transference numbers.

Contents

1. Introduction

Over the 50 years that passed since the appearance of idea of lithium ion batteries (LIBs), these batteries firmly embedded in our lives, being among the most successful inventions of humankind. Currently, LIBs provide energy supply for all portable devices, computing equipment and wireless tools and are being actively implemented in transport vehicles.[1–3] This is due to the remarkable performance characteristics of these batteries, which currently demonstrate the highest energy capacity per both unit volume and unit weight.[4–7] Another important factor is the relatively low cost of LIBs.[8] However,

D.Yu.Voropaeva. PhD, Researcher.
E-mail: voropaeva@igic.ras.ru
Current research interests: polymer electrolytes based on cation exchange membranes for lithium metal batteries, metal ion batteries.
I.A.Stenina. Professor, Doctor of Chemical Sciences, Leading Researcher.
E-mail: stenina@igic.ras.ru
Current research interests: solid electrolytes, ion exchange membranes, metal ion batteries, solid state chemistry.
A.B.Yaroslavtsev. Professor, Academician of RAS, Head of Laboratory.
E-mail: yaroslav@igic.ras.ru
Current research interests: solid electrolytes, ion exchange membranes, metal ion batteries, hydrogen energy, solid state chemistry.

Translation: Z.P.Svitanko

Received 9 April 2024

such a great success could hardly be expected without confidence in the safety of the battery; therefore, initially it was a major challenge to ensure safety. A key problem was the possibility of self-ignition of lithium cobaltite, which was used as a cathode material; this problem was solved by adjusting the operation conditions and restricting the LIB charge. The second serious problem is spontaneous growth of dendrites through the liquid electrolyte when lithium metal is used as the battery anode.[9,10] This finally resulted in short circuits, uncontrolled heating of the battery and evaporation and ignition of the electrolyte. A new LIB technology no longer using lithium metal and thus preventing the dendrite formation was presented only in 1991.[11] This provided a wide use of LIBs in portable devices and later in a number of other applications.

Among other problems that hinder the development of LIBs, the limited lithium reserves and low abundance of lithium are worthy of note. The most probable way out is to use sodium ion batteries, at least for solving problems of energy storage in large-scale power systems and for power backup in electric utilities for night hours where power consumption sharply decreases.[12,13] Hydrogen cycle can also compete with metal ion batteries, especially for balancing the seasonal variations in energy demand, because in this case, the expediency of using batteries is restricted by their self-discharge.[14–16] However, there is one more vitally important problem caused by the pursuit for improvement and high rivalry in the manufacture of LIBs: the capacity limit of a modern battery, equal to approximately 300 W-h kg^{-1}, has been nearly reached.[17] This barrier can be overcome by using conceptually new high-capacity silicon-based anode materials, which, unfortunately, have moderate stability.[18,19]

The concept of turning back to lithium metal anodes, which have the highest capacity, appears much more realistic.[7,20–23] For this purpose, it is necessary to solve the problem of dendrite growth, which was an insurmountable obstacle to the use of such anodes 30 years ago.[24] This problem has been addressed using various approaches. One of them is to increase the affinity of the anode material for lithium; this may provide a more uniform lithium coating of the anode during the battery charging owing to a decrease in the nucleation overpotential,[25–27] which, for example for copper, exceeds 40 mV.[28] It is the nonuniform contact that is responsible for the considerable overpotential and the point growth of dendrites.[29] The majority of researchers attempt to solve this problem by increasing the surface area (the number of nucleation sites) *via* the formation of surface structures, in particular from carbon materials.[30–33] Some authors used surface deposition of metals possessing affinity for lithium or structures containing such metals.[34–37] The same goal can be reached by the deposition of metal oxides on the electrode surface[38,39] or by the formation of artificial solid electrolyte interface (SEI); these structures are mainly deposited on the electrodes during the first cycles.[40–43] Usually, the formation of SEI is considered as an inevitable adverse effect, which somewhat decreases the capacity of the battery. However, once formed, it performs a protective function or, as in this particular case, provides a more efficient interfacial contact. Many researchers believe that SEIs containing fluoride ions, which can come, in particular, from the electrolyte, are more efficient.[44–46] However, it seems that the difference between these approaches is rather terminological, since the essence of both methods is to form porous or solid conductive coatings that prevent the formation of dendrites.

Meanwhile, the development of batteries with a dense solid electrolyte, which both solves the problem of dendrite growth and makes it possible to avoid the use of combustible organic solvents, appears more promising.[47–49] This review addresses the most important classes of these materials.

2. Lithium-conducting solid electrolytes

Usually, modern LIBs make use of liquid electrolytes that have ionic conductivity and are formed rather easily on mixing of some solvents and salts.[50–52] Meanwhile, the major problems of existing LIBs are related exactly to their use. Indeed, without these electrolytes, there would be no risk of leakage or ignition of organic solvents. Freezing of solvents accounts for the sharp decrease in the performance of LIBs at negative temperatures. The penetration of dendrites through the liquid interlayer is possible. Finally, the performance of LIBs markedly decreases due to the low lithium transference numbers, despite the use of salts with relatively large anions in electrolytes.[53,54] The transition to solid electrolytes is expected to solve this problem and to substantially increase the stability and safety of batteries, especially those that use lithium metal anodes. However, it is noteworthy that safety of solid-state batteries depends not only on the stability and characteristics of particular components, but also on the compatibility of the electrolyte with electrode materials; therefore, it is necessary to consider the stability of a battery cell as a whole.[55]

In essence, safety increase alone would be quite sufficient to draw attention to all-solid-state lithium batteries (ASSBs) and even for the commercial production of these batteries. Indeed, in recent years, Chinese manufacturers, who are the leaders in LIB sales, have paid particular attention to their safety, for example,

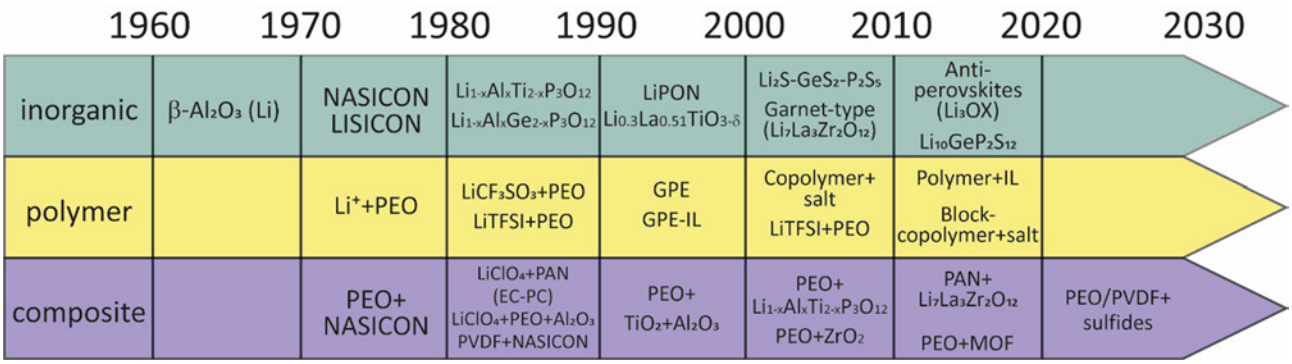

Figure 1. Development of studies of solid electrolytes for ASSBs on the timeline. PEO is polyethylene oxide, PAN is polyacrylonitrile, EC is ethylene carbonate, PC is propylene carbonate, ILis ionic liquid, MOF is metal-organic framework.

cathode materials based on $LiFePO_4$ (LFP) are used, although they are markedly inferior in the capacity to the Li(Ni,Co,Mn)O_2 (NCM) oxides.[56–58] However, there is also an authoritative opinion of J.B.Goodenough that switching to ASSBs would considerably increase the battery capacity.[59] In most cells with solid electrolytes, lithium metal is used as the anode, which provides the highest capacity and operating voltage. Materials such as NCM or LFP, which proved to be efficient, are usually serve as cathodes. The capacity is most often referred to the weight of the cathode material.

Although in most studies, only increased cyclability and safety are demonstrated after the replacement of liquid electrolytes by solid ones, this line of research may obviously be regarded as one of the most stable trends of modern science in the field of energy storage devices.[47,49,60–64]

The term 'solid electrolytes' covers an extensive range of materials; in order to form a systematic view, it is convenient to subdivide them into three large classes: inorganic, polymer and composite electrolytes. Each type of materials has benefits and drawbacks when used in ASSBs.[61,63,65] The development of studies of solid electrolytes for ASSBs on the timeline is shown in Fig. 1.

3. Ion transport in solid electrolytes

The main benefits of inorganic lithium ion electrolytes include high thermal stability and non-flammability and a wide electrochemical stability window, which allows ASSB to operate in a wide range of potential differences.[48,66,67] Particularly inorganic electrolytes were the first to be studied as solid electrolytes. However, an electrolyte suitable for ASSBs should possess a high ionic conductivity of at least 10^{-4} S cm^{-1} at room temperature (25 °C).[68,69]

The highest mobility in most types of materials is inherent in ions with a relatively large radius, with the optimal radius being approximately 1 Å.[70,71] Moreover, singly charged silver and copper ions with easily deformable d-electron shells move most easily in solids. However, low electrochemical potentials of these ions in relation to the corresponding metals makes their use for the design of power sources unpractical.

In ideally packed crystals, the ion transport is impossible. The ions migrate only through structure defects: vacancies (the absence of ion in the site, which is normally occupied) or interstitials (an ion in the site not characteristic of this ion in an ideal structure, C_i). Defects of this type in a pure substance are usually generated in pairs when an ion leaves its site and migrates to an interstice (Frenkel defects), or by simultaneous formation of cation (V_C) and anion (V_A) vacancies (Schottky defects) (Fig. 2). It is obvious that the formation of defects requires a significant energy (the enthalpies are ΔH_F and ΔH_S for the Frenkel and Schottky defects, respectively). Their equilibrium concentration for the formation of, for example, a Schottky defect can be found from the relation

$$[V_C] = [V_A] = K^{1/2} \cdot \exp\left(\frac{\Delta H_S}{2RT}\right) = \exp\left(\frac{\Delta S}{2R}\right) \cdot \exp\left(\frac{\Delta H_S}{2RT}\right) \quad (1)$$

where K is the pre-exponential factor of the defect formation constant, which is in some cases expressed as an entropy factor. In the general case, if n defects are formed simultaneously in the defect formation event, the enthalpy of defect formation under the exponent is divided by n. Only in a small number of crystals, the number of cation sites, the energies of which differ by a value comparable to kT exceeds the number of cations. In this case, the defect concentration in the crystal is very high and, therefore, the ions can move quickly. These are so-called superionic conductors, which include high-temperature polymorphs of compounds such as AgI, $CsHSO_4$, *etc.*[72–74]

However, this situation is not achievable for all materials. Furthermore, in most cases, devices that use solid electrolytes must operate at room or slightly higher temperatures, which are substantially lower than the superionic phase transition temperature. In order to increase the concentrations of defects in these materials, heterovalent substitution (doping) is used most often. For example, in the widely known materials with the NASICON (Na superionic conductor) structure such as lithium titanium phosphate [$LiTi_2(PO_4)_3$], the formation of defects upon the insertion of tri- or pentavalent cations (*e.g.*, aluminium and niobium) can be represented by the following quasi-chemical equations:[67,75,76]

$$Li_3Al_2(PO_4)_3/LiTi_2(PO_4)_3 = Li_{Li} + 2\,Li_i^{*} + 2Al'_{Ti} + 3\,PO_{4(PO_4)} \quad (2)$$

$$NbTi(PO_4)_3/LiTi_2(PO_4)_3 = V'_{Li} + Ti_{Ti} + Nb_{Ti}^{*} + 3\,PO_{4(PO_4)} \quad (3)$$

where the subscripts designate the cation site in the crystal lattice, while the superscripts '*' and ''' correspond to positive and negative charges of the ion or the vacancy relative to this site.[77] In this case, the defect concentration should formally be equal (or proportional) to the dopant concentration. However, usually the dopant solubility in the crystal lattice is limited; moreover, at higher degree of substitution, the association of defects is enhanced; therefore, the concentration of charge carriers is usually lower than the dopant concentration.

One more necessary condition for the existence of ionic conductivity is the possibility for ions to move in the crystal lattice, which is characterized by the ion mobility (μ_i). For migration to a neighbouring site, an ion should leave its coordination polyhedron, having overcome some intermediate state with the maximum energy (bottleneck). This is usually the face of the coordination polyhedron, as the ion that passes through the face is located most closely to other ions. The energy difference usually markedly exceeds the kT value, which makes the residence time of the ion in the activated state very short. Therefore, it is believed that ions move between crystal lattice sites by hopping and that the ion diffusion coefficient (D) exponentially increases with increasing temperature.

$$D = D_0 \cdot \exp\left(-\frac{E_j}{RT}\right) \quad (4)$$

where E_j is the activation energy of the ion jumping from one site to the other, D_0 is the pre-exponential factor. The mobility of ions is related to the diffusion coefficient by the Nernst–Einstein relation

$$\mu_i = \frac{qD_i}{kT} \quad (5)$$

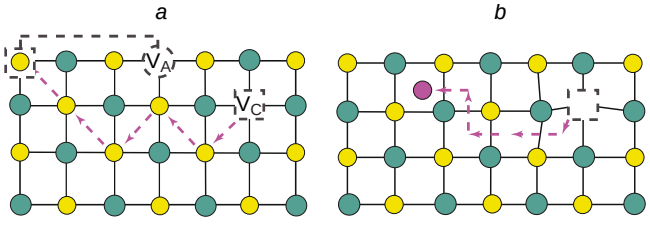

Figure 2. Schottky (*a*) and Frenkel (*b*) defects of the crystal lattice and ion transport by the vacancy (*a*) and interstitial (*b*) mechanisms.

From this, it is possible to obtain the Frenkel equation, which defines the temperature dependence of the ionic conductivity (σ)

$$\sigma T = A \exp\left(-\frac{E_j + \Delta H/2}{kT}\right) \quad (6)$$

A is the pre-exponential factor.

When the temperature change is small, the contribution of the multiplier T to the change of conductivity is insignificant, and it is possible to use the Arrhenius equation

$$\sigma = \sigma_0 \exp\left(-\frac{E_a}{kT}\right) \quad (7)$$

where E_a is the activation energy of conductivity. It is important to understand that for pure (underdoped) substances, the activation energy of conductivity includes some contribution of the enthalpy of defect formation and the activation energy of ion migration in the lattice ($E_a = E_j + \Delta H/2$).

Meanwhile, in the case of superionic phases, the activation energy of conductivity is determined only by the activation energy of ion jumping. The same situation may occur for heterovalent-doped materials. On the other hand, if association of defects with opposite charges is accompanied by a noticeable energy benefit, this can also give an additional contribution to the activation energy of conductivity.

One way to increase the ionic conductivity is to form composite materials.[78–80] For example, finely dispersed oxides of polyvalent elements (silicon, aluminium, *etc.*) can adsorb mobile cations from ionic crystals that are in contact with them. In this case, the concentration of cationic vacancies in a thin Debye layer near the surface of ionic crystal sharply increases, which may result in an increase in the conductivity by a few orders of magnitude. It is noteworthy that the energy of localization of various ions on the crystal surface can also markedly differ, which may lead to preferential surface exposure of ions of the same type.[81] In this case, the near-surface concentration of vacancies of these ions or, conversely, the interstitial concentration of oppositely charged ions increases. Therefore, even in pure substances existing as a nanodispersed phase (when the Debye length of approximately 1–2 nm is comparable with the size of ionic crystals), the ionic conductivity can markedly increase. Due to the fact that the activation energy of ion jumping decreases on this surface, as is the case, for example, for zirconium hydrogen phosphate, which adsorbs water molecules, the ionic conductivity of nanodispersed materials can increase by several orders of magnitude.[82,83] Meanwhile, crossing of the electrical double layer by an ion on this surface can be significantly complicated. In this case, the conductivity of finely dispersed material can be much lower than its bulk conductivity due to high grain boundary resistance. This situation is also characteristic of many NASICON-structured materials.[84–86]

It is noteworthy that there is a wide class of glassy electrolytes both inorganic and polymeric ones, in which the transport occurs in a similar way. Glassy materials have no long-range order; therefore, the structure and the size of polyhedra can somewhat differ. In this case, ion transport is determined by the lowest activation energy pathways. That is why materials existing in the glassy state and glass ceramics containing a mixture of crystalline and glassy phases often have higher ionic conductivity, in particular grain boundary one.[87–90]

In polymers, ions often move in coordination with the segmental mobility of the polymer backbone or side chains, which also results in some acceleration of ion transport. However, the conductivity of ion exchange polymer materials appears to be high only if they are plasticized with polar solvents. In these systems, the ion transport proceeds *via* the system of solvent-filled pores and channels.[91] In this case, the transport mechanism is similar to that in solutions, except that the transport rate is limited by the size of the channels connecting the pores.[92] Typical examples of such systems are Nafion membranes and other ion exchange membranes filled with an aprotic solvent, the charge carriers in which are generated upon dissociation of functional groups.[93–97]

It is worthy of note that two mechanisms of ion transport can be realized in solid electrolytes, namely, the vacancy and interstitial mechanisms (see Fig. 2), which can have markedly different rates. This may be compared with a drop falling in an empty vessel and a bubble rising in a filled vessel. Although both mechanisms lead to one and the same result, the transfer of some volume of a liquid under the action of gravity, the drop falls much faster, because the viscosity of the medium is much lower in this case. Most often, the Schottky disorder predominates in crystals, since the interstitial sites are too small to accommodate the ions. However, for lithium ions that have a small radius, this is usually not a serious obstacle, and the Frenkel disorder and the interstitial transport mechanism are quite often preferred for lithium ions.

The attention of researchers in the field of inorganic solid electrolytes is concentrated on NASICON, garnet and perovskite type materials and sulfides. These types of materials are considered below as the most popular inorganic lithium ion electrolytes used to fabricate ASSL Bs. Polymer electrolytes and composite materials are also used in ASSBs; these types of electrolytes are considered in the subsequent parts of the review. Figure 3 presents a comparison of the most important properties

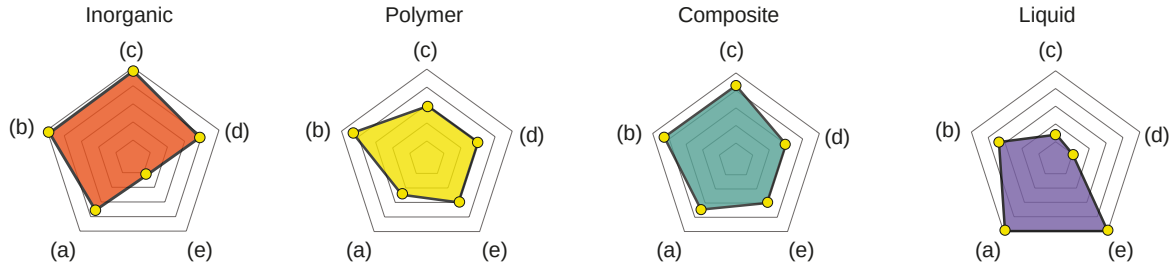

Figure 3. Comparison of the main characteristics of various electrolytes for lithium ion batteries

of these three classes of solid-state electrolytes with those of conventional liquid electrolytes.

4. Inorganic electrolytes

In 1993, Inaguma *et al.*[98] reported a material with the perovskite structure, $Li_{0.34}La_{0.51}TiO_{2.94}$, which had a fairly high ionic conductivity exceeding 2×10^{-5} S cm^{-1}; the authors stated that the bulk conductivity reached 10^{-3} S cm^{-1} at room temperature. Due to the low stability against lithium metal, this material could not be used as an electrolyte for ASSBs and, furthermore, so high bulk conductivity was not confirmed in later publications.[99–101] It is worth noting that this type of materials has a vacancy mechanism of conductivity (see Fig. 2 *a*).[102]

Materials with the general formula $Li_{3x}La_{2/3-x}TiO_3$ refer with the perovskite structural type (ABO_3) in which titanium occupies a half of octahedral sites, while lanthanum partially occupies the sites with the coordination number of 12 (Fig. 4).[103,104] Therefore, lithium ions that substitute lanthanum have a wide choice of free sites for migration by the vacancy mechanism and extensive opportunities for the change in stoichiometry.[105,106] Some authors noted that the conducting properties of such materials are markedly affected by their domain structure.[107,108] It was shown that the lithium content can control the dimensionality of transport processes. In the materials with the lithium content $x < 0.1$, the conductivity is two-dimensional, with the transport along the crystallographic *ab* plane predominating. When the lithium content is higher, lithium and lanthanum ions are randomly arranged in the crystal, and the conductivity is three-dimensional.[109–111] It is noted that a decrease in the conductivity of $Li_{3x}La_{2/3-x}TiO_3$ is usually caused by high resistance of grain boundaries.[112] This resistance can be reduced, for example, by introducing silver ions, which leads to increasing grain size,[113] or by using film materials.[114]

Since titanium ions in these structures are readily reduced, attempts were made to synthesize more stable materials, which resulted in the formation of $Li_{2x-y}Sr_{1-x}Ta_yZr(Hf)_{1-y}O_3$ with room-temperature ionic conductivity in the range of 2×10^{-4}–4×10^{-4} S cm^{-1} and electrochemical stability window of 1.4–4.5 V.[115–118] The stability of titanium- and lanthanum-containing materials can be increased, while maintaining high conductivity, by coating the $Li_{3x}La_{2/3-x}TiO_3$ particles with polydopamine, polyvinylidene fluoride (PVDF) or polyethylene oxide (PEO) with conducting additives.[119–121]

A high conductivity is also inherent in one of the first representatives of solid electrolytes, β-alumina $LiAl_{11}O_{17}$. Its

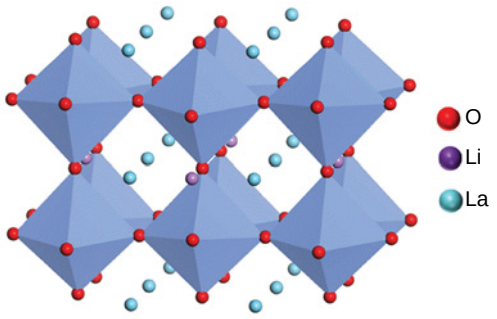

Figure 4. Crystal structure of perovskite. Titanium atoms are located within the octahedra. Reproduced from Ref. 104 with permission from John Wiley and Sons.

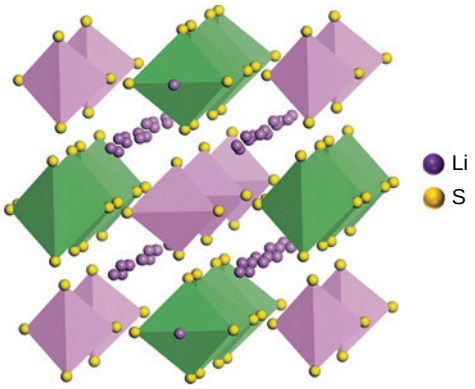

Figure 5. Crystal structure of LISICON. The zinc and germanium atoms are located within the octahedra and tetrahedra, respectively. Reproduced from Ref. 104 with permission from John Wiley and Sons.

structure is formed by four $[Al_{11}O_{16}]_n^{n+}$ layers with close-packed oxygen atoms. Since a layer containing four times less oxygen atoms is located between these layers, there appear intersecting channels that have a set of cavities, the total number of which is five times as great as the number of lithium cations.[122] This provides a high conductivity of the material over a wide temperature range.[123–126]

A number of lithium silicates and germanates with partial substitution of lithium by magnesium and zinc have been reported. The conductivity of the best obtained electrolytes $Li_{14}Zn(GeO_4)_4$ was 10^{-9} S cm^{-1} at room temperature and reached 0.125 S cm^{-1} at 300 °C.[127,128] The structure of these materials, called lithium superionic conductors (LISICON), belongs to space group Pnma (Fig. 5). The materials have a rigid three-dimensional framework, $[Li_{11}Zn(GeO_4)_4]_n^{3n-}$. The other lithium ions form parallel chains along the crystallographic *a* axis and are involved in two-dimensional diffusion. An even higher conductivity (4×10^{-5} S cm^{-1} at 18 °C) was found for $Li_{3.6}Ge_{0.6}V_{0.4}O_4$.[129,130] These materials show high thermal stability, but low chemical stability, because vanadium is easily reduced by lithium metal.

In the last decade, fairly high ionic conductivity was reported for materials with antiperovskite structure, which can be described as Li_3OA, where A is a halide ion or its analogue. For example, Li_3OCl and $Li_3OCl_{0.5}Br_{0.5}$ have a conductivity of 8.5×10^{-4} and 1.9×10^{-3} S cm^{-1}, respectively.[131] The temperature dependences of the ionic conductivity of Li_3OCl and a number of other inorganic and polymeric materials described in this review are shown in Fig. 6. The conductivity can be increased by an order of magnitude by partial substitution of lithium by barium in the glassy material $Li_{2.99}Ba_{0.005}OCl$.[137,138] The authors of a recent review[132] consider antiperovskites as promising electrolytes for ASSBs due to their high conductivity and thermal stability. However, very low stability of these compounds to hydrolysis with water vapour was noted.[132,139] Therefore, quite a few attempts to fabricate ASSBs using electrolytes with the antiperovskite structure have been made to date. Most often, they are markedly inferior in the capacity to batteries with liquid electrolytes.[140,141] The fabrication of the NCM111|$Li_{1.9}(OH)Cl_{0.9}$|$Li_4Ti_5O_{12}$ cell using melting of electrolytes can be considered as the most successful attempt. The cell showed an initial capacity of 150 mAh g^{-1}, with approximately 80% capacity retention after 100 cycles, which is moderate for the so stable anode.[141]

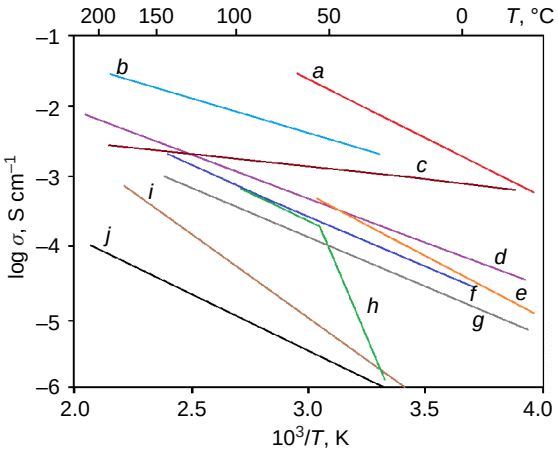

Figure 6. Temperature dependences of the ionic conductivity for $Li_{10}GeP_2S_{12}$ (*a*), glass ceramics $Li_7P_3S_{11}$ (*b*), Li_3OCl (*c*), $Li_{1.2}Al_{0.2}Zr_{0.1}Ti_{1.7}(PO_4)_3$ (*d*), Nafion + propylene carbonate + ethylene carbonate (*e*), PVDF + LiFSI (*f*), $Li_7La_3Zr_2O_{12}$ (*g*), PEO + LiTFSI (*h*), LiPON (*i*), $Li_1Ti_2(PO_4)_3$ (*j*). The Figure was created by the authors using published data.[132–136]

4.1. NASICON-structured materials

Materials with the NASICON structure include two types of complex phosphates containing tri- and tetravalent transition metal ions $[Li_3A^{III}_2(XO_4)_3$ and $LiA^{IV}_2(XO_4)_3$, where A^{III} = Al, Cr, Fe, *etc.*; A^{IV} = Ti, Ge, Sn, Zr, Hf; X = P or Si]. Most of these materials crystallize in the rhombohedral system (space group $R\bar{3}c$), while other compounds correspond to monoclinic or triclinic system. The structures are formed by AO_6 octahedra and XO_4 tetrahedra connected by shared vertices, with conductivity channels being formed between them (Fig. 7). These channels contain two types of vacancies, M1 and M2, the number of which per formula unit is 1 and 3, respectively. According to Francisco *et al.*,[142] the conductivity of such materials is limited by lithium transport through the triangular face of the $(M1)O_6$ distorted octahedron to M2 site.

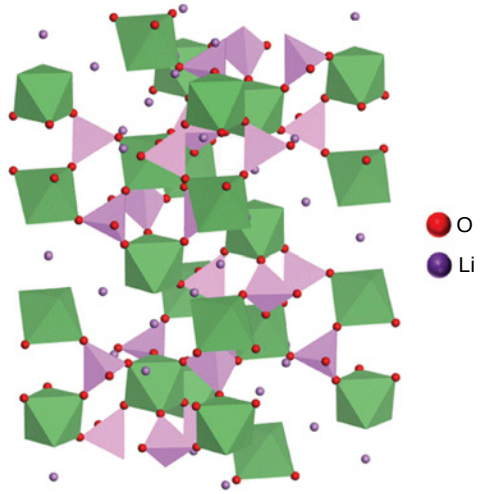

Figure 7. NASICON crystal structure. The A and X atoms are located within the octahedra and tetrahedra, respectively. Reproduced from Ref. 104 with permission from John Wiley and Sons.

Of most interest are materials based on tetravalent transition metal cations in which singly charged lithium or sodium cations completely occupy the M1 site, thus forming an ordered phase. Both A and X ions in these materials easily undergo heterovalent substitution, for example, according to Eqns (2) and (3) to form solid solutions containing a significant number of lithium vacancies or, on the contrary, additional lithium ions in the interstitials. In both cases, this results in a considerable increase in the ionic conductivity (see Fig. 6). By comparing the ionic conductivity and NMR relaxation data for materials based on scandium- and niobium-doped $LiZr_2(PO_4)_3$, Stenina *et al.*[143] arrived at the conclusion that the transport of lithium ions by the interstitial mechanism (see Fig. 2*b*) is preferred. A similar conclusion was drawn by other authors,[102,144,145] who used numerical methods and analysis of published data array. It is worth noting that $Na_2Zr_2SiP_2O_{12}$ with high sodium ion conductivity (0.1 S cm^{-1}), which gave the name to the NASICON structural type, has the interstitial mechanism of conductivity.[146] In some materials, *e.g.*, in lithium zirconium and lithium titanium phosphates, the heterovalent substitution may promote transition to the high-temperature polymorph.[143,147] This is accompanied by the shift of the phase transition temperature to the low temperature range for phosphates doped with trivalent cations $[Li_{1+x}M^{III}Ti_{2-x}(PO_4)_3]$.[148]

The approach involving the formation of defects *via* heterovalent substitution is undoubtedly the key way to fabricate materials with high ionic conductivity; however, as follows from Eqn (6), it is also necessary to take into account the contribution of ion mobility. Since materials of this type are isostructural, the key role in increasing the lithium ion mobility should belong to the activation energy of ion transport, which is determined by the size of the faces of coordination polyhedra that must be crossed by lithium ions moving between the M1 and M2 sites. Considering the clearly pronounced trend of decreasing activation energy of ionic conductivity for NASICON-structured materials following an increase in the bottleneck size in the series $LiGe_2(PO_4)_3$, $LiGeTi(PO_4)_3$, $LiTi_2(PO_4)_3$, $LiSn_2(PO_4)_3$, $LiTiHf(PO_4)_3$, $LiHf_2(PO_4)_3$, it was concluded[149–151] that an increase in the conductivity is favoured by increasing radius of the cation in the A site. This rule works quite well for undoped materials. However, it is far from being always correct. For example, Liu *et al.*[48] stated that the ionic conductivity of $LiTi_2(PO_4)_3$ or $LiGe_2(PO_4)_3$ is much higher than that of $LiZr_2(PO_4)_3$. The conductivity of $LiTi_2(PO_4)_3$ at room temperature is 10^{-7} S cm^{-1}. It can be increased by partial substitution of titanium (ionic radius of 0.61 Å) by either germanium with a smaller radius (0.53 Å) or zirconium with a greater radius (0.72 Å).[152–154] Attention is also attracted by the fact that aluminium-doped lithium titanium phosphates have been studied most intensively in recent years. This is due to the fact that particularly these compounds exhibit the highest conductivity values up to 1.1×10^{-3} S cm^{-1}.[155–161] Note that the conductivity is usually maximized for the $Li_{1.3}Al_{0.3}Ti_{1.7}(PO_4)_3$ composition. The point is that the solubility of aluminium ions in $LiTi_2(PO_4)_3$ is limited and attempts to increase the aluminium content result in the formation of a non-conducting $AlPO_4$ phase at the grain boundaries, which leads to a drop in the ionic conductivity.[162,163] Mention should also be made of the fact that among trivalent metal ions, the best substituting ion is relatively small aluminium, which in no way can increase the size of the coordination polyhedron of A cations. The major drawback of lithium titanium phosphates is the instability against reduction with lithium. Therefore, a lot of attention is paid to methods for

Table 1. Lithium-ion conductivity at room temperature for the main classes of solid inorganic electrolytes.

Inorganic electrolyte	Ionic conductivity, S cm^{-1}	Ref.
$Li_{1.3}Al_{0.3}Sn_{0.35}Ti_{1.35}(PO_4)_3$	4.7×10^{-4}	168
$Li_{1.2}Al_{0.2}Zr_{0.1}Ti_{1.7}(PO_4)_3$	7.9×10^{-4}	133
$Li_{1.3}Al_{0.21}B_{0.08}In_{0.01}Ti_{1.7}(PO_4)_3$	1.1×10^{-3}	169
$Li_{1.4}Al_{0.4}Ti_{1.4}Ge_{0.2}(PO_4)_3$	1.3×10^{-3}	170
$Li_{1.4}Al_{0.15}Fe_{0.25}Ti_{1.6}(PO_4)_3$	2.2×10^{-3}	171
$Li_{1.5}Al_{0.4}Cr_{0.1}Ge_{1.5}(PO_4)_3$	6.6×10^{-3}	172
$Li_{5.85}Al_{0.25}La_3Zr_{1.6}Ta_{0.4}O_{12}$	4.6×10^{-4}	173
$Li_{6.5}Ga_{0.2}La_{2.9}Sr_{0.1}Zr_2O_{12}$	5.5×10^{-4}	174
$Li_{6.46}La_{2.94}Ba_{0.06}Zr_{1.4}Ta_{0.6}O_{12}$	6.0×10^{-4}	175
$Li_{6.6}Al_{0.05}La_3Zr_{1.75}Nb_{0.25}O_{12}$	6.3×10^{-4}	176
$Li_{6.25}La_3Zr_{1.55}Al_{0.1}Ta_{0.45}O_{12}$	6.7×10^{-4}	177
$Li_{6.65}Ga_{0.05}La_{2.95}Ba_{0.05}Zr_{1.75}Ta_{0.25}O_{12}$	7.2×10^{-4}	178
$Li_7La_{2.75}Ca_{0.25}Zr_{1.75}Ta_{0.25}O_{12}$	7.6×10^{-4}	179
$Li_{6.4}Ga_{0.2}La_{2.95}Yb_{0.05}Zr_2O_{12}$	9.0×10^{-4}	180
$Li_{6.4}Ga_{0.2}La_3Zr_{1.7}Y_{0.3}O_{12}$	1.04×10^{-3}	181
$Li_{6.4}Ga_{0.2}La_{2.75}Y_{0.25}Zr_2O_{12}$	1.6×10^{-3}	182
$Li_{6.65}Ga_{0.15}La_3Zr_{1.9}Sc_{0.1}O_{12}$	1.8×10^{-3}	183
Li_3PS_4	1.6×10^{-4}	184
$Li_4P_2S_6$	2×10^{-6}	185
$Li_7P_3S_{11}$	1.3×10^{-3}	186
$Li_{10}GeP_2S_{12}$	1.2×10^{-2}	187
$Li_{10}SnP_2S_{12}$	3.2×10^{-3}	188
$Li_{10}SiP_2S_{12}$	2.3×10^{-3}	189
$Li_{11}AlP_2S_{12}$	8.0×10^{-4}	190
Li_6PS_5Cl	1.3×10^{-3}	191
Li_6PS_5Br	3.1×10^{-3}	192

stabilization of these materials, for example, by doping with magnesium ions[164,165] or coating with a polymer[166] or MoS_2.[167]

Comparison of some characteristic values of lithium-ion conductivity at room temperature for the main classes of solid inorganic electrolytes is presented in Table 1.

The ionic conductivity of $LiZr_2(PO_4)_3$ reaches 3×10^{-6} S cm^{-1} at room temperature and sharply increases after the phase transition to the rhombohedral structure at 40–55 °C.[193] As noted above, this phase can also be stabilized at room temperature by heterovalent substitution.[194] Although the initial $LiZr_2(PO_4)_3$ has a higher conductivity than the titanium-containing material, the replacement of a part of zirconium by lower-valence cations makes it possible only to approach the conductivity of $Li_{1+x}Al_xTi_{2-x}(PO_4)_3$.[195–200] Owing to the markedly larger radius of zirconium ions, a considerable fraction of zirconium can be substituted by even divalent cations, the radius of which is rather large because of the lower charge.

It is of interest that among lithium germanium phosphate-based materials, the highest room-temperature conductivities (10^{-4}–10^{-3} S cm^{-1}) were also achieved by doping with aluminium.[201–206] The lower mobility of lithium caused by smaller unit cell parameters of an aluminium-doped material is largely counterbalanced by higher solubility of Al^{3+} ions because of similarity of the Al^{3+} radius to the radius of Ge^{4+} (the maximum conductivity corresponds to 0.4–0.7 content of aluminium). Nikodimos *et al.*[207] reported that $Li_{1.5}Al_{0.33}Sc_{0.17}Ge_{1.5}(PO_4)_3$ exhibited a high bulk conductivity of 5.8×10^{-3} S cm^{-1}. One more benefit of these materials is a wide electrochemical stability window.[208,209]

Many of the listed facts contradict the assumption that the conductivity is determined by the bottleneck size and, ultimately, by the average size of cations in the A-site. Perhaps, it is more correct to say that created structure distortions result in the formation of conductivity channels in which lithium cations move faster. It is evident that the substitution of some titanium by germanium or aluminium leads to decreasing size of a particular polyhedron; however, the size of a neighbouring polyhedron or, more precisely, the size of section of the faces connecting them may increase. Obviously, the lithium transport rate would be determined exactly by channels with optimal sizes. Other explanations for certain experimental facts can be offered as well. For example, there are data that the presence of germanium promotes the formation of glass ceramics,[210] and its formation at grain boundaries can reduce their resistance. Trivalent ions that occupy titanium sites and are negatively charged with respect to the lattice, may serve as traps for lithium ions by forming associates with them (ion pairs connected by oxygen atoms). Furthermore, aluminium ions with a greater polarizing ability shift the electron density from the oxygen atoms to a greater extent, which leads to a lower binding of lithium ions. This only indicates that it is not always easy to predict which of the factors would predominate in each particular case; therefore, dopants are, most often, selected randomly, especially in the case of double substitution.

We have already noted above that in the case of NASICON materials, the grain boundary resistance usually exceeds the bulk resistance.[84,85,211] This results in considerable differences in the methods used to synthesize these materials. First, unlike the synthesis of most solid-state electrolytes, the preparation of nano-sized materials does not make sense; on the contrary, it is desirable to obtain crystals of larger size. For example, good results are achieved by using various methods of sintering.[150,209,212–217] In addition, it is expedient to introduce additives that increase the ceramic density and sinterability and the grain boundary conductivity. Some authors reported the successful use of lithium, boron and germanium oxides and lithium borates and phosphates for this purpose.[158,210,218–226] One can assume that these additives interact with the surface of crystallites and form amorphous or glassy phases. The highest conductivity of the obtained samples was $(3-4)\times10^{-4}$ S cm^{-1}.[220] There have also been successful attempts to synthesize thin films of $Li_{1+x}Al_xTi_{2-x}(PO_4)_3$ by pulsed laser deposition. After annealing at 800 °C, their ionic conductivity was 1×10^{-4} S cm^{-1} at room temperature. Bachman *et al.*[150] attributed the pronounced increase in the ionic conductivity during annealing to the formation of a glassy grain boundary phase.

Mention may also be made of some other recent studies in which the properties of the interface between $Li_{1+x}Al_xTi_{2-x}(PO_4)_3$ and electrode materials were improved by deposition of polymer coatings containing a lithium salt,[227,228] lithium ion-conducting material,[229] zinc oxide or reduced graphene oxide[230,231] (Table 2). Note also the high lithium-ion conductivity of some other phosphorus-containing materials. For example, Guan *et al.*[232] used the lithium salt of phosphotungstic heteropolyacid with a conductivity of 8.9×10^{-4} S cm^{-1} to design NCM523|Li cells with a potential difference of 4.35 V, which stably operated during 100 cycles.

Table 2. Main characteristics of batteries with solid inorganic electrolytes.

Electrolyte	Interlayer between the electrolyte and lithium	Cell cathode|anode	Cycling rate, temperature	Initial capacity, mAh g^{-1}	Number of cycles	Capacity retention (%)	Ref.
$Li_3PW_{12}O_{40}$	–	NMC523|Li	0.1C, RT	165.6	200	91.5	232
$Li_{6.75}La_3Zr_{1.75}Ta_{0.25}O_{12}$	Al and Si alloy	LFP|Li	0.5C, RT	144	600	86.2	233
$Li_{6.6}La_3Zr_{1.6}Ta_{0.4}O_{12}$	Ag-coated Cu	LFP|Li	0.5C, RT	146	300	81	234
$Li_{6.4}La_3Zr_{1.4}Ta_{0.6}O_{12}$	AlF_3	LFP|Li	1C, RT	115.6	535	80.6	235
$Li_{6.75}La_3Zr_{1.75}Ta_{0.25}O_{12}$	MgF_2	LFP|Li	0.1C, RT	151.4	100	98.3	236
$Li_{6.4}La_3Zr_{1.4}Ta_{0.6}O_{12}$	Porous hard carbon	LFP|Li	0.2C, RT	154.4	150	89	237
$Li_{6.75}La_3Zr_{1.75}Ta_{0.25}O_{12}$	SnS_2	LFP|Li	0.1C, RT	156.9	100	90.4	238
$Li_{6.4}La_3Zr_{1.4}Ta_{0.6}O_{12}$	$InCl_3$	LFP|Li	0.5C, RT	130.3	475	97.8	239
$Li_{6.5}La_3Zr_{1.5}Ta_{0.5}O_{12}$	Ta_2O_5	LFP|Li	0.2C, RT	153	100	~100	240
$Li_{6.4}La_3Zr_{1.4}Ta_{0.6}O_{12}$	α-MoO_3	LFP|Li@Mo	1C, RT	138	200	98	241
$Li_{6.40}La_3Zr_{1.40}Ta_{0.60}O_{12}$	Graphite	LFP|Li	0.1C, RT	149.4	350	83	242
$Li_7La_3Zr_2O_{12}$	Li@C	LFP|Li	0.5C, RT	~142	100	~92	243
$Li_{6.5}La_3Zr_{1.5}Nb_{0.5}O_{12}$	LiPON	LFP|Li	0.2C, 30 °C	139.1	150	99.2	244
$Li_7La_{2.75}Ca_{0.25}Zr_{1.75}Nb_{0.25}O_{12}$	Al	LFP|Li	0.1 mA cm^{-2}, 20 °C	132	100	90.9	245
$Li_7La_{2.75}Ca_{0.25}Zr_{1.75}Nb_{0.25}O_{12}$	Al_2O_3	$Li_2FeMn_3O_8$|Li	0.1C, RT	110	100	~100	246
$Li_{1.5}Al_{0.5}Ge_{1.5}(PO)_4$	ZnF_2	LFP|Li	0.1C, RT	154	40	~100	247
$Li_{1.5}Al_{0.5}Ge_{0.5}(PO_4)_3$	ZnO + reduced graphene oxide	LFP|Li	0.5C, RT	131.6	100	93.8	230
$Li_{1.5}Al_{0.5}Ge_{1.5}(PO_4)_3$	PVDF-HFP – LiTFSI	LFP|Li	0.2C, RT	150.7	200	98.8	248
$Li_{1.3}Al_{0.3}Ti_{1.7}(PO_4)_3$	Boron nitride	LFP|Li	0.5C, RT	150.9	500	92	249
$Li_{1.3}Al_{0.3}Ti_{1.7}(PO_4)_3$	PEO	LFP|Li	0.3C, RT	139	100	97.3	250
$Li_{1.3}Al_{0.3}Ti_{1.7}(PO_4)_3$	PEO + LiTFSI + $Li_{1.3}Al_{0.3}Ti_{1.7}(PO_4)_3$	LFP|Li	0.05C, 80 °C	113.1	45	80.7	251
$Li_{1.3}Al_{0.3}Ti_{1.7}(PO_4)_3$	PEGDA + $Pyr_{13}TFSI$	LFP|Li	0.5C, 60 °C	152.5	200	91.5	252
$Li_{1.4}Al_{0.4}Ti_{1.6}(PO_4)_3$	ZnO	LFP|Li	0.1C, RT	167.3	200	88	253
$Li_{1.3}Al_{0.3}Ti_{1.7}(PO_4)_3$	PEO + BN	LFP|Li	0.5C, 60 °C	139.2	500	96.6	254
$Li_{1.4}Al_{0.4}Ti_{1.6}(PO_4)_3$	PAN (cathode), PEO (anode)	NCM622|Li	0.5C, 60 °C	168.2	120	89	255
$Li_{1.4}Al_{0.4}Ti_{1.6}(PO_4)_3$	Liquid electrolyte (300 μL)	LFP|Li	1C, RT	125	500	92	256
$Li_{10}SnP_2S_{12}$	–	LFP|Li	0.1C, RT	139.6	100	76.7	257
$Li_7P_3S_{11}$	–	$Li_4Ti_5O_{12}$|Li	1C, RT	158	600	85	258
$Li_{2.96}P_{0.98}S_{3.92}O_{0.06} - Li_3N$	–	$LiNbO_3$@ NCA|Li	0.1 mA cm^{-2}, RT	165.8	50	93.5	259
$Li_{10}GeP_2S_{12}$	–	LFP|Li	1C, RT	105.7	200	99	260
Li_6PS_5Cl	Polypropylene carbonate + LiTFSI	LFP|Li	1C, RT	~150	900	~90	261

Note. @ means a composite or alloy, RT is room temperature; PVDF-HFP is poly(vinylidene fluoride-co-hexafluoropropylene); PEGDA is polyethylene glycol diacrylate; Pyr13TFSI is ionic liquid, *N*-propyl-*N*-methylpyrrolidinium bis(trifluoromethanesulfonyl)imide; PAN is polyacrylonitrile.

4.2. Garnet structure materials

Solid-state electrolytes based on $Li_7La_3Zr_2O_{12}$ (LLZO) with the garnet structure are among the newest and most in-demand types of materials for ASSBs (Fig. 8). The benefits of these materials include relatively high lithium-ion conductivity and stability against lithium metal. Only in the beginning of the 21st century, it was found that the materials $Li_5La_3M_2O_{12}$ (M = Ta, Nb) have relatively high lithium-ion conductivity of approximately 10^{-6} S cm^{-1} at room temperature.[262] Four more years later, a zirconium compound of a similar composition, LLZO, was obtained and showed a two orders of magnitude higher ionic conductivity.[263]

The tetragonal phase of LLZO is formed by connected ZrO_6 octahedra and two types of eight-vertex lanthanum polyhedra (see Fig. 8). Lithium ions fully occupy the tetrahedral and two types of distorted octahedral voids.[264] Due to the low

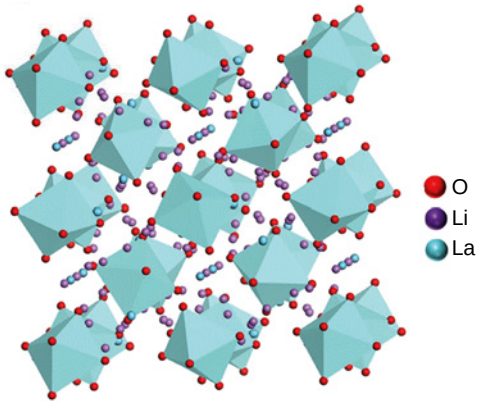

Figure 8. Crystal structure of garnet type LLZO. Zirconium is located inside the octahedra. Reproduced from Ref. 104 with permission from John Wiley and Sons.

concentration of defects, the tetragonal phase has a conductivity of 1.6×10^{-6} S cm^{-1} at room temperature.[265]

The cubic LLZO phase has a similar framework structure, although all zirconium and lanthanum ions occupy each one type of sites and are structurally equivalent.[266] Lithium ions occupy only two types of sites, the first of which (Li1) has a tetrahedral environment of oxygen atoms and is almost completely filled. The second one (Li2) has a distorted octahedral environment and is filled by about 1/3. In combination with the small distance between two sites, this provides conditions for high ionic conductivity.[267]

It is noteworthy that, according to many researchers, the cubic phase can exist only owing to the presence of dopant impurities, in particular, its stabilization in the early studies was due to a minor amount of aluminium from the crucible used for annealing.[48,268,269] This stabilization can be achieved by replacement of any type of cations present in LLZO and is accompanied by increase in the ionic conductivity (see Fig. 6). In some cases, it is difficult to know exactly in which lattice the substitution will take place, because ionic radii of lithium and zirconium ions with coordination number of 6 are similar, and the authors usually do not undertake special investigation to determine localization of the dopant. The assumptions on the dopant localization site are usually based on the component ratio taken initially, which cannot be regarded as accurate, because of incomplete crystallization, evaporation of lithium compounds, and possible interaction with the crucible material. In this review, we give information on substitution in a particular sublattice relying on the data from the original publications.

Miara *et al.*[270] calculated the energies of defect formation and preferable positions occupied by all possible dopants in the LLZO structure using the density functional theory (DFT) method (Fig. 9); this can be considered as a theoretical justification of doping experiments. Partial substitution of zirconium seems to be the most attractive and reasonable option. Evidently, the most expedient is heterovalent substitution, which should be accompanied by the formation of structural defects to maintain the electroneutrality of the whole material. Nevertheless, there are studies related to partial substitution of zirconium ions by Ti^{4+} (Ref. 271) and Ge^{4+} (Ref. 272), in which cubic LLZO was stabilized and showed conductivity of $2 \times 10^{-4} - 5 \times 10^{-4}$ S cm^{-1}.

The replacement of a part of zirconium by divalent or trivalent ions should be accompanied by the insertion of additional lithium ions into partially occupied octahedral voids in LLZO and by increasing concentration of mobile Li^+ ions. It is well known that for heterovalent substitution, it is most expedient to use ions with a charge differing by unity from the charge of the replaced ion and with similar size at the same coordination number. From this standpoint, scandium is the ion of choice to substitute zirconium. Even at a low degree of zirconium substitution (2.5%), the conductivity was 1.65×10^{-4} S cm^{-1} at 20 °C.[273] However, scandium is fairly expensive; therefore, yttrium is used most often to stabilize the high-temperature zirconium oxide phase, despite the significant difference in the ion size. Kotobuli and Koishi[274] obtained the material $Li_{7.06}La_3Y_{0.06}Zr_{1.94}O_{12}$, the conductivity of which at 25 °C approached 10^{-3} S cm^{-1}. The results of partial substitution of zirconium by samarium and gadolinium were more modest: the conductivity of the best samples did not exceed 2.5×10^{-4} S cm^{-1} at room temperature.[275,276] When 5% of zirconium was substituted by magnesium possessing a similar radius, an ionic conductivity of 2.9×10^{-4} S cm^{-1} at 20 °C was achieved.[273]

One more approach is to introduce higher-valence ions instead of zirconium, which may increase the concentration of lithium vacancies. Among pentavalent elements, niobium and

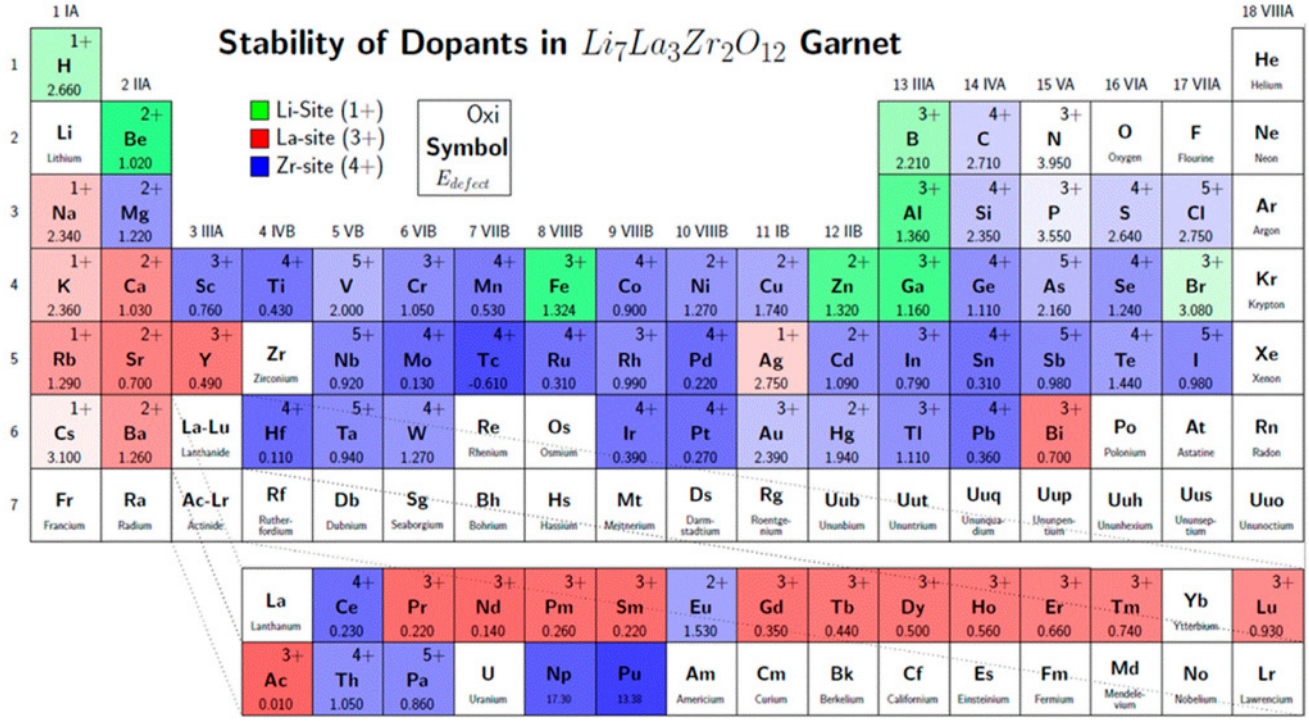

Figure 9. Preferable sites and oxidation numbers of doping elements and energies of defects (in eV) in LLZO. The colours highlight the cation sites in which the dopants are located (Li sites are green, La sites are red, and Zr sites are blue). A darker colour corresponds to lower energies of defects in these positions.[270] Reproduced with permission from the American Chemical Society.

tantalum with ion radii similar to that of zirconium are the dopants of choice. The conductivity of the best samples for both niobium and tantalum doping reached 8.0×10^{-4} S cm^{-1}.[277,278] However, it is worth noting that these results were not reproduced in subsequent studies. Materials with different degrees of substitution of zirconium had room-temperature conductivities of 1.4×10^{-4}–6×10^{-4} S cm^{-1}.[279–285] The substitution of zirconium by bismuth and antimony gave even more modest results.[286,287]

The attempts at partial substitution of zirconium by hexavalent cations (chromium, molybdenum, tungsten and tellurium) were also made. The authors of some studies reported fairly high conductivity values of up to 10^{-3} S cm^{-1} at room temperature.[288–290] However, due to easy reduction of dopants, these materials are unstable against lithium metal, unlike most other garnet type materials.

Finally, it is appropriate to mention a number of studies in which zirconium ions of LLZO were simultaneously substituted by different ions. For example, co-doping with tantalum and cerium may bring about an increase in both the concentration of lithium vacancies and the size of conductive channels. As a result, the ionic conductivity was increased to 10^{-3} S cm^{-1} at room temperature.[291] Tong *et al*.[292] reported the synthesis of $Li_{6.4}La_3Zr_{1.4}Ta_{0.3}Nb_{0.3}O_{12}$ containing equal amounts of niobium and tantalum with a conductivity of 6×10^{-4} S cm^{-1}.[292]

The authors of other studies introduced simultaneously pentavalent niobium and trivalent rare earth elements into zirconium sites. This could have resulted in generation of mutually annihilating defects. However, the authors reported fairly high conductivity of 8×10^{-3}–10×10^{-3} S cm^{-1} for the obtained materials.[293–295]

The substitution of lithium by multicharged cations is an equally popular approach. It seems that the success of this approach is hindered by the fact that multicharged cations that occupy lithium sites should limit the lithium mobility. However, according to density functional theory calculations, there are eight non-equivalent paths of lithium diffusion over the three-dimensional lattice in the cubic structure;[284] in combination with the relatively low degree of substitution, this can minimize the adverse effect. Partial substitution of lithium by aluminium is the most popular approach. As opposed to the existing view that the high concentration of lithium is responsible for high conductivity,[296] the stream of studies along this line does not decrease. Partial lithium substitution by aluminium results only in a decrease in the Li^+ content, but the ionic conductivity of materials increases upon this substitution by, on average, two orders of magnitude.[279,297–301]

The attempts to replace some of Li^+ ions by Ga^{3+} ions with a size similar to the lithium size also appear reasonable. These studies proved to be quite successful: some authors reported conductivity of 3.5×10^{-4}–9.6×10^{-4} S cm^{-1}.[302–306] There is information on the synthesis of gallium-containing materials the conductivity of which ranged from 1.2×10^{-3} to 1.25×10^{-3} S cm^{-1}.[307,308] It was also reported that partial substitution of lithium ions in LLZO by gallium ions produces a new crystalline phase with space group I-$\bar{4}$3d with enhanced lithium diffusion.[309] The improvement of lithium diffusion was also observed by Fritsch *et al*.,[310] who substituted zirconium by tantalum and niobium.

Other authors describe materials in which lithium was partly replaced by trivalent iron,[311] rare earth elements,[312–314] divalent magnesium and zinc[273,315] and tetravalent germanium.[316] However, the results were modest in most cases. The highest ionic conductivity (3.2×10^{-4} S cm^{-1}) was observed for the yttrium-containing sample.[313]

Numerous attempts are made to perform simultaneous substitution in the lithium and zirconium sublattices. Since the heterovalent substitution of lithium can give only additional vacancies, it seems most appropriate to use a second dopant that could enhance this effect or increase the mobility of lithium by changing the lattice parameters. Il'ina *et al*.[176] described the material $Li_{6.6}Al_{0.05}La_3Zr_{1.75}Nb_{0.25}O_{12}$ with a lithium ion conductivity of 6.3×10^{-4} S cm^{-1} at room temperature. A number of authors[173,177,317,318] reported LLZO materials with partial lithium substitution by aluminium and zirconium substitution by tantalum; the conductivity of these materials ranged from 4.6×10^{-4} to 10^{-3} S cm^{-1} at 25 °C. The gallium-doped material $Li_{6.4}Ga_{0.133}La_3Zr_{1.8}Ta_{0.2}O_{12}$ had a conductivity of 6.1×10^{-4} S cm^{-1}.[319] Somewhat lower conductivity was obtained when pentavalent antimony (4.1×10^{-4} S cm^{-1})[320] or hexavalent molybdenum (4.4×10^{-4} S cm^{-1})[321] was used for doping. When a part of zirconium was replaced by titanium and a part of lithium was replaced by aluminium ($Li_{6.25}Al_{0.25}La_3Zr+Ti_{0.25}O_{12}$), the conductivity was much lower (1.5×10^{-4} S cm^{-1}).[322] Presumably, this is caused by decreasing size of the conductivity channels.

The results of partial substitution of lithium by gallium and zirconium by scandium (1.8×10^{-3} S cm^{-1} at 27 °C)[183] or yttrium (1×10^{-3} S cm^{-1} at 25 °C) were among the best.[181] This is not fully understandable, since doping of these materials with gallium is expected to generate lithium vacancies, while the replacement of zirconium, on the contrary, should decrease the vacancy concentration. The opposite effect is also expected to be induced by the partial substitution of lanthanum by calcium and zirconium by niobium, which was reported by Zhang *et al*.[179] and Chen *et al*.[323] The maximum conductivity of 7.6×10^{-4} S cm^{-1} at room temperature was attained for $Li_7La_{2.75}Ca_{0.25}Zr_{1.75}Ta_{0.25}O_{12}$,[179] in which, according to the presented stoichiometry, no additional disorder should have been generated. It can be assumed that the substitution in such materials does not proceed according to a strictly specified pattern, but involves, for example, simultaneous inclusion of aluminium from the crucible or separation of amorphous phases, which leads to an increase in the defect concentration.

The authors of a few other papers simultaneously replaced all three elements in LLZO. Lithium was substituted by gallium or aluminium, lanthanum was substituted by barium, while yttrium, tantalum or tungsten were used to substitute zirconium. In the case of $Li_{6.52}Al_{0.2}La_{2.98}Ba_{0.02}Zr_{1.9}Y_{0.1}O_{12}$, no such high conductivity was obtained: 2×10^{-4}–3×10^{-4} S cm^{-1}.[324,325] The conductivity of $Li_{6.65}Ga_{0.05}La_{2.95}Ba_{0.05}Zr_{1.75}Ta_{0.25}O_{12}$ and $Li_{5.72}Al_{0.2}La_{2.98}Ba_{0.02}Zr_{1.65}W_{0.35}O_{12}$, in which two main dopants should have induced the formation of lithium vacancies, proved to be higher: 7.2×10^{-4} and 5.3×10^{-4} S cm^{-1}, respectively.[178,324] An opinion was stated[48,296] that the ionic conductivity is correlated with the lithium ion content. Meanwhile, it can be noted that in these materials, like in the above-described materials, no definite correlation can be found between the conductivity and the lithium content; probably, this emphasizes once again that the heterovalent substitution in LLZO is determined by not only the stoichiometric ratio of the reactants. In some samples, doping may also improve the morphology or grain contacts.

Most LLZO electrolytes are stable against the lithium anode.[326] However, the lack of plasticity of LLZO results in low efficiency of its contacts with the cathode and anode and increases the battery's internal resistance.[327,328] One more result

is the non-uniform deposition of lithium on the anode during the charging, which may lead to dendrite growth.[329] The situation is exacerbated by the low wettability of LLZO with lithium.[330] The most popular approach to address this problem is to form interlayers (interfaces) that possess lithium ion and electronic conductivity, *e.g.*, lithium alloys with indium and aluminium[245,331] and lithium nitride,[332] and to use of a special trimethyl phosphate-based electrolyte, which is distinguished by high electrochemical stability[333] (see Table 2).

Unfortunately, some of the elements used for LLZO modification can be reduced by lithium, which complicates the use of the obtained materials. As shown previously, high conductivity values were obtained for gallium-doped LLZO samples. The authors reported the capacity of the Li|L(Ga)LZO|LFP cell equal to 150 mAh g^{-1}, which slightly changed after 50 cycles.[334] However, there are also data that contradict the above, indicating the instability of gallium-doped LLZO against lithium metal.[334] The reduction of gallium with lithium is accompanied by the formation of impurity phases[335,336] and the growth of dendrites, which, as indicated by Li *et al*.,[335] can be prevented by adding SiO_2. According to Shen *et al*.,[337] dendrite penetration is prevented by the use of dense pore-free ceramic, while Liu *et al*.[338] proposed coating the L(Ga)LZO surface with a gel-polymer electrolyte layer, which provides for more than 82% capacity retention after 100 cycles at a 0.5C rate. Methods of stabilization of electrochemical contacts in these systems are being actively developed.

4.3. Sulfide electrolytes

Sulfide electrolytes are similar to their oxide counterparts in both the structure and transport mechanisms. However, they still have specific features, which make them a separate class of solid electrolytes. Sulfur ions have a larger radius than oxygen and a substantially higher polarizability of the electron shell. This results in a greater size of conductivity channels and additionally facilitates the transport of lithium ions along the channels *via* deformation of their electron shells (polarizability). Thus, the ionic conductivity significantly increases and the activation energy of conductivity decreases.[71,339,340] In addition, because of the same reasons, sulfides are more plastic and less brittle than oxides.[341] Meanwhile, it is evident that sulfides are markedly inferior to oxides in the chemical and thermal stability.[150,342,343] According to some authors, sulfides are also characterized by a wide electrochemical stability window[344,345] and make it possible to obtain high-power ASSBs.[346]

The simplest representatives of sulfide electrolytes are lithium thiophosphates Li_3PS_4, $Li_7P_3S_{11}$ and $Li_4P_2S_7$, formed in the $Li_2S-P_2S_5$ system[347] and $Li_4P_2S_6$.[348] These materials are composed of isolated single (PS_4^{3-}) and/or paired ($P_2S_7^{4-}$ or $P_2S_6^{4-}$) thiophosphate ions with tetrahedral environment of phosphorus and lithium cations.[349,350]

Li_3PS_4 has three structural phases differing in the degree of ordering. The low-temperature γ-Li_3PS_4 phase has a relatively low ionic conductivity of $3-7\times10^{-7}$ S cm^{-1} at room temperature and an ordered arrangement of lithium ions in tetrahedral sites.[351] However, as the temperature is raised, the disorder of lithium ions with their partial shift into octahedral voids induces a phase transition to the β-phase, a sharp increase in the ionic conductivity up to 3×10^{-2} S cm^{-1} and decrease in the activation energy of conductivity down to 15.5 kJ mol^{-1}.[352,353] Note that the estimated ionic conductivity values for the β-phase stable above 450 °C are only slightly greater.[354] One more benefit of Li_3PS_4 is the stability against lithium metal and a wide electrochemical stability window of up to 5 V.[355] It was also reported that the conductivity of glass ceramic Li_3PS_4 at room temperature reaches 7.5×10^{-4} S cm^{-1}.[356]

The ionic conductivities of $Li_2P_2S_6$ and $Li_4P_2S_6$ at room temperature are relatively low, being only 8×10^{-11} and 1.6×10^{-10} S cm^{-1}, respectively.[357,358] A markedly higher conductivity, reaching 8×10^{-5} S cm^{-1} at room temperature, is inherent in $Li_7P_3S_{11}$, and when glass ceramic is used, it may increase to 1.7×10^{-2} S cm^{-1}.[359–362] The opinions concerning the stability of these materials are contradictory. For example, it was reported that $Li_7P_3S_{11}$ can operate with a lithium metal anode, but is unstable to air and water.[363,364] However, other data attest to the lack of stability of all materials of this class against lithium and, furthermore, the decomposition products do not effectively passivate the anode.[361,365–367] The protection can be provided by using a lithium–indium alloy as the anode[368] or by depositing protective coatings[369–373] (see Table 2).

Li_6PS_5X are complex-anion materials the lattice of which with a cubic symmetry and space group $F\bar{4}3m$ belongs to the argyrodite structure type. It contains PS_4^{3-}, S^{2-} and X^- anions and lithium cations in tetrahedral voids.[374–376] The ionic conductivity of these materials is comparable with that of liquid electrolytes; therefore, they can be considered among the most promising for ASSBs.[343]

As the reference point to start the description of the conductivity of various argyrodites, one should consider Li_7PS_6. The low-temperature orthorhombic phase of this material obtained by solid-state synthesis has a conductivity of 8×10^{-5} S cm^{-1} at room temperature.[378] The high-temperature cubic polymorph is stable only above 210 °C;[379] however, Ziolkowska *et al*.[380] were able to obtain it from a solution. The conductivity of this material reached 1.1×10^{-3} S cm^{-1} at room temperature. Rao and Adams[381] showed that the conductivity of materials such as Li_6PS_5Cl, prepared by ball milling, is $1\times10^{-3}-1.3\times10^{-3}$ S cm^{-1} at room temperature. Even higher conductivity values of approximately $3\times10^{-3}-5\times10^{-3}$ S cm^{-1} were obtained by other authors.[192,382–387] Some authors successfully used the heterovalent substitution of a part of phosphorus[388,389] or sulfur.[390] In addition, high electrochemical stability of these electrolytes of up to 7–10 V has been reported.[391,392] Despite the fact that Li_6PS_5I has a relatively low conductivity (10^{-6} S cm^{-1}) at room temperature, the highest conductivity values ($1.8\times10^{-2}-2.4\times10^{-2}$ S cm^{-1}) are attained particularly for iodine-containing $Li_{7-x}E^{5+}_{1-x}M^{4+}_xS_5I$, in which the pentavalent cation is partly substituted by a tetravalent cation.[393–395]

Quite a few complex lithium halides with indium and rare earth metals like $Li_3MCl(Br)_6$ (M = In, Y, Er, *etc*.) with a high room temperature conductivity of $1\times10^{-3}-3\times10^{-3}$ S cm^{-1} have been obtained.[396–400] There are data on using these electrolytes in ASSBs with a relatively high capacity and stability.[401,402]

The use of the Li_6PS_5Cl and Li_6PS_5Br electrolytes in ASSBs with anodes made of the lithium–indium alloy has been reported. In the opinion of the authors,[403–405] the batteries based on these electrolytes showed fairly high capacity and stability. Therefore, argyrodite type Li_6PS_5X compounds can be considered to be promising electrolytes for ASSBs.[343,406,407]

One more large group of sulfide electrolytes includes materials similar to LISICON complex phosphates discussed above. The first materials of this type were detected in the Li_3PS_4 and Li_4GeS_4 system in which the compound $Li_{10}GeP_2S_{12}$ with a broad homogeneity range is formed[408,409] (see Fig. 6). The structure of $Li_{10}GeP_2S_{12}$ refers to the tetragonal space group $P4_2/nmc$. It is formed by isolated tetrahedra $(Ge,P)S_4$, with

lithium ions being located in the tetrahedral and octahedral voids between them (see Fig. 5).[410,411] The lithium transport occurs *via* one-dimensional channels along the ⟨001⟩ crystallographic direction.[412]

These materials attract attention for their high ionic conductivity,[413] which is a record high for sulfide electrolytes (up to 1.4×10^{-2} S cm^{-1}) in the opinion of some researchers, and are quite competitive with liquid electrolytes.[69,410,414,415] The conductivity of $Li_{10}GeP_2S_{12}$ reaches 10^{-2} S cm^{-1} only at temperatures of 50–80 °C.[187] However, the materials of this group are characterized by certain problems, for example, high resistance of grain boundaries, as is the case for NASICON ceramics. As a result, contrary to expectations, a decrease in the grain size also leads only to increasing resistance of the materials.[260,416–419]

Another obvious disadvantage of these materials regarding their commercialization is the presence of expensive germanium. Therefore, many researchers have attempted to replace germanium by more common elements. For example, the preparation of $Li_{10}SnP_2S_{12}$ with the ionic conductivity of 2×10^{-3}–7×10^{-3} S cm^{-1} has been reported.[420–423] However, these materials are not stable against the lithium metal anode. Vinado *et al*.[424] and Tarhouchi *et al*.[425] reported the possibility of increasing stability of these electrolytes by deposition of surface layers.

One more alternative is $Li_{10}SiP_2S_{12}$. Although Kuhn *et al*.[420] reported a high ion mobility in these structures according to NMR data, the ionic conductivity determined by impedance spectroscopy was 4×10^{-3} S cm^{-1}, which is somewhat lower than that for germanium-containing materials. Markedly higher conductivity was reported for materials with partial substitution by tetravalent cobalt (6.1×10^{-3} S cm^{-1})[426] or complete substitution of germanium by silicon (6×10^{-3} S cm^{-1}).[427] An ionic conductivity of 3.1×10^{-3} and 2.5×10^{-2} S cm^{-1} at room temperature was reported[345,428] for materials in which sulfur was partially replaced by oxygen and chlorine, respectively. Finally, an aluminium-containing material, $Li_{11}AlP_2S_{12}$ had a higher stability, but a lower conductivity of 8×10^{-4} S cm^{-1} at 25 °C with an activation energy of 25.4 kJ mol^{-1} and electrochemical stability of up to 5.0 V. It was shown that partial substitution of tin in $Li_{10}SnP_2S_{12}$ by aluminium resulted in a conductivity of 2×10^{-3} S cm^{-1}.[427]

While evaluating the potential of sulfide electrolytes, one can state that they have a higher ionic conductivity (see Fig. 6) than the above-described oxide systems, but are noticeably inferior to them in the chemical and electrochemical stability, which restricts their use in electrochemical current sources.[339,340,429,430]

5. Polymer electrolytes

Despite the high ionic conductivity of solid inorganic electrolytes, their commercialization is hindered by the relatively high resistance at the electrode/electrolyte interface and the necessity of high-temperature treatment. Polymer electrolytes (PEs) usually possess excellent flexibility and mechanical properties with improved interfacial contact, which attracts attention of researchers specializing in ASSBs.[431] Polymer electrolytes can be classified by the presence or absence of a liquid phase (gel-polymer and solid), by phase composition (homogeneous and composite), by the number of types of charge carriers (with parallel transport of co-ions and counter-ions or with selective transport of cations).[432–435]

The most popular PEs correspond to the polymer/salt-type electrolytes. These systems contain a lithium salt with a bulky anion, the most widely used among them being bis(trifluoromethanesulfonyl)imide (LiTFSI), bis(fluorosulfonyl)imide (LiFSI), hexafluorophosphate ($LiPF_6$) and perchlorate ($LiClO_4$) (Table 3). To ensure the dissolution of this salt, the polymer must contain a sufficient number of electronegative atoms capable of coordinating lithium ions and participating in their transport. Therefore, the most commonly used inert polymer matrices include PEO, PVDF, polymethyl methacrylate (PMMA), polyacrylonitrile (PAN), *etc*. (see Table 3).

Table 3. Structural formulas of the most common lithium salts and polymer matrices used in electrolytes.

$LiPF_6$	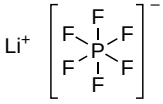	PEO	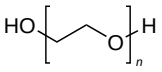
$LiClO_4$	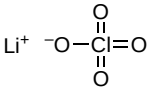	PVDF	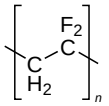
LiTFSI	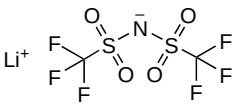	PAN	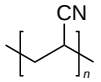
LiFSI	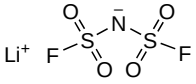	PMMA	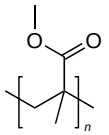

Most polymers contain crystalline and amorphous phases, in which cation movement occurs by different mechanisms. The greatest contribution to the ionic conductivity of polymer electrolytes is made by the movement of lithium cations in amorphous parts of the polymer, which is implemented by the solvation/desolvation mechanism *via* their interaction with electronegative atoms of the macromolecule or the salt and involves the segmental mobility of polymer groups. At temperatures below the glass transition temperature T_g, the segmental mobility of the polymer matrix is inhibited, and the cation movement in the polymer occurs by hopping between neighbouring sites able to coordinate lithium. Thus, ionic conductivity in solid PEs is determined by the degree of crystallinity, free volume and segmental mobility of the polymer, and studies are mainly focused on varying the above parameters. Effective strategies for the manufacture of uniform solid PEs with enhanced characteristics include copolymerization, graft polymerization and blending of different polymers.[431,436] The use of polymer chains with various bulky moieties, cross-linking agents, rigid frameworks and various functional groups makes it possible to reduce the polymer crystallinity and/or coordinate ion transport pathways and also to improve the mechanical properties of PEs to prevent dendrite growth.

The methods used to prepare PE films can be classified into *ex situ* methods in which an electrolyte film is obtained separately and then used in the assembly of the battery and *in situ* methods in which a polymer film is formed directly on the electrode surface. Solution casting is the most common method to fabricate film PEs. The polymer and the lithium salt are dissolved, cast on a substrate and dried.[437] An advantage of *ex situ* methods is the control over the composition, the possibility of simple characterization of the resulting electrolyte and the use of a wide range of polymers. According to the *in situ*

polymerization technique, a liquid solution of a polymer precursor is injected into the electrode and then polymerized using thermal or photo initiators.[96] Polymer electrolytes obtained by polymerization *in situ* can provide an easy pathway for Li^+ ion transport in the electrodes and considerably reduce the interfacial resistance owing to good interfacial contact between the electrode and polymer electrolyte.[438] The precursor used in *in situ* polymerization is mainly composed of a monomer with a functional group, a lithium salt, a solvent and an initiator.

5.1. Polymer/salt-type electrolytes

Below we consider some examples of formation of electrolytes based on PEO and PVDF, which appreciably differ in the transport mechanism, because in the case of PEO, coordination of lithium ions by the polymer oxygen is possible, while the transport in PVDF occurs through clusters formed by ions and polar groups.

Currently, PEO is the most widely used electrolyte because of its low cost and ease of production.[439] The chain flexibility endows the polymer with good mechanical properties. Owing to the high concentration of oxygen atoms, PEO readily dissolves lithium salts, thus forming partially crystallized systems. However, below the melting temperature (~65 °C),[440] the PEO crystallinity is usually 75–80%, which accounts for the low ionic conductivity of PEO-based electrolytes, ranging from 10^{-8} to 10^{-7} S cm^{-1} at room temperature.[441,442] The ion transport in PEO-based amorphous polymer electrolytes or in their amorphous parts is determined by segmental mobility of the macromolecules and polymer relaxation. The movement of cations induced by an electric field is accompanied by ion desolvation/solvation by the polymer polar groups.[443] A correlation between the ionic conductivity of electrolytes and the polymer viscosity made it possible to propose a transport model, which implies a correlation between the hopping of cations and rotation of polymer chain segments, resulting in a change in the cation environment. The cation transport in amorphous PEO is shown schematically in Fig. 10. The ion hopping from one position to another occurs in concert with the chain rearrangement, resulting in optimization of the cation environment in the new position.

According to literature data, PEO-based polymer electrolytes are incompatible with high-voltage cathodes based on layered oxides such as $LiCoO_2$ or NCM due to the oxidative degradation of PEO in contact with these cathode materials.[444,445] According to Yang *et al*.,[446] this is due to decomposition and oxidation of the terminal –OH and/or C–O–C ether groups in PEO to give C=O and COOH(Li) groups at >4 V voltage (*vs*. Li/Li^+). Huang *et al*.[447] found that the oxidation of PEO-based electrolytes may be accompanied by the release of protons, which results in the uncontrolled structural degradation of layered NCM at the cathode/electrolyte interface. The interfacial structural degradation of NCM leads to a rapid increase in cell impedance and a sharp decrease in the capacity. Homann *et al*.[448] that the failure of cells based on PEO and layered cathode materials is due to the short circuit caused by the formation of lithium dendritic layers with a large surface area rather than to PEO oxidation on contact with layered oxides. Later this assumption was confirmed by other authors.[449] It was shown that the use of high-molecular-weight PEO (MW = 8×10^6 g mol^{-1}),[449] which has a higher viscosity and, hence, supresses the penetration of dendrites, or increase in the salt concentration in the electrolyte[450] substantially improves the cyclability of batteries by inhibiting the dendrite formation.

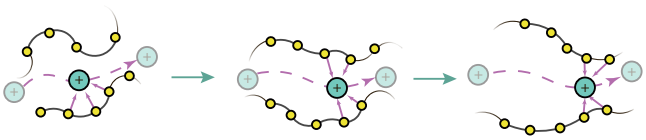

Figure 10. Schematic picture of lithium cation transport in the amorphous part of PEO.

The technology of lithium metal battery presented in 2011 is based particularly on PEO-based polymer electrolytes. This resulted in the manufacturing of more than 8000 electric vehicles. However, relatively low ionic conductivity of PEO-based materials below its melting point is the main obstacle to commercialization of these batteries on a larger scale.

One way of decreasing the PEO degree of crystallinity is copolymerization. In this case, structurally different moieties in the polymer prevent the regular packing of the polymer chains. The copolymerization of polar and nonpolar monomers affords phase-separated microdomains, in which the polar PEO domains are involved in the ion transport, while the nonpolar domains disrupt the packing and, hence, provide a decrease in the PEO degree of crystallinity. For example, various researchers investigated copolymerization of ethylene oxide with styrene-based monomers.[451–454] It was shown that inclusion of styrene molecules suppresses crystallization of ethylene oxide units and improves the mechanical properties of electrolytes. Butzelaar *et al*.[455] synthesized copolymers of ethylene oxide with vinyl ethers with different side chain lengths and grafting degrees. This approach decreased the degree of crystallinity of an electrolyte containing the LiTFSI salt from 98% to 39%. The maximum ionic conductivity (2.2×10^{-5} S cm^{-1} at 20 °C) was attained for a polymer with 50% grafting degree and [LiTFSI] : [EO] ratio of 1 : 20.

In the case of statistical copolymerization, the monomers are distributed randomly. St-Onge *et al*.[456] demonstrated that approximately 26 mol.% propylene oxide is sufficient for complete amorphization of the parent polymer (Fig. 11 *a*). The copolymer containing 10 mol.% propylene oxide and 18 wt.% LiTFSI had an ionic conductivity of 3×10^{-5} S cm^{-1} at room temperature (Fig. 11 *b*), while the all-solid-state LFP|Li battery had a capacity of 120 mAh g^{-1} at room temperature. Notably, the presence of statistical defects not only prevents crystallization, but also decreases the strength of the PEO–Li^+ coordination; as a result, the Li^+ transference number can increase from 0.21 characteristic of pure PEO to 0.58 for the polymer containing 10 mol.% propylene oxide.

The use of fluorine-containing PEO block copolymers not only improves the mechanical strength of the electrolyte, but also provides the formation of a LiF-containing SEI layer on the lithium anode surface,[457] which increases the battery lifetime. The use of poly(ethylene oxide)-co-(heptadecafluorodecyl methacrylate) block copolymer containing LiTFSI (ionic conductivity of 2.7×10^{-4} S cm^{-1} at 70 °C and lithium transference number of 0.41) as the electrolyte in the LFP|Li battery provided an initial capacity of 157 mAh g^{-1} and 95.8% capacity retention after 250 cycles.[457] The characteristics of highly stable batteries with electrolytes made of PEO-based copolymers are described in the literature[458,459] and are summarized in Table 4.

One more method to decrease the crystallinity and improve the electrochemical performance of PEO is to blend several polymers or fabricate continuous films by pore filling. Wang

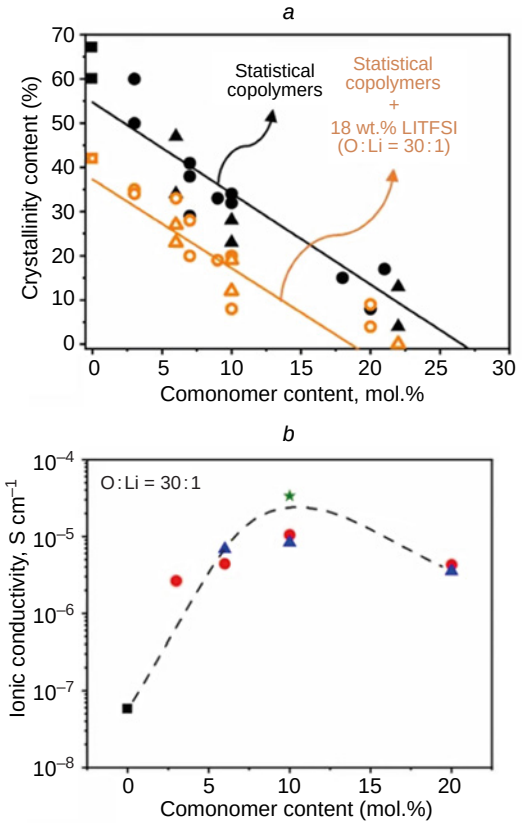

Figure 11. Degree of crystallinity (*a*) and ionic conductivity *vs.* the comonomer content in the statistical copolymerization (*b*). Reproduced in accordance with the Creative Commons Attribution 4.0 International License.[456]

et al.[463] showed that blending of polyamide containing an N-substituted pyrrolidone ring (IBD) with PEO+LiTFSI decreases the polymer crystallinity, which provides an increase in the ionic conductivity (Fig. 12*a*), electrochemical stability window from 4.25 V (for PEO+LiTFSI) to 4.80 V (Fig. 12*b*), and lithium transference number from 0.17 (for PEO+LiTFSI) to 0.43 owing to the presence of carbonyl groups. As a result 80.5% of the initial capacity was retained in the LFP|Li battery with the modified electrolyte after 580 cycles at 50 °C; meanwhile, in the cell with the PEO+LiTFSI electrolyte, the capacity retention was only ~10% even after 250 cycles (Fig. 12*c*).

Blending of PEO with poly(vinylpyrrolidone) and $LiNO_3$ resulted in the fabrication of highly conductive polymer electrolyte with a lithium transference number of 0.3 and an ionic conductivity reaching 1.1×10^{-3} S cm^{-1} at room temperature.[487] Gao *et al.*[460] obtained a composite electrolyte with a framework of poly(*m*-phenyleneisophthalamide) nanofibres filled with PEO and LiTFSI, which had an ionic conductivity of 2.9×10^{-4} S cm^{-1} at 30 °C. Wan *et al.*[488] reported a thin polyamide film (8.6 μm) filled with PEO+LiTFSI with an ionic conductivity of 2.3×10^{-4} S cm^{-1} at 30 °C.

Ionic liquids (ILs) have a good potential for the use in lithium batteries due to their low volatility and low flammability.[489–491] Polymeric ionic liquids (PILs) combine the flexibility of a polymer and the ionic conductivity of ILs.[467,490,492–494] The insertion of imidazolium ion-based PIL into PEO would decrease the PEO crystallinity and induce the microphase separation, responsible for fast ion transport.[464] The resulting electrolyte also shows a high transference number (0.63) and a wide electrochemical stability window (>5.0 V).

Polyvinyl difluoride is characterized by a higher dielectric constant, which promotes dissociation of lithium salts and

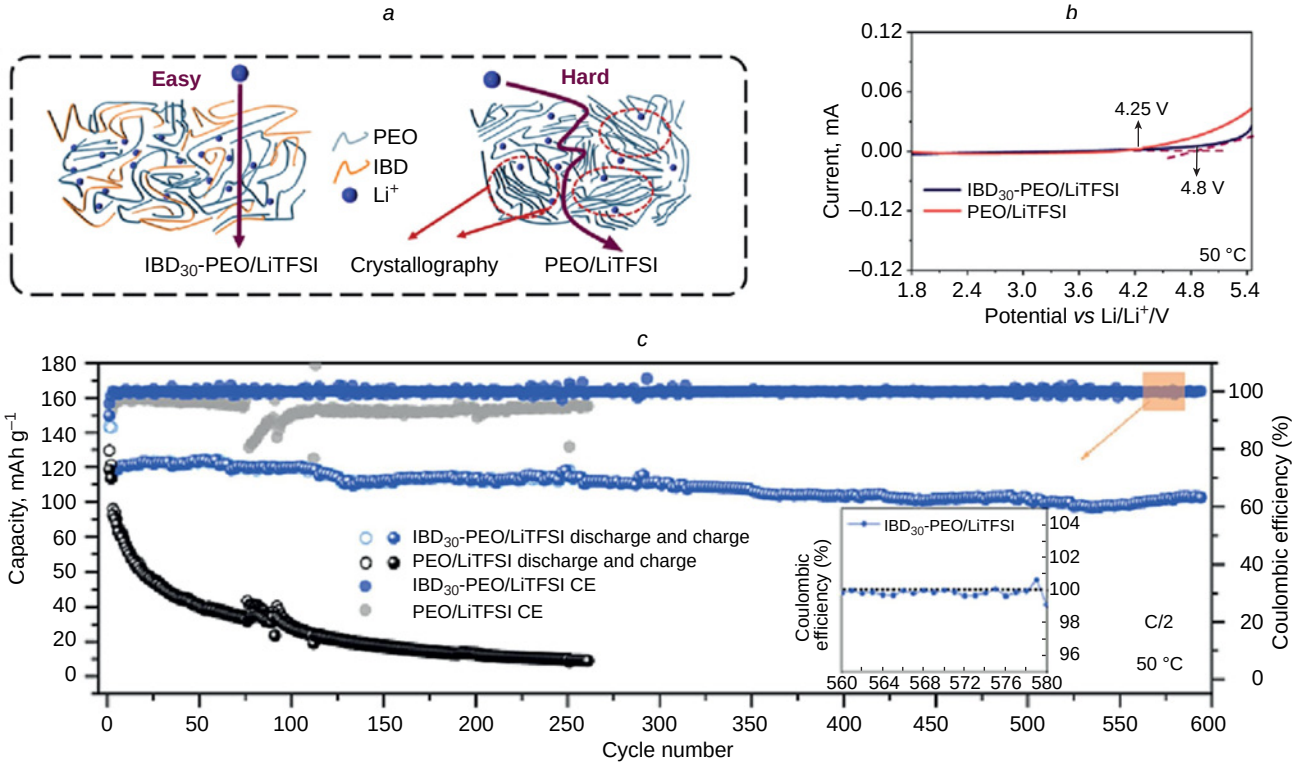

Figure 12. Scheme of ion transport (*a*), voltammetric curve (*b*) and capacity change during long-term cycling of LFP|Li batteries at 50 °C with polymer electrolytes based on polymer blends: (IBD+PEO+LiTFSI) and PEO+LiTFSI (*c*).[463] Reproduced with permission from Elsevier.

Table 4. Lithium ion conductivity, oxidative stability and lithium transference numbers for some polymer electrolytes and key characteristics of lithium metal batteries based on these electrolytes.

Polymer	Salt/plasticizer	Conductivity, S cm^{-1}/T (°C)	Oxidative stability, V	Lithium transference number	Cell cathode|anode	Cycling rate, temperature	Initial capacity, mAh g^{-1}	Number of cycles	Capacity retention (%)	Ref.
Polyphenyleneisophthalamide+PEO[a]	LiTFSI/–	2.9×10^{-4}/30 °C	5.4	–	LFP|Li	1C, RT	146.5	400	87.4	460
PEO block copolymer with polystyrene-based side chain	LiTFSI/–	1.6×10^{-5}/25 °C	4.75	0.13	NCM622|Li	0.1C, 60 °C	175	100	57	453
PEO–propylene oxide statistical copolymer	LiTFSI/–	3×10^{-5}/25 °C	–	0.58	LFP|Li	0.04C	120	–	–	456
PEO+porphyrin molecules modified with polyether chains	LiTFSI/–	5.7×10^{-4}/60 °C	5.15	0.2	LFP|Li	0.2C, 60 °C	158.2	120	97.1	461
PEO–heptadecafluorodecyl methacrylate block copolymer	LiTFSI/–	2.68×10^{-4}/70 °C	4.9	0.41	LFP|Li	0.2C, 60 °C	157.1	250	96.2	457
PEO-filled polyamide	LiTFSI/–	2.05×10^{-4}/30 °C	4.7	0.53	LFP|Li	1C, 60 °C	125	300	82	462
PEO+copolymer of itaconic acid, 1,4-butanediamine and 1,10-decanediamine	LiTFSI/–	4.26×10^{-4}/50 °C	4.8	0.43	LFP|Li	0.5C, 50 °C	124.4	580	80.5	463
Imidazolium-based polymerized ionic liquid (poly(ethylene glycol) monomethacrylate in PEO matrix	LiTFSI/–	2.2×10^{-4}/60 °C	5.0	0.63	LFP|Li	0.2C, 60 °C	160	50	63	464
Bilayer PVDF/polypropylene	$LiClO_4$/–	1.53×10^{-4}/RT	4.8	0.24	LFP|Li	0.3C, RT	134	180	97	465
Electrospun high-polarity β-phase multilayer structure, PVDF–HFP/PEO+LiTFSI/PVDF–HFP	LiTFSI/–	2.57×10^{-3}/80 °C	5.22	0.23	LFP|Li	1C, 80 °C	160	100	80	466
Cross-linked [$Vmim_1O_2$]TFSI in the PVDF–HFP matrix	LiTFSI/–	1.06×10^{-3}/25 °C	5.5	0.59	LFP|Li	0.1C, 25 °C	153.7	–	–	467
Poly(vinylidene fluoride-co-trifluoroethylene-co-chlorotrifluoroethylene)	LiTFSI/–	3.1×10^{-4}/25 °C	4.6	0.33	LFP|Li	0.5C, 25 °C	146.4	150	98.5	468
Poly(vinylidene fluoride-co-trifluoroethylene)	LiTFSI/–	4.48×10^{-4}/25 °C	4.5	0.455	NCM811|Li	1C, 25 °C	178	300	92.1	469
PEG-filled PVDF	LiTFSI/–	8×10^{-5}/30 °C	5.2	0.432	LFP|Li	1C, 60 °C	142.2	1000	86.4	470
Cross-linked polyurethane	LiTFSI/ succinonitrile	2.86×10^{-4}/RT	4.06	0.511	LFP|Li	0.5C, RT	134	700	92	471
β-Cyclodextrin-based triblock copolymer	$LiClO_4$/–	1.5×10^{-3}/100 °C	4.2	0.42	LFP|Li	0.1C, 60 °C	167	100	98	472
PVDF–HFP+sulfonated PVDF–HFP	–/–	2.84×10^{-4}/RT	<5.4	0.81	LFP|Li	0.2C, RT	147.9	200	89.1	473
Lithium 4-styrenesulfonyl(4-(trifluoro-methoxy)benzenesulfonyl)imide)+ polyethylene glycol	–/–	1.96×10^{-5}/30 °C	–	~0.9 (40 °C)	LFP|Li	0.1C, 80 °C	~155	100	64.5	474
PVDF+copolymer of vinyl ethylene carbonate and lithium 3-sulfonyl(trifluoro-methanesulfonyl)imide propyl methacrylate	–/succinonitrile	1.72×10^{-4}/RT	4.5	0.93	LFP|Li	0.5C, 25°C	160	400	≈99	475

Table 4 (continued).

Polymer	Salt/plasticizer	Conductivity, S cm^{-1}/T (°C)	Oxidative stability, V	Lithium transference number	Cell cathode|anode	Cycling rate, temperature	Initial capacity, mAh g^{-1}	Number of cycles	Capacity retention (%)	Ref.
Phosphorylated nanocellulose + hydroxypropyl methyl cellulose	$LiPF_6$/DMSO	2.0×10^{-3}/RT	4.5	0.56	LFP|Li	0.2C, RT	138.5	80	89	476
PVDF-HFP + branched acrylate	LiTFSI/DOL + DME + $[Py_{13}]$TFSI	9.5×10^{-4}/RT	5.0	0.25	LFP|Li	0.5C, RT	153.7	500	92.7	477
PVDF-HFP modified with polyethylene glycol and lithium montmorillonite	LiTFSI/fluoro-ethylene carbonate + PC	1.82×10^{-3}/25 °C	5.1	0.513	LFP|Li	1C, RT	136	1000	92	478
PVDF – HFP	$LiPF_6$/EC + DMC + $[Py_{14}]PF_6$	1.62×10^{-3}/RT	5.14	0.47	$LiNi_{0.5}Mn_{1.5}O_4$|Li	0.2C, RT	112	150	98.2	479
PVDF + copolymer of borate-containing poly(ethylene glycol) methyl methacrylate and 4-vinyl-1,3-dioxolan-2-one	LiTFSI/EC + PC	1.32×10^{-3}/30 °C	4.7	0.6	LFP|Li	0.2C, RT	143	150	96	480
Pentaerythritol tetraacrylate-graft-butyl methacrylate	$LiPF_6$/EC + DEC + EMC	1×10^{-3}/RT	5.2	0.41	NCM523|Li	2C, RT	108	100	63.9	481
PVDF + lithium poly(4-styrenesulfonyl-(benzenesulfonyl)imide)	–/EC + DMC	1.1×10^{-3}/RT	4.5	0.87	LFP|Li	0.1C, RT	148	–	–	482
Lithium (4-styrenesulfonyl)-(trifluoromethanesulfonyl)imide cross-linked with polyethylene glycol dimethacrylate	LiTFSI + $LiNO_3$/DOL + DME	2.74×10^{-5}/RT	4.7	0.622	LFP|Li	0.1C, RT	132.1	150	80	483
Copolymer of lithium (4-styrenesulfonyl)-(trifluoromethanesulfonyl)imide, pentaerythritol tetrakis(2-mercaptoacetate) and pentaerythritol tetraacrylate	–/EC + DMC	8.4×10^{-4}/RT	5.2	0.93	LFP|Li	1C, RT	133	400	83	484
Poly(ethylene-ran-butylene)-block-polystyrene functionalized with lithium benzenesulfonylimide	–/EC + DMA	6×10^{-4}/25 °C	4.1	0.72	LFP|Li	0.1C, RT	100	40	≈99	485
Nafion-212	–/EC + PC	1.9×10^{-4}/25 °C	6	0.8	LFP|Li	0.1C, RT	141	50	≈99	134
Aquivion-87	–/EC + DMA	1.08×10^{-3}/25 °C	–	0.69	LFP|Li	0.1C, RT	142	70	98.8	486

Note. $[Vmim_1O_2]$TFSI is 1-ethoxymethyl-3-vinylimidazolium bis(trifluoromethanesulfonyl)imide, DOL is dioxolane, $[Py_{13}]$TFSI is 1-methyl-1-propylpyrrolidinium bis(trifluoromethanesulfonyl)imide, $[Py_{14}]PF_6$ is 1-butyl-1-methylpyrridium hexafluorophosphate. [a] Mixture/solution.

provides a high concentration of charge carriers.[495] In addition, PVDF has other useful properties, including flexibility and mechanical strength, wide electrochemical stability window and thermal stability. Therefore, PVDF is a promising base for solid-state PEs attracting considerable attention of researchers. Solid electrolyte interface containing LiF can be formed at the interface between a PVDF-based electrolyte and lithium metal anode; this facilitates the interfacial ionic conductivity and improves the mechanical strength.[496]

Since PVDF is a non-coordinating polymer, unlike PEO, lithium salts do not interact directly with the backbone. The addition of a lithium salt to the polymer matrix gives rise to aggregates in which Li^+ is coordinated by electronegative atoms of salt anions. The salt clusters can form a percolation network where Li^+ moves along the channels formed by anions by hopping from one stable position to another (Fig. 13).[495,497] The conductivity of the PVDF+LiTFSI electrolyte amounts to 1.8×10^{-5} S cm^{-1} at room temperature.

The degree of crystallinity of PVDF is relatively high, being 65–78% at room temperature.[498] However, the introduction of other units can disrupt the ordered matrix structure, thus increasing the proportion of amorphous domains and ionic conductivity. The copolymer of PVDF with hexafluoropropylene (PVDF-HFP) is used most often. The CF_3 groups of the latter effectively reduce the degree of crystallinity.[496,499] Electrolytes based on this copolymer have high ionic conductivity and mechanical strength.[500] The high dielectric constant of the electrolyte based on poly(vinylidene fluoride-co-trifluoroethylene-co-chlorotrifluoroethylene) triblock copolymer containing LiTFSI, which was reported by Huang *et al.*,[468] provided an ionic conductivity of 3.1×10^{-4} S cm^{-1} at 25 °C. It was shown[469] that conformation of molecular chains also affects the ionic conductivity of electrolytes based on PVDF. The *trans*-planar conformation in which all fluorine atoms are located on one side and hydrogen atoms are on the other side is characterized by higher polarity, which provides higher ionic conductivity. Zeng *et al.*[469] produced an electrolyte with an ionic conductivity of 4.5×10^{-4} S cm^{-1} at 25 °C based on PVDF in this conformation by introducing 20–50 mol.% trifluoroethylene blocks. The NCM811|Li cells containing this copolymer retained 92% of the initial capacity after 300 cycles at 25 °C, while the capacity retention for similar cells based on pure PVDF electrolyte was only 20%.

One more promising approach for improving the polymer properties is to introduce functional groups chemically bound to the backbone. Mi *et al.*[501] obtained electrolytes based on lithium phenyl phosphate uniformly grafted to PVDF. The introduction of functional groups resulted in decreasing glass transition temperature and degree of crystallinity of the DMF-solvated electrolyte and in increasing ionic conductivity. The NCM811|Li cell demonstrated 71% capacity retention after 1550 cycles.

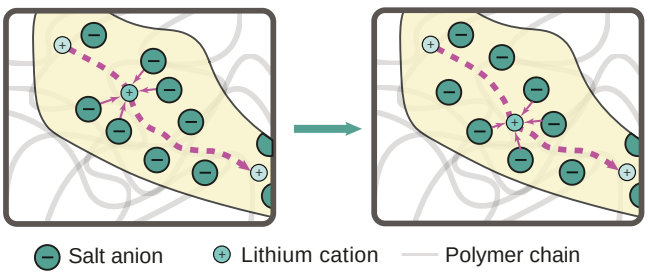

Figure 13. Scheme of the lithium cation transport through the channels formed by anions in PVDF.

Polymer blending is a much simpler approach to enhancing the transport properties of PVDF-based electrolytes. Li *et al.*[502] fabricated an electrolyte by mixing solutions of polyvinylpyrrolidone, polyether imide, PVDF and LiTFSI. The microporous material formed after the solvent evaporation had an ionic conductivity of 5.1×10^{-4} S cm^{-1} and Li transference number of 0.51 at room temperature. The LFP|Li batteries with this electrolyte demonstrated a discharge capacity of 122 mAh g^{-1} by the 100th cycle with a Coulombic efficiency of more than 99%. Wang *et al.*[470] filled the pores in a PVDF film with polyethylene glycol (PEG) with subsequent thermal curing. The ionic conductivities achieved for this structure were 8×10^{-5} S cm^{-1} at 30 °C and 2.9×10^{-4} S cm^{-1} at 60 °C. The LFP|Li battery retained 86.4% of the capacity after 1000 cycles.[470] The electrolyte based on PILs, PVDF-HFP and LiTFSI showed an ionic conductivity of 1×10^{-3} S cm^{-1} at 25 °C and a wide electrochemical stability window (5.5 V).[467] The LFP|Li cell demonstrated a reversible capacity of 154 mAh g^{-1} at a 0.1C rate, and the Li|Li symmetrical cell maintained a stable voltage for 1000 h.[467]

It is worth noting that most PVDF-based solid electrolytes are prepared by polymer solution casting using DMF as a solvent. After drying, electrolytes may contain residual amounts of DMF, which causes their high ionic conductivity.[503,504] Zhang *et al.*[503] demonstrated that the solvation effect, caused by the minor residual amount of bound DMF, plays the key role in the ion transport, interfacial stability and the cell performance. Since the residual DMF occurs in the electrolytes in the bound state rather than as the free solvent, the ionic conductivity can be implemented *via* the transport of lithium ions between the sites of interaction of bound DMF molecules with PVDF chains. The control of the solvation effect in electrolytes can significantly improve the cycling characteristics of PVDF-based solid-state lithium metal batteries at 25 °C (for example, more than 1000 cycles with capacity retention of more than 94%).[503,504]

The polymer plasticization with solvents giving gel-polymer electrolytes (GPEs) is the most efficient way to obtain polymer electrolytes with a high conductivity at relatively low temperatures (see Fig. 6).[96] If the polymer is non-conductive, GPE includes the polymer, liquid low-molecular-weight plasticizer and a lithium salt. Lithium transport in GPE is accomplished *via* Li^+ diffusion through the liquid phase encapsulated in the polymer matrix.

Apart from meeting the general requirements to electrolyte components, such as inertness to all electrochemical cell components and thermal stability, plasticizers should have a high dielectric constant that would facilitate dissociation of the salt[505] and low viscosity to provide ion transport.[506] The plasticizers used most often are aprotic solvents that contain carbonyl (>C=O), nitrile (–C≡N), sulfonyl (>S=O) or ether (–O–) groups, which ensure the dissolution of salts.[507] Various cyclic and linear organic carbonates that are used in liquid electrolytes are most popular. Examples of matrices frequently employed to obtain polymer/salt gel-polymer electrolytes are PAN, PVDF-HFP, PMMA, polyvinyl chloride and so on.[444,506–508] In many cases, in GPEs, PVDF is considered only as a polymer framework which absorbs a large amount of a liquid electrolyte.[509] Saikia and Kumar[510] showed that GPEs based on PVDF-HFP plasticized with a mixture of propylene carbonate (PC) and diethyl carbonate (DEC) has a higher ionic conductivity (7.5×10^{-3} S cm^{-1}) than PVDF (1.3×10^{-3} S cm^{-1}). A sandwich structure containing a PVDF-coated polypropylene

separator was plasticized with DMF. The system demonstrated an ionic conductivity of 1.5×10^{-4} S cm^{-1} at room temperature and prevented the dendrite formation.[465] The specific capacity of the LFP|Li cell was 134 mAh g^{-1} with 97% capacity retention after 180 cycles.

In addition to the fact that the introduction of low-molecular-weight solvents is detrimental to safety, batteries with carbonate solvents are susceptible to fast decrease in the capacity at temperatures above 55 °C due to decomposition of the electrolyte.[511] At temperatures above 69 °C, SEI formed by a carbonate electrolyte decomposes and induces exothermic reactions that result in battery failure.[512] A possible solution to the battery safety problem is to add fire retardants to the electrolyte. In particular, of interest are fire-resistant phosphate compositions[513–515] and organic fluorinated solvents, which are compatible with high-voltage cathodes, have low flammability and provide durable SEI with high conductivity.[516,517] For example, GPEs based on poly(ethylene glycol dimethyl acrylate) plasticized with triethyl-2-fluoro-2-phosphonoacetate had an ionic conductivity of 3.15×10^{-3} S cm^{-1} and lithium transference number of 0.47, and the LFP|Li battery showed 94.6% capacity retention after 700 cycles.[515] Deng *et al*.[516] reported polymer electrolytes with a high ionic conductivity of 4.4×10^{-3} S cm^{-1} at 30 °C and a wide electrochemical stability window of 5.6 V using the PVDF matrix plasticized with solutions of LiFSI, $LiPF_6$ or lithium difluoro(oxalato)borate in a mixture of ethylene carbonate (EC), fluoroethylene carbonate and methyl 2,2,2-trifluoroethyl carbonate. The LFP|Li batteries with this electrolyte showed 81% capacity retention after 1000 cycles.[516] The key characteristics of various polymer electrolytes and batteries based on them are summarized in Table'4.

5.2. Solid polymer electrolytes based on cation exchange membranes

According to the space–charge model proposed by Chazalviel and co-workers,[518] the application of direct current induces a cation concentration gradient in the electrolyte. The depletion of cations near the anode surface at high current density leads to accumulation of local spatial charge and formation of branched dendrites. The dendrite growth can be retarded by increasing the initial cation concentration and decreasing the concentration of mobile anions in the electrolyte, *e.g*., by using cation exchange membranes as electrolytes, so-called single-ion-conducting polymer electrolytes.[62,64,519,520] In cation exchange membranes, anions are covalently bound to the polymer matrix. These electrolytes possess only cationic conductivity and should be characterized by lithium transference numbers close to unity. In order to maximize cation mobility, functional groups are often arranged on the side chains of the polymer backbone. A great benefit of cation exchange membranes is the ability to provide their own lithium conductivity. It is of interest that the addition of lithium salts does not increase the conductivity.[521]

Among recent studies dealing with the development of single-ion-conducting electrolytes for ASSBs, most popular are cation exchange membranes containing sulfonic acid R–SO_3^- and bis(sulfonyl)imide R–$SO_2N^{(-)}SO_2$–X functional groups, which are analogues of the widely used LiTFSI. The bis(sulfonyl) imide groups can effectively delocalize negative charge[522–526] and decrease the dissociation energy with the release of Li^+ cations, thus promoting ion transport. The negative charge distribution in R–$SO_2N^{(-)}SO_2$–X can be further improved by introducing various electronegative or bulky groups such as –CF_3, –Ph or –$PhCF_3$.[482,527–529]

It was shown that PEO binds to functional groups of bis(trifluoromethanesulfonyl)imide thus giving a material with ion transport channels.[530] Mixtures with a high content of PEO (up to [O]/[Li^+] = 10) were fully amorphous and had ionic conductivity of 10^{-5} and 10^{-4} S cm^{-1} at 90 and 130 °C, respectively. An electrolyte based on a mixture of lithium poly(4-styrene sulfonyl(trifluoromethylsulfonyl)imide) with PEO showed an ionic conductivity of 9.5×10^{-6} S cm^{-1} at 70 °C.[531] The material cross-linked with α,ω-diaminopolyethylene glycol had an ionic conductivity of 2.0×10^{-5} S cm^{-1} at 30 °C and Li^+ transference number of 0.9.[474]

Zhang *et al*.[532] developed ionomers containing fluorinated aryl sulfonimide anions as side chains blended with PEO, which showed a conductivity of 10^{-4} S cm^{-1} and electrochemical oxidative stability (> 5.0 V). The best samples of these materials demonstrated ionic conductivity of up to 1.72×10^{-4} S cm^{-1} at room temperature.[475] The PVDF-HFP sulfonated copolymer mixed with non-sulfonated polymer exhibited an ionic conductivity of 2.8×10^{-4} S cm^{-1} at room temperature and a lithium transference number of 0.81.[473]

The introduction of low-molecular-weight plasticizers into cation exchange membranes may markedly increase the ionic conductivity. Zhong *et al*.[533] reported a polymer electrolyte containing a lithium [(4-styrenesulfonyl)(fluorosulfonyl)imide] copolymer solvated with a mixture of EC and dimethyl carbonate (DMC) in the PVDF matrix. The ionic conductivity of this electrolyte was 5.8×10^{-3} S cm^{-1} at 28 °C and the lithium transference number was 0.91. Another copolymer containing (4-styrenesulfonyl)(trifluoromethanesulfonyl)imide solvated with a mixture of EC and DMC showed an ionic conductivity of 8.4×10^{-4} S cm^{-1} at room temperature and a lithium transference number of 0.93.[484] The LFP|Li battery based on this copolymer retained 83% of the capacity after 400 cycles.

Owing to good transport properties and thermal and electrochemical stability, perfluorinated Nafion type sulfonated cationic membranes, in which the functional SO_3^- groups are bound to the perfluorinated polymer matrix, attract the greatest attention.[95,534] The solvation of these membranes with organic aprotic solvents provides high ionic conductivity, which can reach 10^{-4}–10^{-3} S cm^{-1} at room temperature (see Fig. 6). A few examples of using Nafion-type membranes in lithium-ion or lithium metal batteries have been reported in the literature.[95,535–543] For example, the ionic conductivity of Nafion-211 solvated with PC was 2.1×10^{-3} S cm^{-1} at 70 °C, while the discharge capacity of a lithium-sulfur battery was 895 mAh g^{-1} (in terms of sulfur) with 89% capacity retention after 100 cycles.[535] The membrane electrolyte obtained by casting a 20 wt.% dispersion of Nafion in water and in lower aliphatic alcohols solvated with an EC–PC mixture was characterized by an ionic conductivity of 3.6×10^{-4} S cm^{-1} at 20 °C and a discharge capacity of the LFP|Li cell of ≈80 mAh g^{-1} at a 0.05C rate.[536] The properties of these electrolytes are described in more detail in reviews.[95,432]

6. Composite electrolytes

The data given in the previous Sections indicate that inorganic electrolytes often do not have sufficiently high conductivity, or, as in the case of sulfides, they are not sufficiently stable. Furthermore, it is often difficult to make a tight barrier between a cathode and anode with such electrolytes. Conversely, in the case of polymer systems, it is easy to produce electrolytes, including those suitable for being used in flexible batteries, but they often have insufficient strength and do not completely

prevent the formation of lithium dendrites. In addition, to achieve high conductivity, they are often plasticized with solvents, which preserves the possibility of evaporation upon depressurization or fire if temperature conditions are violated. Therefore, there is an opinion that the most promising approach is to fabricate composite electrolytes (CEs) that would combine the benefits of both types of materials and decrease risks during application in real devices. Composite electrolytes are usually made of a polymer, an inorganic filler and, often, a solvent and/or a lithium salt. The ionic conductivity of CEs largely depends on the interaction between the listed components.[544–546] To attain the optimal results, it is necessary to understand why properties of polymer electrolytes are improved when inorganic fillers are introduced into them. The fillers not only increase the mechanical strength of the polymer matrix, but also act as a sort of plasticizers, which prevent the polymer crystallization and increase the ionic conductivity of the electrolyte.[547,548] In addition, the use of dopants that have their own lithium conductivity (so-called active fillers) can provide an increase in the concentration of charge carriers and improvement of battery performance. However, an increase in the concentration of charge carriers can also be achieved with an inert filler as a result of surface sorption processes that increase the concentration of defects. An increase in the lithium transference numbers, together with increase in the composite strength and generation of steric hindrances for the transport of much larger anions reduce the risk of dendrite penetration (Fig. 14) and substantially increase the battery safety.

According to the existing views, the transport of lithium ions proceeds *via* polar regions of the polymer matrix and is facilitated by the segmental mobility of polymer chain fragments in amorphous domains.[549,550] The inorganic electrolyte prevents an ordered packing of the polymer and decreases the degree of crystallinity. According to some authors, the interaction of the filler with the polymer increases the redox stability of the electrolyte, thus expanding the electrochemical stability window.[551]

To be competitive with commercial liquid electrolytes, CEs should be thin (not more than 30 μm thick) and ensure fast transport of lithium ions.[549,552] A combination of a lithium metal anode with a cathode operating at relatively high potentials (⩾4 V *vs*. Li^+/Li) provides high energy density, which, of course, attracts the attention of many researchers. However, new, rather serious limitations appear simultaneously due to the need to ensure the electrolyte stability at both high and low potentials.[553]

In addition, the use of both inorganic electrolytes and CEs with higher ceramic contents is often faced with an additional problem related to the poor contact between the electrolyte and the electrodes. A poor contact, which is conventionally called point-to-point contact, generates a significant interfacial resistance and non-uniform distribution of local current density, which induces the growth of dendrites. The change in the electrode volume during cycling leads to accumulation of structural stresses, which further deteriorates the ion transport at the electrolyte/electrode interface.[554] This complications can be overcome by switching to composite electrolytes with high plasticity.[555–558] The foregoing gives reasons to believe that composite electrolytes with a relatively high ionic conductivity, electrochemical stability and mechanical strength have a huge potential for the design of next-generation ASSBs

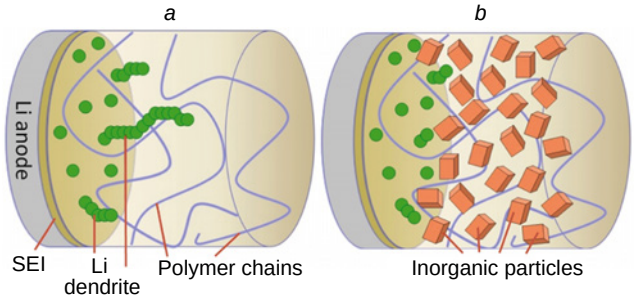

Figure 14. Scheme of dendrite penetration in a polymer (*a*) and composite (*b*) electrolytes.

6.1. Composite electrolytes with inert fillers

The inorganic fillers used in composite electrolytes can be classified into inert and active ones depending on the presence of lithium conductivity. Among inert fillers, note a number of oxides such as Al_2O_3, SiO_2, ZrO_2, *etc*., while active fillers are most often represented by materials described among inorganic electrolytes.[549,559,560] In the materials with high concentration of active fillers, the polymer matrix provides enhancement of mechanical properties, and lithium diffusion can proceed *via* the network formed by the inorganic electrolyte and can be fast enough without addition of lithium salts.[561–563]

Inert fillers may increase the strength and thermal stability of the polymer matrix. In addition, while acting as rigid barriers or cross-linking agents, they can increase the free volume in the polymer matrix *via* increasing the segmental mobility and decreasing the degree of crystallinity.[564,565] It is often noted that some acidic fillers may adsorb anions and, hence, restrict their mobility and increase the lithium transference number.[549] Fillers with small particle size form multiple interfaces providing increasing concentration of charge carriers represented by lithium defects.[81,566]

It was shown[567] that the introduction of silica into PMMA+LiTFSI electrolyte resulted in an increase in the polymer segmental mobility and in the conductivity (7.3×10^{-5} S cm^{-1} at 30 °C). The *in situ* synthesis of SiO_2 particles in PEO produced a high ionic conductivity (1.2×10^{-3} S cm^{-1} at 60 °C; 4.4×10^{-5} S cm^{-1} at 30 °C) and expanded the electrochemical stability window up to 5.5 V.[568] The addition of 1 wt.% TiO_2 into the PMMA+$LiClO_4$ system increased the ionic conductivity up to 3×10^{-4} S cm^{-1} at room temperature.[569] The introduction of 20 wt.% TiO_2 into lithium ion poly(ethylene citrate) increased the ionic conductivity of PMMA+$LiClO_4$ by two orders of magnitude up to 1.7×10^{-4} S cm^{-1}.[570] A higher conductivity can also be attained by adding zirconium oxide to polymer electrolytes. For example, the conductivity of the polypropylene oxide+LiTFSI and PVDF-HFP+$LiClO_4$ systems increased after the addition of ZrO_2 up to 9.6×10^{-4} and 2.5×10^{-3} S cm^{-1}, respectively. In addition, this ensured the electrochemical stability of CEs up to 5 V.[571,572]

As noted above, the lithium transference number is also an important parameter. The non-uniform lithium deposition and dendrite formation are caused by low lithium transference numbers, which are only 0.1–0.2 in most composite electrolytes.[573] An increase in the transference numbers leads to more uniform deposition of lithium and prevents dendrite formation.[574,575] They can be increased by using polymers with a high dielectric constant or a lithium salt with a low crystal lattice energy.[576] In addition, by introduction of functional groups, it is possible to enhance the binding of anions to the

matrix or the filler, or simply restrict the movement of a bulky anion due to the steric factor (see Fig. 14 *b*). For example, the lithium transference number can be increased to 0.8 by introducing boron nitride nanosheet structures,[577] negatively charged imidazole structures[578] or layered lithium montmorillonite[579] into the polymer to suppress the transport of anions.

An efficient approach is modification of polymer electrolytes with zeolites possessing high surface area, which is involved in the generation of defects that contribute to lithium ion transport. Indeed, modification of the PEO+LiTFSI system with SSZ-13 and YNa zeolites increased the ionic conductivity to 5.3×10^{-2} and 1.7×10^{-2} S cm^{-1} at 70 and 60 °C, respectively, with simultaneous increase in the lithium transference numbers to ≈0.85; ASSBs based on these electrolytes showed a high stability.[580,581] Meanwhile, it is noteworthy that the use of metal-organic frameworks (MOFs) with an equally high surface area provided a much more modest conductivity,[582] probably indicating an important role of the nature of the surface of such materials. A comparison of properties of composite electrolytes filled with various inert and active particles is given in Table 5.

6.2. Composite electrolytes with active fillers

Materials of this class appear to be of most interest in terms of the diversity of lithium ion transport pathways. If the filler particles form a one-, two- or three-dimensional framework, cations can move due to migration of charge carriers (vacancies or interstitials) from one particle to another. Conversely, if the polymer predominates in the material, then lithium transport activated by the polymer segmental mobility prevails.[625] On the other hand, defect formation processes at the interfaces and the interfacial migration between the fillers and the polymer can play an important role. The ion transport mechanisms in composite electrolytes are described in quite a few publications.[86,150,549,550,626,627] Meanwhile, it is obvious that nature and energy of the bond between lithium and the anion are rather similar in such fillers and in ion salts generating charge carriers in polymer electrolytes. This markedly decreases the efficiency of defect formation processes due to sorption phenomena at the interface between the inorganic and polymer phases.[81] However, this does not eliminate the significance of using such composites to improve the transport processes across the interfaces by filling the gaps between the hard ceramic particles and improving the wettability of interfaces and the contact between the active filler particles.

As an intermediate approach between inert and active fillers, consider the tight composite electrolyte with $MoSe_2$ nanosheets in PVDF containing a LiFSI solution in DMF, which was reported by Wu *et al*.[628] The reaction of $MoSe_2$ with lithium metal gives rise to the Li_2Se interlayer, possessing a reasonably good conductivity, at the interface, thus increasing the battery performance. The material demonstrates an ionic conductivity of 6.4×10^{-4} S cm^{-1} and electrochemical stability window of up to 4.7 V. The NCM811|Li battery based on this electrolyte showed a high performance.

According to Marchiori *et al*.,[629] the addition of lithium salts alone is able to decrease the polymer stability to oxidation. Cathodes such as $LiCoO_2$ and NCM have high specific surface area and exhibit an even more pronounced catalytic activity in redox reactions owing to transition metal ions or conducting carbon, which accelerates the electrolyte degradation.[630,631] The introduction of inorganic electrolytes may restrict the direct contact of polymers with a lithium metal anode or a high-voltage cathode. However, according to some authors, inorganic particles can also contribute to polymer stabilization due to the acid–base interactions leading to electron density redistribution.[632–634]

Wang *et al*.[635] reported composite electrolytes based on a liquid crystalline polymer in combination with ILs and Li salts ($LiBF_4$ and LiFSI). The resulting electrolytes had a conductivity of up to 2.1×10^{-3} S cm^{-1} at 25 °C, lithium transference numbers of <0.6 and electrochemical stability window of 5.6 V. In the authors' opinion, the high conductivity was caused by the presence of a nano-sized conductive network.

Garnet type materials are among the most demanded fillers[636] (see Table 5). The composite membranes based on the PEO matrix containing 52 wt.% $Li_7La_3Zr_2O_{12}$ had an ionic conductivity of 4.4×10^{-4} S cm^{-1} at 55 °C, while retaining high flexibility inherent in the polymer matrix.[637] UV cross-linked PEO containing tetraethylene glycol dimethyl ether, LiTFSI and LLZO showed an ionic conductivity of more than 10^{-4} S cm^{-1} and lithium transference number of more than 0.5 at 20 °C. The LFP|Li cell with this electrolyte retained a high capacity after 400 cycles.[638] An electrolyte based on PEO and graphene oxide containing LiTFSI also had a conductivity of more than 10^{-4} S cm^{-1} at 55 °C. The LFP|Li cell retained a capacity of 139 mAh g^{-1} with Coulombic efficiency of approximately 93.6% after 100 cycles.[626]

The composite electrolyte based on PEO+$LiClO_4$ and $Li_{6.4}La_3Zr_{1.4}Ta_{0.6}O_{12}$ demonstrated a lithium ion conductivity of 4.8×10^{-4} S cm^{-1} at 60 °C.[639] Composite electrolytes based on PVDF and PEG dimethyl ether filled with $Li_7La_3Zr_2O_{12}$ had an ionic conductivity of 4.7×10^{-4} S cm^{-1} at 60 °C and an electrochemical stability window of 4.5 V.[640] The NCM622|Li ASSB based on this material demonstrated a capacity of 156 mAh g^{-1} at a 0.1C rate. Huo *et al*.[641] investigated the characteristics of composite electrolytes containing $Li_{6.4}La_3Zr_{1.4}Ta_{0.6}O_{12}$ over a wide range of filler concentrations ranging from 'ceramic-in-polymer' to 'polymer-in-ceramic'. The highest conductivity was 1.6×10^{-4} S cm^{-1} at 30 °C, while the LFP|Li battery provided a specific capacity of 99 mAh g^{-1} with 82.4% capacity retention after 200 cycles.

Some authors also pay considerable attention to the orientation of filler particles in the composite. In terms of the percolation theory, the presence of continuous networks or even one-dimensional structures should provide certain advantages for the conductivity An electrolyte with oriented one-dimensional $Li_{0.35}La_{0.55}TiO_3$ structure in the PEO+LiTFSI matrix[613] demonstrated an ionic conductivity of 1.3×10^{-4} S cm^{-1}. The ordered $Li_{0.33}La_{0.557}TiO_3$ nanowires showed an ionic conductivity of 6.0×10^{-5} S cm^{-1} at 30 °C, which was an order of magnitude higher than the conductivity of the material with randomly oriented nanowires.[642] As other examples of formation of ordered filler structures with increased conductivity in polymer matrices, mention may be made of one-dimensional LLZO garnet structures in PEO (1.8×10^{-4} S cm^{-1})[643] and anodic aluminium oxide with PEO-filled channels (5.8×10^{-4} S cm^{-1}).[644]

Considerable attention is also paid to composite electrolytes incorporating NASICON type particles (see Table 5). For example, Wang *et al*.[645] fabricated a flexible electrolyte based on PEO+PEG with $Li_{1.5}Al_{0.5}Ge_{1.5}(PO_4)_3$ particles forming one-dimensional channels for fast diffusion of lithium ions. The conductivity of the material reached 1.7×10^{-4} S cm^{-1} at 25 °C. An ASSB based on this material with an LFP cathode showed a more than 93% capacity retention after 300 cycles. Zhai *et al*.[646] also investigated one-dimensionally oriented structures of

Table 5. Comparison of properties of composite electrolytes doped with inert and active filler particles.

Polymer + salt	Dopant	Conductivity, S cm^{-1}/*T*, °C	Stability, V	Li transference numbers	Cell cathode|anode	Cycling rate, temperature	Initial capacity, mAh g^{-1}	Number of cycles	Capacity retention (%)	Ref.
PEO + LiTFSI	Al_2O_3	9.6×10^{-4}/25	5	0.43	CNT@S|Li	0.1C, 60 °C	1415	120	45.2	583
PPC + LiTFSI	SiO_2	8.5×10^{-4}/60	4.8	0.86	LFP|Li	1C, 60 °C	103	200	76	584
PPC + LiTFSI	TiO_2	1.52×10^{-4}/25	4.6	–	LFP|Li	0.3C, RT	140	100	63.3	585
PPC + LiTFSI	TiO_2 nanorods	1.2×10^{-4}/25	4.6	–	LFP|Li	0.3C, RT	162	100	93	585
PVDF–HFP + $LiClO_4$	ZrO_2	2.5×10^{-3}/25	5	0.57	–	–	–	–	–	572
PVDF–HFP + $LiPF_6$	ZrO_2	3.6×10^{-3}/25	5	0.41	$LiCoO_2$|Li	2C, RT	126.4	150	85.2	586
PEO + LiTFSI	CeO_2	1.1×10^{-3}/60	–	0.47	LFP|Li	0.1C, 60 °C	167	280	91	587
PEO + LiTFSI	MnO_2	1.95×10^{-5}/30	–	0.378	LFP|Li	0.5C, 60 °C	110	300	86.7	588
PEO + LiTFSI	$BaTiO_3$	1.5×10^{-5}/25	>4.5	0.197	LFP|Li	0.1C, 80 °C	140.7	50	97.8	589
PEO + LiTFSI	$Mg_2B_2O_5$	1.5×10^{-4}/40	4.75	0.44	LFP|Li	1C, 50 °C	117	230	≈100	590
PEO + LiTFSI	$Al_2Si_2O_5(OH)_4$	1.1×10^{-4}/25	6.35	0.4	S|Li	0.1C, 25 °C	747	100	87	591
PEO + LiTFSI	ZIF-8 (MOF)	2.2×10^{-5}/30	~5	0.36	LFP|Li	0.5C, 60 °C	130.6	350	85	592
PEO+ LiFSI	MIL-53(Al) (MOF)	3.4×10^{-3}/120	5.1	0.343	LFP|Li	5C, 120 °C	136.4	300	94.7	593
PEO + LiTFSI	UiO-66 (MOF)	1.3×10^{-4}/30	4.5	0.26	LFP|Li	0.5C, 60 °C	151	100	95	594
PEO + LiTFSI	SSZ-13(MOF)	1.7×10^{-2}/60	4.65	0.84	LFP|Li	0.1C, 60 °C	156.6	100	95.2	580
PAN + $LiClO_4$	Graphene oxide	4×10^{-4}/30	4.3	0.42	LFP|Li	0.2C, 60 °C	166	50	99.6	595
PEO + LiTFSI	Halloysite NT	9.2×10^{-5}/25	5.14	0.46	LFP|Li	0.3C, 25 °C	~158	300	≈82	596
PAN + $LiClO_4$	$Li_7La_3Zr_2O_{12}$	1.3×10^{-4}/30	5	0.3	–	–	–	–	–	597
PEO + LiTFSI	$Li_7La_3Zr_2O_{12}$	2.4×10^{-4}/25	6	–	LFP|Li	0.5C, 60 °C	163	70	97.4	598
PEO + LiTFSI	$Li_7La_3Zr_2O_{12}$	9×10^{-5}/25	5.5	0.27	LFP|Li	0.2C, 30 °C	157.6	50	≈100	599
PMMA + $LiClO_4$	$Li_{6.4}La_3Zr_2Al_{0.2}O_{12}$	1.5×10^{-4}/30	4.7	0.47	LFP|Li	1C, RT	151.8	200	95.2	600
PMMA + $LiClO_4$	$Li_{6.4}La_3Zr_2Al_{0.2}O_{12}$	1.2×10^{-4}/30	6	–	$LiNi_{0.8}Co_{0.15}Al_{0.05}O_2$|Li	0.2C, RT	213	14	≈82	601
PEO + $LiClO_4$	$Li_{6.25}Al_{0.25}La_3Zr_2O_{12}$	3.0×10^{-4}/24	5	–	NCM424|Li	0.1C, 70 °C	122	100	≈80	602
PMMA + $LiClO_4$	$Li_{6.75}La_3Zr_{1.75}Nb_{0.25}O_{12}$	2.2×10^{-5}/25	4.67	0.45	$LiCoO_2$|Li	0.2C, 60 °C	134.6	80	92.3	603
PEO + LiTFSI	$Li_{6.75}La_3Zr_{1.75}Ta_{0.25}O_{12}$	1.1×10^{-5}/25	5.5	0.58	LFP|Li	0.1C, 60 °C	150	100	87	604
PPC + LiTFSI	$Li_{6.75}La_3Zr_{1.75}Ta_{0.25}O_{12}$	5.2×10^{-4}/20	4.6	0.75	LFP|Li	1C, 20 °C	~127	200	95	605
PEO + LiTFSI	$Li_{1.5}Al_{0.5}Ge_{1.5}(PO_4)_3$	1.25×10^{-4}/25	>3.8	–	LFP|Li	0.5C, 60 °C	145.8	300	92	606
PEO + LiTFSI	$Li_{1.5}Al_{0.5}Ge_{1.5}(PO_4)_3$	1.7×10^{-4}/20	5	–	LFP|Li	0.1C, 80 °C	160	–	–	607
PPO + LiTFSI	$Li_{1.5}Al_{0.5}Ge_{1.5}(PO_4)_3$	3.5×10^{-4}/25	4.8	0.83	NCM622|Li	0.3C, RT	175	230	80	608
PEO + LiTFSI	$Li_{1.3}Al_{0.3}Ti_{1.7}(PO_4)_3$	7.5×10^{-4}/60	5.1	–	LFP|Li	1C, 60 °C	122.1	200	80	609
PVDF–HFP + LiTFSI	$Li_{1.5}Al_{0.5}Ti_{1.5}(PO_4)_3$	2.3×10^{-4}/25	>4	–	LFP|Li	0.2C, RT	148	50	87.8	610
PVDF + LiTFSI	$Li_{1.3}Al_{0.3}Ti_{1.7}(PO_4)_3$, PMMA-coated	1.2×10^{-3}/25	4.8	0.85	NCM532|Li	0.5C, RT	131.8	150	91.2	611
PEO + LiTFSI	$Li_{0.35}La_{0.55}TiO_3$	8.8×10^{-5}/25	5.1	–	–	–	–	–	–	612
PEO + LiTFSI	$Li_{0.33}La_{0.557}TiO_3$	1.3×10^{-4}/25	>3.8	0.55	LFP|Li	1C, 60 °C	144.6	100	96	613

Table 5 (continued).

Polymer + salt	Dopant	Conductivity, S cm^{-1}/*T*, °C	Stability, V	Li transference numbers	Cell cathode|anode	Cycling rate, temperature	Initial capacity, mAh g^{-1}	Number of cycles	Capacity retention (%)	Ref.
PEO + LiTFSI	$Li_{0.33}La_{0.557}TiO_3$	1.6×10^{-3}/25	4.7	0.48	LFP|Li	2C, 60 °C	135	300	79	614
PEO + LiTFSI	$Li_{0.33}La_{0.557}TiO_3$	2.4×10^{-4}/25	5	–	–	–	–	–	–	615
Poly(glycidyl methacrylate)	Li_3PS_4	1.8×10^{-4}/25	4.8	–	–	–	–	–	–	616
PVDF–HFP + LiTFSI	Li_7PS_6	1.1×10^{-4}/25	>4	–	LFP|Li	0.2C, RT	160	150	72	617
PEO + (3-chloropropyl) trimethoxysilane + LiTFSI on a nylon mesh	$Li_{10}GeP_2S_{12}$	2.4×10^{-4}/25	4.7	0.43	$LiNbO_3$-coated NCM622|Li	0.1C, RT	142.4	100	≈80	618
PVDF + LiTFSI	$78Li_2S–22P_2S_5$	5.9×10^{-4}/25	>3	–	Si@C|Li alloy with In	0.176 mA cm^{-2}, RT	778	100	93.2	619
PVDF + LiTFSI	$3Li_2S$-P_2S_5	3.4×10^{-4}/25	>3.8	0.44	LFP|Li	0.05 mA cm^{-2}, RT	153	150	99.5	620
PEO + $LiClO_4$	$Li_6PS_5Cl + SiO_2$	3×10^{-3}/25	>4.2	–	NCM721|Li alloy with In	1C, 60 °C	134.3	1000	74	621
PEO	Li_6PS_5Cl	~0.3×0^{-4}/25	>4	–	NCM811|Li	0.05C, 30 °C	75.6	200	91	622
Poly(vinylidene fluoride-co-trifluoroethylene)	Li_6PS_5Cl	1.2×10^{-3}/25	5	0.99	$LiNbO_3$-coated NCM622|Li alloy with In	1 мА · см$^{-2}$, RT	108	1000	92	563
PEO + LiTFSI	Li_6PS_5Cl	1.1×10^{-3}/25	4.9	–	Al_2O_3-coated NCM532|Li	0.05C, 25 °C	135.8	200	81.6	623
PEO +LiTFSI	$Li_{10}SnP_2S_{12}$	1.7×10^{-4}/50	5	0.38	S@C|Li	0.5C, 60 °C	562	150	92.2	624

Note. CNT are carbon nanotubes.

$Li_{1+x}Al_xTi_{2-x}(PO_4)_3$ in PEO+PEG with 5.2×10^{-5} S cm^{-1} conductivity.

Ding and co-workers[647] found that a layer of the PEO+LiTFSI coating can effectively prevent the side reactions between $Li_{1.5}Al_{0.5}Ge_{1.5}(PO_4)_3$ and Li anode. This electrolyte was stable at potentials of up to 5.12 V. The assembled $LiMn_{0.8}Fe_{0.2}PO_4$|Li cell with this electrolyte had a discharge capacity of 161 mAh g^{-1} and a good cyclability at 50 °C.

The composite electrolytes based on sulfides have received a lot of research attention in recent years. The high conductivity in combination with enhanced plasticity inherent in sulfides, in comparison with oxide systems, make them very attractive for the fabrication of composites with various polymers. Whiteley *et al*.[648] developed a membrane composed of 77 wt.% $78Li_2S-22P_2S_5$ with a self-reducing polymer matrix, the ionic conductivity of which was 10^{-4} S cm^{-1} at room temperature. Similar membranes with an even higher sulfide content (80–97 wt.%) were reported by Zhang *et al*.[619] The composites containing PEO and PVDF polymers with addition of lithium salts provided an ionic conductivity of 2×10^{-4}–4×10^{-4} S cm^{-1} at room temperature, while after the addition of lithium salts, the conductivity increased to 4×10^{-4}–7×10^{-4} S cm^{-1}. The PEO-based electrolytes containing 1 wt.% $Li_{10}GeP_2S_{12}$ had the highest ionic conductivity of 1.2×10^{-3} S cm^{-1} at 80 °C and a wide electrochemical stability window of up to 5.7 V.[649]

Electrolytes based on Li_6PS_5Cl and poly(vinylidene fluoride-co-trifluoroethylene) obtained by electrospinning and hot-pressing had an ionic conductivity of 1.2×10^{-3} S cm^{-1}, while ASSBs based on them with the NCM811 cathode retained 71% capacity after 20 000 cycles.[563] A PEO+LiTFSI-based electrolyte filled with $Li_{3.25}Ge_{0.25}P_{0.75}S_4$ had an ionic conductivity of 4.2×10^{-4} S cm^{-1} and a lithium transference number of 0.87.[650] Meanwhile, it should be noted that the practical application of composites based on sulfides, which show conductivity and plasticity values outstanding for inorganic electrolytes (see Table 5), is currently limited by their low electrochemical and chemical stability, in particular, the tendency to oxidation and especially to hydrolysis in the presence of water vapour.

The advantages of composite electrolytes appear especially beneficial for lithium-sulfur batteries characterized by high energy density (500–600 W-h kg^{-1}). However, the shuttle effect of the soluble lithium polysulfides (Li_2Sn, $3<n<8$) formed during their operation leads to a decrease in the capacity and Coulombic efficiency.[651] Polymers such as PEO can solvate polysulfides[652] and deteriorate the interfacial contact;[653] however, inorganic fillers can reduce the contact of polysulfides with polymers and lead to higher transference numbers.[654,655]

While concluding the review of composite electrolytes, one more class of composites containing a pair of inorganic components and no polymer is worthy of note. More than half a century ago, the Liang's[656] unexpected discovery of the sharp increase in the ionic conductivity of rather ordinary solid electrolyte AgI in composites with highly dispersed oxides stimulated the interest of researchers in composite electrolytes. This increase was due to the adsorption of mobile ions on the oxide surface, resulting in a pronounced increase in the vacancy concentration in the silver sites and, hence, in an increase in the charge carrier concentration. The stream of research has shifted rather quickly to lithium electrolytes, which have much higher prospects for practical application.[81] It was especially important that the conductivity was reasonably high even at room temperature. In this regard, the significantly less common examples of composites with two inorganic phases deserve mention. Thus, the addition of only 2 wt.%Al_2O_3 increases the ionic conductivity of β-Li_3PS_4 to 2.3×10^{-4} S cm^{-1} and ensures stability against lithium metal up to 5 V.[411] The composite electrolyte consisting of $Li_7La_3Zr_2O_{12}$ and β-Li_3PS_4 had a conductivity of 5.4×10^{-4} S cm^{-1} at room temperature.[657] Notably, its conductivity was also much higher compared to the starting electrolytes.

A high ionic conductivity of $LiBH_4$, which increased by three orders of magnitude after the orthorhombic to hexagonal phase transition to reach 10^{-3} S cm^{-1} at 120 °C has been reported.[658,659] The ionic conductivity of the $LiBH_4$–LiI system reached 10^{-5} S cm^{-1} even at room temperature,[660] while that of the 2 Li_3PS_4–$LiBH_4$ glassy electrolyte was 1.6×10^{-3} S cm^{-1}, with the electrochemical stability window of the latter being up to 5 V (*vs*. Li^+/Li).[661]

7. Conclusion

The desire to increase the specific capacity of lithium-ion batteries persistently stimulates researchers to return to the use of lithium metal anodes, improve cathode materials and restrict the electrolyte and separator thickness. However, this increases the risks of lithium dendrite growth and penetration and deteriorates the battery safety. A solution to these problems can be provided by the design of all-solid-state lithium batteries, the key role in which is played by a solid electrolyte. Therefore, recent studies have been focused on the search for solid electrolytes capable of competing with liquid electrolytes in terms of ionic conductivity and, at the same time, ensuring a proper safety of the battery.

These studies are conducted along three interrelated directions, including the development of inorganic, polymer and composite electrolytes. Among inorganic electrolytes, most success was attained in the field of garnet type complex oxides, NASICON-structured complex phosphates and sulfide and halosulfide materials. The heterovalent substitution in the cation sublattice, which increases the concentration of charge carriers, vacancies or interstitials, still remains the most useful approach. The highest conductivity values have been currently achieved for sulfide materials, but their further advancement is limited by low electrochemical and chemical stability.

Polymer electrolytes are highly popular; they provide not only a high conductivity, but also plasticity, which is important for the design of prospective flexible devices. Among polymer electrolytes, two developing clusters can be distinguished, one using inert polymers with a dissolved lithium salt. The other, perhaps more interesting, cluster is related to the use of ion exchange membranes in the lithium form plasticized with organic solvents.

The studies devoted to the development of composite electrolytes containing a polymer electrolyte together with an inorganic filler appear to be the most promising. It is believed that this approach would give efficient electrolytes combining high conductivity and good mechanical properties. Composite electrolytes can also be divided into two extensive classes, first, those incorporating inert fillers that may improve mechanical and conductive properties of polymers. Electrolytes that incorporate active fillers possessing their own lithium conductivity appear even more promising. Of particular note is the development of systems incorporating percolation networks of active fillers and materials that improve the contact at the interface between the electrolyte and electrode materials. In addition, the use of composite electrolytes may help to solve the problem of the loss of ionic conductivity caused by phase

separation, for example, at low temperatures, which often occurs in polymer electrolytes plasticized with organic solvents.

Higher safety resulting from elimination of leakages of a liquid electrolyte, removal of restrictions on the decomposition potential, increase in the lithium transference numbers, prevention of uncontrolled metal deposition on the electrode surface and, as a consequence, increase in the cycling stability– all this makes solid electrolytes increasingly attractive.

Meanwhile, despite numerous studies and publications in this field, some fundamental issues remain unsolved; in particular, note the insufficiently high ionic conductivity of solid electrolytes in comparison with liquid ones and problems of electrolyte/electrode contact. Therefore, the design of the interface between solid electrolytes and lithium metal anode or cathode material is a challenging problem requiring further research and development of effective strategies.

This work was financially supported by the Russian Science Foundation, Grant No. 23-19-00642, https://rscf.ru/project/23-19-00642/.

8. List of abbreviations and symbols

ASSB — all-solid-state lithium metal battery,
CE — composite electrolyte,
DME — dimethoxyethane,
DMA — *N*,*N*-dimethylacetamide,
DMC — dimethyl carbonate,
DMF — *N*,*N*-dimethylformamide,
DOL — dioxolane,
EC — ethylene carbonate,
EMC — ethyl methyl carbonate
GPE — gel polymer electrolyte,
IL — ionic liquid,
LIB — lithium-ion batteries,
LiTFSI — lithium bis(trifluoromethanesulfonyl)imide,
LFP — $LiFePO_4$,
LLZO — $Li_7La_3Zr_2O_{12}$,
MOF — metal-organic frameworks,
NCM — $Li(Ni,Co,Mn)O_2$,
NCMXYZ — $Li(Ni_{0,x}Co_{0,y}Mn_{0,z})O_2$,
PAN — polyacrylonitrile,
PC — propylene carbonate,
PE — polymer electrolyte,
PEG — polyethylene glycol,
PEO — polyethylene oxide,
PIL — polymer ionic liquid,
PMMA — polymethyl methacrylate,
PPC — polypropylene carbonate,
PPO — polypropylene oxide,
PVDF — polyvinylidene fluoride,
PVDF-HFP — poly(vinylidene fluoride-co-hexafluoropropylene),
RT — room temperature,
SEI — solid electrolyte interface.

9. References

1. T.Kim, W.Song, D.-Y.Son, L.K.Ono, Y.Qi. *J. Mater. Chem. A*, **7**, 2942 (2019)
2. K.Sashmitha, M.U.Rani. *Polym. Bull.*, **80**, 89 (2023)
3. B.Dunn, H.Kamath, J.-M.Tarascon. *Science,* **334**, 928 (2011)
4. A.B.Yaroslavtsev, I.A.Stenina, T.L.Kulova, A.M.Skundin, A.V.Desyatov. In *Comprehensive Nanoscience and Technology*. (2nd Edn). (Elsevier, 2019). Vol. 5. P. 165
5. A.Varzi, K.Thanner, R.Scipioni, D.Di Lecce, J.Hassoun, S.Dörfler, H.Altheus, S.Kaskel, C.Prehal, S.A.Freunberger. *J. Power Sources*, **480**, 228803 (2020)
6. Y.Chen, Y.Kang, Y.Zhao, L.Wang, J.Liu, Y.Li, Z.Liang, X.He, X.Li, N.Tavajohi, B.Li. *J. Energy Chem.*, **59**, 83 (2021)
7. Y.Li, Y.Li, L.Zhang, H.Tao, Q.Li, J.Zhang, X.Yang. *J. Energy Chem.*, **77**, 123 (2023)
8. D.Karabelli, K.P.Birke, M.Weeber. *Batteries*, **7**, 18 (2021)
9. X.Xu, C.Carr, X.Chen, B.D.Myers, R.Huang, W.Yuan, S.Choi, D.Yi, C.Phatak, S.M.Haile. *Adv. Energy Mater.*, **11**, 2003309 (2021)
10. C.Zhu, T.Fuchs, S.A.L.Weber, F.H.Richter, G.Glasser, F.Weber, H.-J.Butt, J.Janek, R.Berger. *Nat. Commun.*, **14**, 1300 (2023)
11. Y.Nishi. *J. Power Sources*, **100**, 101 (2001)
12. K.M.Abraham. *ACS Energy Lett.*, **5**, 3544 (2020)
13. T.P.Nguyen, I.T.Kim. *Materials*, **16**, 6869 (2023)
14. I.A.Stenina, A.B.Yaroslavtsev. *Pure Appl. Chem.*, **89**, 1185 (2017)
15. P.-A.Le, V.D.Trung, P.L.Nguyen, T.V.Bac Phung, J.Natsuki, T.Natsuki. *RSC Adv.*, **13**, 28262 (2023)
16. I.A.Stenina, A.B.Yaroslavtsev. *Membr. Membr. Technol.*, **6**, 15 (2024)
17. S.Xia, X.Wu, Z.Zhang, Y.Cui, W.Liu. *Chem*, **5**, 753 (2019)
18. M.Je, D.-Y.Han, J.Ryu, S.Park. *Acc. Chem. Res.*, **56**, 2213 (2023)
19. J.Lee, G.Oh, H.-Y.Jung, J.-Y.Hwang. *Inorganics*, **11**, 182 (2023)
20. C.Wei, Y.Zhang, Y.Tian, L.Tan, Y.An, Y.Qian, B.Xi, S.Xiong, J.Feng, Y.Qian. *Energy Storage Mater.*, **38**, 157 (2021)
21. X.Rao, Y.Lou, S.Zhong, L.Wang, B.Li, Y.Xiao, W.Peng, X.Zhong, J.Huang. *J. Electroanal. Chem.*, **897**, 115499 (2021)
22. H.Liang, L.Wang, L.Sheng, H.Xu, Y.Song, X.He. *Electrochem. Energy Rev.*, **5**, 23 (2022)
23. E.Goikolea, V.Palomares, S.Wang, I.R.de Larramendi, X.Guo, G.Wang, T.Rojo. *Adv. Energy Mater.*, **10**, 1 (2020)
24. S.Ye, X.Chen, R.Zhang, Y.Jiang, F.Huang, H.Huang, Y.Yao, S.Jiao, X.Chen, Q.Zhang, Y.Yu. *Nano-Micro Lett.*, **14**, 187 (2022)
25. X.-B.Cheng, R.Zhang, C.-Z.Zhao, Q.Zhang. *Chem. Rev.*, **117**, 10403 (2017)
26. Z.Hou, J.Zhang, W.Wang, Q.Chen, B.Li, C.Li. *J. Energy Chem.*, **45**, 7 (2020)
27. C.Fang, B.Lu, G.Pawar, M.Zhang, D.Cheng, S.Chen, M.Ceja, J.-M.Doux, H.Musrock, M.Cai, B.Liaw, Y.S.Meng. *Nat. Energy*, **6**, 987 (2021)
28. G.Luo, H.Wu. *Nat. Energy*, **1**, 16001 (2016)
29. Y.He, X.Ren, Y.Xu, M.H.Engelhard, X.Li, J.Xiao, J.Liu, J.-G.Zhang, W.Xu, C.Wang. *Nat. Nanotechnol.*, **14**, 1042 (2019)
30. R.Pathak, Y.Zhou, Q.Qiao. *Appl. Sci.*, **10**, 4185 (2020)
31. K.Lin, X.Xu, X.Qin, S.Wang, C.Han, H.Geng, X.Li, F.Kang, G.Chen, B.Li. *Carbon*, **185**, 152 (2021)
32. Z.Yu, J.Zhou, X.Lv, C.Li, X.Liu, S.Yang, Y.Liu. *J. Alloys Compd.*, **925**, 166691 (2022)
33. Y.Chen, M.Li, Y.Liu, Y.Jie, W.Li, F.Huang, X.Li, Z.He, X.Ren, Y.Chen, X.Meng, T.Cheng, M.Gu, S.Jiao, R.Cao. *Nat. Commun.*, **14**, 2655 (2023)
34. H.Ye, Z.Zheng, H.Yao, S.Liu, T.Zuo, X.Wu, Y.Yin, N.Li, J.Gu, F.Cao, Y.Guo. *Angew. Chem., Int. Ed.*, **58**, 1094 (2019)
35. Y.Zhang, C.Wei, J.Sun, J.Jian, C.Jin, C.Lu, L.Peng, S.Li, M.H.Rümmeli, R.Yang. *Solid State Ionics*, **364**, 115636 (2021)
36. Z.Liu, S.Ha, Y.Liu, F.Wang, F.Tao, B.Xu, R.Yu, G.Wang, F.Ren, H.Li. *J. Mater. Sci. Technol.*, **133**, 165 (2023)
37. T.Xu, L.Hou, C.Yan, J.Hou, B.Tian, H.Yuan, D.Kong, H.Wang, X.Li, Y.Wang, G.Zhang. *Scr. Mater.*, **229**, 115352 (2023)
38. F.Zhao, X.Zhou, W.Deng, Z.Liu. *Nano Energy*, **62**, 55 (2019)
39. C.Xu, H.Wang, X.Liu, G.Liu, Z.Zhang, C.Wu, J.Li. *J. Power Sources*, **562**, 232778 (2023)

40. C.Yan, H.-R.Li, X.Chen, X.-Q.Zhang, X.-B.Cheng, R.Xu, J.-Q.Huang, Q.Zhang. *J. Am. Chem. Soc.*, **141**, 9422 (2019)
41. D.Chen, S.Huang, L.Zhong, S.Wang, M.Xiao, D.Han, Y.Meng. *Adv. Funct. Mater.*, **30**, (2020)
42. P.Zhai, Y.Wei, J.Xiao, W.Liu, J.Zuo, X.Gu, W.Yang, S.Cui, B.Li, S.Yang, Y.Gong. *Adv. Energy Mater.*, **10**, 1903339 (2020)
43. X.Zhang, C.Sun. *Phys. Chem. Chem. Phys.*, **24**, 19996 (2022)
44. X.Fan, X.Ji, L.Chen, J.Chen, T.Deng, F.Han, J.Yue, N.Piao, R.Wang, X.Zhou, X.Xiao, L.Chen, C.Wang. *Nat. Energy*, **4**, 882 (2019)
45. Y.Gao, T.Rojas, K.Wang, S.Liu, D.Wang, T.Chen, H.Wang, A.T.Ngo, D.Wang. *Nat. Energy*, **5**, 534 (2020)
46. P.Shi, X.Wang, X.Cheng, Y.Jiang. *Batteries*, **9**, 345 (2023)
47. T.Yang, C.Wang, W.Zhang, Y.Xia, H.Huang, Y.Gan, X.He, X.Xia, X.Tao, J.Zhang. *J. Energy Chem.*, **84**, 189 (2023)
48. J.Liu, T.Wang, J.Yu, S.Li, H.Ma, X.Liu. *Materials*, **16**, 2510 (2023)
49. F.Thomas, L.Mahdi, J.Lemaire, D.M.F.Santos. *Materials*, **17**, 239 (2024)
50. H.Wang, Z.Yu, X.Kong, S.C.Kim, D.T.Boyle, J.Qin, Z.Bao, Y.Cui. *Joule*, **6**, 588 (2022)
51. Y.Liu, C.Zhao, J.Du, X.Zhang, A.Chen, Q.Zhang. *Small*, **19**, 2205315 (2023)
52. Q.Wang, C.Zhao, J.Wang, Z.Yao, S.Wang, S.G.H.Kumar, S.Ganapathy, S.Eustace, X.Bai, B.Li, M.Wagemaker. *Nat. Commun.*, **14**, 440 (2023)
53. S.A.Novikova, D.Y.Voropaeva, A.B.Yaroslavtsev. *Inorg. Mater.*, **58**, 333 (2022)
54. P.Zhou, X.Zhang, Y.Xiang, K.Liu. *Nano Res.*, **16**, 8055 (2023)
55. K.Yoon, S.Lee, K.Oh, K.Kang. *Adv. Mater.*, **34**, 2104666 (2022)
56. D.V.Safronov, S.A.Novikova, A.M.Skundin, A.B.Yaroslavtsev. *Inorg. Mater.*, **48**, 57 (2012)
57. B.Ramasubramanian, S.Sundarrajan, V.Chellappan, M.V.Reddy, S.Ramakrishna, K.Zaghib. *Batteries*, **8**, 133 (2022)
58. S.-P.Chen, D.Lv, J.Chen, Y.-H.Zhang, F.-N.Shi. *Energy Fuels*, **36**, 1232 (2022)
59. R.Fang, Y.Liu, Y.Li, A.Manthiram, J.B.Goodenough. *Mater. Today*, **64**, 52 (2023)
60. L.Wang, J.Li, G.Lu, W.Li, Q.Tao, C.Shi, H.Jin, G.Chen, S.Wang. *Front. Mater.*, **7**, 111 (2020)
61. Q.Zhao, S.Stalin, C.-Z.Zhao, L.A.Archer. *Nat. Rev. Mater.*, **5**, 229 (2020)
62. D.Y.Voropaeva, E.Y.Safronova, S.A.Novikova, A.B.Yaroslavtsev. *Mendeleev Commun.*, **32**, 287 (2022)
63. J.Minkiewicz, G.M.Jones, S.Ghanizadeh, S.Bostanchi, T.J.Wasely, S.A.Yamini, V.Nekouie. *Open Ceram.*, **16**, 100497 (2023)
64. H.Zhang, C.Li, M.Piszcz, E.Coya, T.Rojo, L.M.Rodriguez-Martinez, M.Armand, Z.Zhou. *Chem. Soc. Rev.*, **46**, 797 (2017)
65. A.-G.Nguyen, C.-J.Park. *J. Membr. Sci.*, **675**, 121552 (2023)
66. H.Xu, H.Zhang, J.Ma, G.Xu, T.Dong, J.Chen, G.Cui. *ACS Energy Lett.*, **4**, 2871 (2019)
67. S.Kundu, A.Kraytsberg, Y.Ein-Eli. *J. Solid State Electrochem.*, **26**, 1809 (2022)
68. J.Schnell, T.Günther, T.Knoche, C.Vieider, L.Köhler, A.Just, M.Keller, S.Passerini, G.Reinhart. *J. Power Sources*, **382**, 160 (2018)
69. A.Kraytsberg, Y.Ein-Eli. *Energy Technol.*, **11**, 2201291 (2023)
70. P.Verma, P.Maire, P.Novák. *Electrochim. Acta*, **55**, 6332 (2010)
71. A.B.Yaroslavtsev. *Russ. Chem. Rev.*, **85**, 1255 (2016)
72. B.Ma, Q.Jiao, Y.Zhang, C.Lin, X.Zhang, H.Ma, S.Dai, G.Jia. *Ceram. Int.*, **46**, 24882 (2020)
73. D.Aili, Y.Gao, J.Han, Q.Li. *Solid State Ionics*, **306**, 13 (2017)
74. S.F.Parker, H.Cavaye, S.K.Callear. *Molecules*, **25**, 1271 (2020)
75. A.Yaroslavtsev. *Solid State Ionics*, **176**, 2935 (2005)
76. Y.Wang, Y.Wu, Z.Wang, L.Chen, H.Li, F.Wu. *J. Mater. Chem. A*, **10**, 4517 (2022)
77. H.Schmalzried. *Ber. Bunsenges. Phys. Chem.*, **68**, 608 (1964)
78. J.Maier. *Prog. Solid State Chem.*, **23**, 171 (1995)
79. J.Maier. *Solid State Ionics*, **131**, 13 (2000)
80. N.F.Uvarov, V.G.Ponomareva, G.V.Lavrova. *Russ. J. Electrochem.*, **46**, 722 (2010)
81. A.B.Yaroslavtsev. *Rus. J. Inorg. Chem.*, **45**, S249 (2000)
82. J.Maier. *Solid State Ionics*, **175**, 7 (2004)
83. J.Maier. *Phys. Chem. Chem. Phys.*, **11**, 3011 (2009)
84. C.R.Mariappan. *Appl. Phys. A*, **117**, 847 (2014)
85. D.H.Kothari, D.K.Kanchan. *Phys. B: Condens. Matter*, **627**, 413599 (2022)
86. I.Stenina, S.Novikova, D.Voropaeva, A.Yaroslavtsev. *Batteries*, **9**, 407 (2023)
87. N.Oueldna, N.Sabi, H.Ben youcef. *J. Energy Storage*, **86**, 111254 (2024)
88. M.Tatsumisago, A.Hayashi. *Int. J. Appl. Glas. Sci.*, **5**, 226 (2014)
89. V.Viallet, V.Seznec, A.Hayashi, M.Tatsumisago, A.Pradel. In *Springer Handbook of Glass*. (Springer, 2019). P. 1697
90. Z.Chen, T.Du, S.S.Sørensen, R.Christensen, Q.Zhang, L.R.Jensen, O.V.Magdysyuk, M.Diaz-Lopez, M.Bauchy, Y.Yue, M.M.Smedskjaer. *J. Power Sources*, **553**, 232302 (2023)
91. I.A.Stenina, A.B.Yaroslavtsev. *Membranes*, **11**, 198 (2021)
92. V.I.Volkov, N.A.Slesarenko, A.V.Chernyak, V.A.Zabrodin, D.V.Golubenko, V.A.Tverskoy, A.B.Yaroslavtsev. *Membr. Membr. Technol.*, **4**, 189 (2022)
93. N.Kononenko, V.Nikonenko, D.Grande, C.Larchet, L.Dammak, M.Fomenko, Y.Volfkovich. *Adv. Colloid Interface Sci.*, **246**, 196 (2017)
94. P.Fan, H.Liu, V.Marosz, N.T.Samuels, S.L.Suib, L.Sun, L.Liao. *Adv. Funct. Mater.*, **31**, 2101380 (2021)
95. O.V.Bushkova, E.A.Sanginov, S.D.Chernyuk, R.R.Kayumov, L.V.Shmygleva, Y.A.Dobrovolsky, A.B.Yaroslavtsev. *Membr. Membr. Technol.*, **4**, 433 (2022)
96. W.Chae, B.Kim, W.S.Ryoo, T.Earmme. *Polymers*, **15**, 803 (2023)
97. D.Y.Voropaeva, A.B.Yaroslavtsev. *Membr. Membr. Technol.*, **4**, 276 (2022)
98. Y.Inaguma, C.Liquan, M.Itoh, T.Nakamura, T.Uchida, H.Ikuta, M.Wakihara. *Solid State Commun.*, **86**, 689 (1993)
99. R.Jiménez, A.del Campo, M.L.Calzada, J.Sanz, S.D.Kobylianska, S.O.Solopan, A.G.Belous. *J. Electrochem. Soc.*, **163**, A1653 (2016)
100. T.Polczyk, W.Zając, M.Ziąbka, K.Świerczek. *J. Mater. Sci.*, **56**, 2435 (2021)
101. L.Porz, M.Scherer, Q.K.Muhammad, K.Higuchi, Y.Li, S.Koga, A.Nakamura, W.Rheinheimer, T.Frömling. *J. Am. Ceram. Soc.*, **105**, 7030 (2022)
102. Y.-Y.Lin, A.X.Bin Yong, W.J.Gustafson, C.N.Reedy, E.Ertekin, J.A.Krogstad, N.H.Perry. *Curr. Opin. Solid State Mater. Sci.*, **24**, 100875 (2020)
103. A.S.Bhalla, R.Guo, R.Roy. *Mater. Res. Innov.*, **4**, 3 (2000)
104. Y.Liu, P.He, H.Zhou. *Adv. Energy Mater.*, **8**, 1701602 (2018)
105. X.Gao, C.A.J.Fisher, T.Kimura, Y.H.Ikuhara, H.Moriwake, A.Kuwabara, H.Oki, T.Tojigamori, R.Huang, Y.Ikuhara. *Chem. Mater.*, **25**, 1607 (2013)
106. A.Okos, C.F.Ciobota, A.M.Motoc, R.-R.Piticescu. *Materials*, **16**, 7088 (2023)
107. X.Zhou, C.Gao, D.Wang, S.Peng, L.Huang, W.Yang, W.-H.Zhang, X.Gao. *J. Energy Chem.*, **73**, 354 (2022)
108. S.Kobayashi, D.Yokoe, Y.Fujiwara, K.Kawahara, Y.Ikuhara, A.Kuwabara. *Nano Lett.*, **22**, 5516 (2022)
109. K.Mitsuishi, T.Ohnishi, Y.Tanaka, K.Watanabe, I.Sakaguchi, N.Ishida, M.Takeguchi, T.Ohno, D.Fujita, K.Takada. *Appl. Phys. Lett.*, **101**, 073903 (2012)
110. Z.Zhang, Y.Shao, B.Lotsch, Y.-S.Hu, H.Li, J.Janek, L.F.Nazar, C.-W.Nan, J.Maier, M.Armand, L.Chen. *Energy Environ. Sci.*, **11**, 1945 (2018)

111. Y.Sun, P.Guan, Y.Liu, H.Xu, S.Li, D.Chu. *Crit. Rev. Solid State Mater. Sci.*, **44**, 265 (2019)
112. L.Xu, L.Zhang, Y.Hu, L.Luo. *Nano Energy*, **92**, 106758 (2022)
113. M.Ling, Y.Jiang, Y.Huang, Y.Zhou, X.Zhu. *J. Mater. Sci.*, **55**, 3750 (2020)
114. S.Yan, C.-H.Yim, V.Pankov, M.Bauer, E.Baranova, A.Weck, A.Merati, Y.Abu-Lebdeh. *Batteries*, **7**, 75 (2021)
115. K.Kimura, K.Wagatsuma, T.Tojo, R.Inada, Y.Sakurai. *Ceram. Int.*, **42**, 5546 (2016)
116. B.Huang, B.Xu, Y.Li, W.Zhou, Y.You, S.Zhong, C.-A.Wang, J.B.Goodenough. *ACS Appl. Mater. Interfaces*, **8**, 14552 (2016)
117. H.Xu, P.-H.Chien, J.Shi, Y.Li, N.Wu, Y.Liu, Y.-Y.Hu, J.B.Goodenough. *Proc. Natl. Acad. Sci.*, **116**, 18815 (2019)
118. S.-T.Ko, T.Lee, J.Qi, D.Zhang, W.-T.Peng, X.Wang, W.-C. Tsai, S.Sun, Z.Wang, W.J.Bowman, S.P.Ong, X.Pan, J.Luo. *Matter*, **6**, 2395 (2023)
119. H.T.T.Le, R.S.Kalubarme, D.T.Ngo, H.S.Jadhav, C.-J.Park. *J. Mater. Chem A*, **3**, 22421 (2015)
120. M.Jia, Z.Bi, C.Shi, N.Zhao, X.Guo. *ACS Appl. Mater. Interfaces*, **12**, 46231 (2020)
121. S.Yan, H.Al-Salih, C.-H.Yim, A.Merati, E.A.Baranova, A.Weck, Y.Abu-Lebdeh. *Front. Chem.*, **10**, 966274 (2022)
122. C.Zhao, L.Liu, X.Qi, Y.Lu, F.Wu, J.Zhao, Y.Yu, Y.Hu, L.Chen. *Adv. Energy Mater.*, **8**, 1703012 (2018)
123. G.Farrington, B.Dunn, J.Briant. *Solid State Ionics*, **3**–**4**, 405 (1981)
124. M.T.Chowdhury, R.Takekawa, Y.Iwai, N.Kuwata, J.Kawamura. *J. Chem. Phys.*, **140**, 124509 (2014)
125. K.Li, Y.Yang, X.Zhang, S.Liang. *J. Mater. Sci.*, **55**, 8435 (2020)
126. L.Zhu, A.V.Virkar. *Crystals*, **11**, 293 (2021)
127. H.-P.Hong. *Mater. Res. Bull.*, **13**, 117 (1978)
128. U.V.Alpen, M.F.Bell, W.Wichelhaus, K.Y.Cheung, G.J.Dudley. *Electrochim. Acta*, **23**, 1395 (1978)
129. J.Kuwano, A.R.West. *Mater. Res. Bull.*, **15**, 1661 (1980)
130. S.Woo, B.Kang. *J. Mater. Chem. A*, **10**, 23185 (2022)
131. Y.Zhao, L.L.Daemen. *J. Am. Chem. Soc.*, **134**, 15042 (2012)
132. W.Xia, Y.Zhao, F.Zhao, K.Adair, R.Zhao, S.Li, R.Zou, Y.Zhao, X.Sun. *Chem. Rev.*, **122**, 3763 (2022)
133. I.Stenina, A.Pyrkova, A.Yaroslavtsev. *Batteries*, **9**, 59 (2023)
134. D.Voropaeva, S.Novikova, I.Stenina, A.Yaroslavtsev. *Polymers*, **15**, 4340 (2023)
135. B.A.Fortuin, L.Meabe, S.R.Peña, Y.Zhang, L.Qiao, J.Etxabe, L.Garcia, H.Manzano, M.Armand, M.Martínez-Ibañez, J.Carrasco. *J. Phys. Chem. C*, **127**, 1955 (2023)
136. A.K.Sahu, K.S.K.Varadwaj, S.K.Nayak, S.Mohanty. *Nano Energy*, **122**, 109261 (2024)
137. M.H.Braga, J.A.Ferreira, V.Stockhausen, J.E.Oliveira, A.El-Azab. *J. Mater. Chem. A*, **2**, 5470 (2014)
138. M.H.Braga, A.J.Murchison, J.A.Ferreira, P.Singh, J.B.Goodenough. *Energy Environ. Sci.*, **9**, 948 (2016)
139. Y.Li, W.Zhou, S.Xin, S.Li, J.Zhu, X.Lü, Z.Cui, Q.Jia, J.Zhou, Y.Zhao, J.B.Goodenough. *Angew. Chem.*, **128**, 10119 (2016)
140. A.Sakuda, A.Hayashi, Y.Takigawa, K.Higashi, M.Tatsumisago. *J. Ceram. Soc. Jpn*, **121**, 946 (2013)
141. X.Lü, J.W.Howard, A.Chen, J.Zhu, S.Li, G.Wu, P.Dowden, H.Xu, Y.Zhao, Q.Jia. *Adv. Sci.*, **3**, 1500359 (2016)
142. B.E.Francisco, C.R.Stoldt, J.-C.M'Peko. *Chem. Mater.*, **26**, 4741 (2014)
143. I.A.Stenina, I.Y.Pinus, M.N.Kislitsyn, I.V.Arkhangel'skij, N.A.Zhuravlev, A.B.Yaroslavtsev. *Zh. Neorg. Khim.*, **50**, 906 (2005)
144. X.Lu, S.Wang, R.Xiao, S.Shi, H.Li, L.Chen. *Nano Energy*, **41**, 626 (2017)
145. H.R.Arjmandi, S.Grieshammer. *Phys. Chem. Chem. Phys.*, **21**, 24232 (2019)
146. W.Baur, J.Dygas, D.Whitmore, J.Faber. *Solid State Ionics*, **18**–**19**, 935 (1986)
147. I.Y.Pinus, I.V.Arkhangel'skii, N.A.Zhuravlev, A.B.Yaroslavtsev. *Russ. J. Inorg. Chem.*, **54**, 1173 (2009)
148. I.Y.Pinus, A.V.Khoroshilov, K.S.Gavrichev, V.P.Tarasov, A.B.Yaroslavtsev. *Solid State Ionics*, **212**, 112 (2012)
149. A.Martínez-Juárez, C.Pecharromán, J.E.Iglesias, J.M.Rojo. *J. Phys. Chem. B*, **102**, 372 (1998)
150. J.C.Bachman, S.Muy, A.Grimaud, H.-H.Chang, N.Pour, S.F.Lux, O.Paschos, F.Maglia, S.Lupart, P.Lamp, L.Giordano, Y.Shao-Horn. *Chem. Rev.*, **116**, 140 (2016)
151. K.Pramanik, K.Sau, P.P.Kumar. *J. Phys. Chem. C*, **124**, 4001 (2020)
152. K.Arbi, J.M.Rojo, J.Sanz. *J. Eur. Ceram. Soc.*, **27**, 4215 (2007)
153. A.Venkateswara Rao, V.Veeraiah, A.V.Prasada Rao, B.Kishore Babu, K.V.Kumar. *Ceram. Int.*, **40**, 13911 (2014)
154. E.A.Kurzina, I.A.Stenina, A.Dalvi, A.B.Yaroslavtsev. *Inorg. Mater.*, **57**, 1035 (2021)
155. R.DeWees, H.Wang. *ChemSusChem*, **12**, 3713 (2019)
156. N.Tolganbek, A.Mentbayeva, B.Uzakbaiuly, K.Kanamura, Z.Bakenov. *Mater. Today Proc.*, **25**, 97 (2020)
157. K.Yang, L.Chen, J.Ma, Y.He, F.Kang. *InfoMat*, **3**, 1195 (2021)
158. G.B.Kunshina, O.O.Shichalin, A.A.Belov, E.K.Papynov, I.V.Bocharova, O.B.Shcherbina. *Russ. J. Electrochem.*, **59**, 173 (2023))
159. P.Wu, W.Zhou, X.Su, J.Li, M.Su, X.Zhou, B.W.Sheldon, W.Lu. *Adv. Energy Mater.*, **13**, 2203440 (2023)
160. C.-E.Yu, D.H.Gregory, W.-R.Liu. *Surf. Coat. Technol.*, **481**, 130671 (2024)
161. J.Yin, H.Zhang, Z.Zeng, G.Xu, P.Guo, H.Jiang, J.Li, Y.Wang, S.Yu, H.Zhu. *J. Alloys Compd.*, **988**, 174346 (2024)
162. P.-Y.Yen, M.-L.Lee, D.H.Gregory, W.-R.Liu. *Ceram. Int.*, **46**, 20529 (2020)
163. C.Luo, M.Yi, Z.Cao, W.Hui, Y.Wang. *ACS Appl. Electron. Mater.*, **6**, 641 (2024)
164. A.Mashekova, Y.Baltash, M.Yegamkulov, I.Trussov, Z.Bakenov, A.Mukanova. *RSC Adv.*, **12**, 29595 (2022)
165. S.Stegmaier, K.Reuter, C.Scheurer. *Nanomaterials*, **12**, 2912 (2022)
166. N.Tolganbek, M.Sarsembina, A.Nurpeissova, K.Kanamura, Z.Bakenov, A.Mentbayeva. *Nanoscale Adv.*, **4**, 4606 (2022)
167. C.Huang, Z.Li, S.Duan, S.Xie, S.Yuan, S.Hou, G.Cao, H.Jin. *J. Power Sources*, **536**, 231491 (2022)
168. A.Xu, R.Wang, M.Yao, J.Cao, M.Li, C.Yang, F.Liu, J.Ma. *Nanomaterials*, **12**, 2082 (2022)
169. S.-F.Wang, D.Shieh, Y.-A.Ko, Y.-F.Hsu, M.-K.Wu. *Solid State Ionics*, **393**, 116174 (2023)
170. P.Zhang, M.Matsui, A.Hirano, Y.Takeda, O.Yamamoto, N.Imanishi. *Solid State Ionics*, **253**, 175 (2013)
171. P.Zhang, M.Matsui, Y.Takeda, O.Yamamoto, N.Imanishi. *Solid State Ionics*, **263**, 27 (2014)
172. M.Illbeigi, A.Fazlali, M.Kazazi, A.H.Mohammadi. *Solid State Ionics*, **289**, 180 (2016)
173. S.Yan, Q.Cui, C.Sun, J.Hao, X.Chu, H.Xie, S.Lin, X.Zhang. *J. Solid State Chem.*, **295**, 121949 (2021)
174. L.Shen, L.Wang, Z.Wang, C.Jin, L.Peng, X.Pan, J.Sun, R.Yang. *Solid State Ionics*, **339**, 114992 (2019)
175. C.Wang, P.-P.Lin, Y.Gong, Z.-G.Liu, T.-S.Lin, P.He. *J. Alloys Compd.*, **854**, 157143 (2021)
176. E.A.Il'ina, E.D.Lyalin, B.D.Antonov, A.A.Pankratov, E.G.Vovkotrub. *Ionics*, **26**, 3239 (2020)
177. M.Xue, W.Lu, S.Xue, C.Zhang. *J. Mater. Sci.*, **56**, 19614 (2021)
178. Y.Meesala, Y.-K.Liao, A.Jena, N.-H.Yang, W.K.Pang, S.-F.Hu, H.Chang, C.-E.Liu, S.-C.Liao, J.-M.Chen, X.Guo, R.-S.Liu. *J. Mater. Chem. A*, **7**, 8589 (2019)
179. Y.Zhang, D.Hu, J.Deng, F.Chen, Q.Shen, A.Li, L.Zhang, S.Dong. *J. Alloys Compd.*, **767**, 899 (2018)
180. Y.Li, Z.Cao, Z.Jiang, Y.Cao, J.Liu, L.Wang, G.Li. *Ionics*, **28**, 5321 (2022)
181. S.M.Alizadeh, I.Moghim, M.Golmohammad. *Solid State Ionics*, **397**, 116260 (2023)
182. Y.Luo, X.Li, Y.Zhang, L.Ge, H.Chen, L.Guo. *Electrochim. Acta*, **294**, 217 (2019)

183. L.Buannic, B.Orayech, J.-M.López Del Amo, J.Carrasco, N.A.Katcho, F.Aguesse, W.Manalastas, W.Zhang, J.Kilner, A.Llordés. *Chem. Mater.*, **29**, 1769 (2017)
184. S.Iikubo, K.Shimoyama, S.Kawano, M.Fujii, K.Yamamoto, M.Matsushita, T.Shinmei, Y.Higo, H.Ohtani. *AIP Adv.*, **8**, (2018)
185. F.Mizuno, A.Hayashi, K.Tadanaga, M.Tatsumisago. *Solid State Ionics*, **177**, 2721 (2006)
186. S.Wenzel, D.A.Weber, T.Leichtweiss, M.R.Busche, J.Sann, J.Janek. *Solid State Ionics*, **286**, 24 (2016)
187. N.Kamaya, K.Homma, Y.Yamakawa, M.Hirayama, R.Kanno, M.Yonemura, T.Kamiyama, Y.Kato, S.Hama, K.Kawamoto, A.Mitsui. *Nat. Mater.*, **10**, 682 (2011)
188. J.Yi, L.Chen, Y.Liu, H.Geng, L.-Z.Fan. *ACS Appl. Mater. Interfaces*, **11**, 36774 (2019)
189. J.M.Whiteley, J.H.Woo, E.Hu, K.-W.Nam, S.-H.Lee. *J. Electrochem. Soc.*, **161**, A1812 (2014)
190. P.Zhou, J.Wang, F.Cheng, F.Li, J.Chen. *Chem. Commun.*, **52**, 6091 (2016)
191. S.Boulineau, M.Courty, J.-M.Tarascon, V.Viallet. *Solid State Ionics*, **221**, 1 (2012)
192. S.Yubuchi, M.Uematsu, C.Hotehama, A.Sakuda, A.Hayashi, M.Tatsumisago. *J. Mater. Chem. A*, **7**, 558 (2019)
193. F.Sudreau, D.Petit, J.P.Boilot. *J. Solid State Chem.*, **83**, 78 (1989)
194. I.A.Stenina, I.Y.Pinus, A.I.Rebrov, A.B.Yaroslavtsev. *Solid State Ionics*, **175**, 445 (2004)
195. H.Xie, J.B.Goodenough, Y.Li. *J. Power Sources*, **196**, 7760 (2011)
196. S.Smith, T.Thompson, J.Sakamoto, J.L.Allen, D.R.Baker, J.Wolfenstine. *Solid State Ionics*, **300**, 38 (2017)
197. M.Harada, H.Takeda, S.Suzuki, K.Nakano, N.Tanibata, M.Nakayama, M.Karasuyama, I.Takeuchi. *J. Mater. Chem. A*, **8**, 15103 (2020)
198. Y.Lu, E.Hu, M.Yousaf, L.Ma, J.Wang, F.Wang, P.Lund. *Energy Fuels*, **36**, 15154 (2022)
199. X.Li, E.Hu, F.Wang, P.Lund, B.Zhu, J.Wang. *J. Mater. Chem. A*, **12**, 4796 (2024)
200. S.Terny, C.López, G.Narda, M.A.Frechero. *Ceram. Int.*, **48**, 31755 (2022)
201. G.B.Kunshina, I.V.Bocharova, E.P.Lokshin. *Inorg. Mater.*, **52**, 279 (2016)
202. G.B.Kunshina, I.V.Bocharova, V.I.Ivanenko. *Inorg. Mater. Appl. Res.*, **8**, 238 (2017)
203. M.A.Moshareva, S.A.Novikova. *Russ. J. Inorg. Chem.*, **63**, 319 (2018)
204. S.V.Pershina, E.A.Il'ina, K.V.Druzhinin, A.S.Farlenkov. *J. Non. Cryst. Solids*, **527**, 119708 (2020)
205. J.A.Dias, S.H.Santagneli, A.C.M.Rodrigues, N.V.Bôas, Y.Messaddeq. *J. Phys. Chem. C*, **127**, 6207 (2023)
206. A.Curcio, A.G.Sabato, M.Nuñez Eroles, J.C.Gonzalez-Rosillo, A.Morata, A.Tarancón, F.Ciucci. *ACS Appl. Energy Mater.*, **5**, 14466 (2022)
207. Y.Nikodimos, M.-C.Tsai, L.H.Abrha, H.H.Weldeyohannis, S.-F.Chiu, H.K.Bezabh, K.N.Shitaw, F.W.Fenta, S.-H.Wu, W.-N.Su, C.-C.Yang, B.J.Hwang. *J. Mater. Chem. A*, **8**, 11302 (2020)
208. S.Kaboli, G.Girard, W.Zhu, A.Gheorghe Nita, A.Vijh, C.George, M.L.Trudeau, A.Paolella. *Chem. Commun.*, **57**, 11076 (2021)
209. V.M.Zallocco, J.M.Freitas, N.Bocchi, A.C.M.Rodrigues. *Solid State Ionics*, **378**, 115888 (2022)
210. Z.Liu, S.Venkatachalam, H.Kirchhain, L.van Wüllen. *Solid State Ionics*, **295**, 32 (2016)
211. H.Gan, W.Zhu, L.Zhang, Y.Jia. *Electrochim. Acta*, **423**, 140567 (2022)
212. X.Xu, Z.Wen, X.Yang, L.Chen. *Mater. Res. Bull.*, **43**, 2334 (2008)
213. H.Zhu, A.Prasad, S.Doja, L.Bichler, J.Liu. *Nanomaterials*, **9**, 1086 (2019)
214. N.Hamao, Y.Yamaguchi, K.Hamamoto. *Materials*, **14**, 4737 (2021)
215. Z.Zhang, Z.Chen, H.Zhu, Y.Ji, J.Duan, H.Hu, M.Bai. *J. Alloys Compd.*, **979**, 173610 (2024)
216. H.Cai, T.Yu, D.Xie, B.Sun, J.Cheng, L.Li, X.Bao, H.Zhang. *J. Alloys Compd.*, **939**, 168702 (2023)
217. S.Valiyaveettil-SobhanRaj, P.Głuchowski, P.López-Aranguren, F.Aguesse, R.Sampathkumar, T.Thompson, C.Rojviriya, W.Manalastas Jr, M.Srinivasan, M.Casas-Cabanas. *Materialia*, **33**, 101999 (2024)
218. M.Rumpel, L.Appold, J.Baber, W.Stracke, A.Flegler, G.Sextl. *Mater. Adv.*, **3**, 8157 (2022)
219. V.A.Vizgalov, T.Nestler, L.A.Trusov, I.A.Bobrikov, O.I.Ivankov, M.V.Avdeev, M.Motylenko, E.Brendler, A.Vyalikh, D.C.Meyer, D.M.Itkis. *CrystEngComm*, **20**, 1375 (2018)
220. S.V.Pershina, A.A.Pankratov, E.G.Vovkotrub, B.D.Antonov. *Ionics*, **25**, 4713 (2019)
221. K.Kwatek, W.Ślubowska, C.Ruiz, I.Sobrados, J.Sanz, J.E.Garbarczyk, J.L.Nowiński. *J. Alloys Compd.*, **838**, 155623 (2020)
222. D.H.Kothari, D.K.Kanchan. *Phys. B: Condens. Matter*, **600**, 412489 (2021)
223. Y.Luo, H.Gao, X.Zhao. *Ceram. Int.*, **48**, 8387 (2022)
224. J.Kang, X.Guo, R.Gu, Y.Tang, H.Hao, Y.Lan, L.Jin, X.Wei. *J. Alloys Compd.*, **941**, 168857 (2023)
225. S.-P.Shen, G.Tang, H.-J.Li, L.Zhang, J.-C.Zheng, Y.Luo, J.-P.Yue, Y.Shi, Z.Chen. *Ceram. Int.*, **48**, 36961 (2022)
226. K.Kwatek, W.Ślubowska-Walkusz, J.L.Nowiński, A. Krawczyńska, I.Sobrados, V.Diez-Gomez, J.Sanz. *Ceram. Int.*, **50**, 12450 (2024)
227. J.Tang, L.Wang, C.Tian, C.Chen, T.Huang, L.Zeng, A.Yu. *ACS Appl. Mater. Interfaces*, **14**, 4170 (2022)
228. W.Zha, Y.Ruan, Z.Wen. *Chem. Eng. J.*, **429**, 132506 (2022)
229. S.Lee, S.Jung, S.Yang, J.-H.Lee, H.Shin, J.Kim, S.Park. *Appl. Surf. Sci.*, **586**, 152790 (2022)
230. N.Ci, L.Zhang, J.Li, D.Li, J.Cheng, Q.Sun, Z.Xi, Z.Xu, G.Zhao, L.Ci. *Carbon*, **187**, 13 (2022)
231. C.-F.Li, R.Murugangantham, W.-C.Hsu, M.Ihrig, C.-T.Hsieh, C.-C.Wang, W.-R.Liu. *J. Taiwan Inst. Chem. Eng.*, **144**, 104681 (2023)
232. D.Guan, X.Wang, L.Song, C.Miao, J.Li, X.Yuan, X.Ma, J.Xu. *Angew. Chem., Int. Ed.*, **63**, e202317949 (2024)
233. L.Zhai, K.Yang, F.Jiang, W.Liu, Z.Yan, J.Sun. *J. Energy Chem.*, **79**, 357 (2023)
234. Y.Shi, Y.Cai, J.Zhao, T.Wu, X.Xue, T.Lin, P.Lin, C.Wang, H.Peng. *Chem. Eng. J.*, **469**, 144090 (2023)
235. G.Lu, W.Liu, Z.Yang, Y.Wang, W.Zheng, R.Deng, R.Wang, L.Lu, C.Xu. *Adv. Funct. Mater.*, **33**, 2304407 (2023)
236. J.Jiang, Y.Ou, S.Lu, C.Shen, B.Li, X.Liu, Y.Jiang, B.Zhao, J.Zhang. *Energy Storage Mater.*, **50**, 810 (2022)
237. L.Chen, J.Zhang, R.Tong, J.Zhang, H.Wang, G.Shao, C.Wang. *Small*, **18**, 2106142 (2022)
238. B.Zhao, W.Ma, B.Li, X.Hu, S.Lu, X.Liu, Y.Jiang, J.Zhang. *Nano Energy*, **91**, 106643 (2022)
239. J.Leng, H.Liang, H.Wang, Z.Xiao, S.Wang, Z.Zhang, Z.Tang. *Nano Energy*, **101**, 107603 (2022)
240. S.Guo, T.Wu, Y.Sun, S.Zhang, B.Li, H.Zhang, M.Qi, X.Liu, A.Cao, L.Wan. *Adv. Funct. Mater.*, **32**, 2201498 (2022)
241. B.Liu, M.Du, B.Chen, Y.Zhong, J.Zhou, F.Ye, K.Liao, W.Zhou, C.Cao, R.Cai, Z.Shao. *Chem. Eng. J.*, **427**, 131001 (2022)
242. C.Cui, Q.Ye, C.Zeng, S.Wang, X.Xu, T.Zhai, H.Li. *Energy Storage Mater.*, **45**, 814 (2022)
243. J.Duan, W.Wu, A.M.Nolan, T.Wang, J.Wen, C.Hu, Y.Mo, W.Luo, Y.Huang. *Adv. Mater.*, **31**, 1807243 (2019)
244. Y.Niu, Z.Yu, Y.Zhou, J.Tang, M.Li, Z.Zhuang, Y.Yang, X.Huang, B.Tian. *Nano Res.*, **15**, 7180 (2022)
245. K.(Kelvin) Fu, Y.Gong, B.Liu, Y.Zhu, S.Xu, Y.Yao, W.Luo, C.Wang, S.D.Lacey, J.Dai, Y.Chen, Y.Mo, E.Wachsman, L.Hu. *Sci. Adv.*, **3**, e1601659 (2017)

246. X.Han, Y.Gong, K.Fu, X.He, G.T.Hitz, J.Dai, A.Pearse, B.Liu, H.Wang, G.Rubloff, Y.Mo, V.Thangadurai, E.D.Wachsman, L.Hu. *Nat. Mater.*, **16**, 572 (2017)
247. J.Yu, Q.Liu, X.Hu, S.Wang, J.Wu, B.Liang, C.Han, F.Kang, B.Li. *Energy Storage Mater.*, **46**, 68 (2022)
248. L.Pan, S.Sun, G.Yu, X.X.Liu, S.Feng, W.Zhang, M.Turgunov, Y.Wang, Z.Sun. *Chem. Eng. J.*, **449**, 137682 (2022)
249. L.Zhu, Y.Wang, Y.Wu, W.Feng, Z.Liu, W.Tang, X.Wang, Y.Xia. *Adv. Funct. Mater.*, **32**, 2201136 (2022)
250. Z.Yang, H.Yuan, C.Zhou, Y.Wu, W.Tang, S.Sang, H.Liu. *Chem. Eng. J.*, **392**, 123650 (2020)
251. Y.Jin, C.Liu, X.Zong, D.Li, M.Fu, S.Tan, Y.Xiong, J.Wei. *J. Power Sources*, **460**, 228125 (2020)
252. Y.Lin, K.Liu, M.Wu, C.Zhao, T.Zhao. *ACS Appl. Energy Mater.*, **3**, 5712 (2020)
253. X.Hao, Q.Zhao, S.Su, S.Zhang, J.Ma, L.Shen, Q.Yu, L.Zhao, Y.Liu, F.Kang, Y.He. *Adv. Energy Mater.*, **9**, 1901604 (2019)
254. Q.Cheng, A.C.A.Li, N.Li, S.Li, A.Zangiabadi, T.-D.Li, W.Huang, A.C.A.Li, T.Jin, Q.Song, W.Xu, N.Ni, H.Zhai, M.Dontigny, K.Zaghib, X.Chuan, D.Su, K.Yan, Y.Yang. *Joule*, **3**, 1510 (2019)
255. J.-Y.Liang, X.-X.Zeng, X.-D.Zhang, T.-T.Zuo, M.Yan, Y.-X.Yin, J.-L.Shi, X.-W.Wu, Y.-G.Guo, L.-J.Wan. *J. Am. Chem. Soc.*, **141**, 9165 (2019)
256. C.Wang, Q.Sun, Y.Liu, Y.Zhao, X.Li, X.Lin, M.N.Banis, M.Li, W.Li, K.R.Adair, D.Wang, J.Liang, R.Li, L.Zhang, R.Yang, S.Lu, X.Sun. *Nano Energy*, **48**, 35 (2018)
257. J.Zhang, S.Ming, Y.Ning, S.Zhen, Y.Jiang, Y.Liu, X.Wu, Y.Zhang, Z.Wang. *J. Power Sources*, **584**, 233625 (2023)
258. G.-L.Zhu, C.-Z.Zhao, H.Yuan, B.-C.Zhao, L.-P.Hou, X.-B.Cheng, H.-X.Nan, Y.Lu, J.Zhang, J.-Q.Huang, Q.-B.Liu, C.-X.He, Q.Zhang. *Energy Storage Mater.*, **31**, 267 (2020)
259. N.Ahmad, S.Sun, P.Yu, W.Yang. *Adv. Funct. Mater.*, **32**, 2201528 (2022)
260. J.Zhang, J.Lv, W.Lu, X.Li, Y.Liu, J.Lang, J.Liu, Z.Wang, M.Lu, H.Sun. *Chem. Eng. J.*, **487**, 150452 (2024)
261. Y.Chen, W.Li, C.Sun, J.Jin, Q.Wang, X.Chen, W.Zha, Z.Wen. *Adv. Energy Mater.*, **11**, 2002545 (2021)
262. V.Thangadurai, H.Kaack, W.J.F.Weppner. *J. Am. Ceram. Soc.*, **86**, 437 (2003)
263. R.Murugan, V.Thangadurai, W.Weppner. *Angew. Chem., Int. Ed.*, **46**, 7778 (2007)
264. J.Awaka, N.Kijima, H.Hayakawa, J.Akimoto. *J. Solid State Chem.*, **182**, 2046 (2009)
265. E.Il'ina. *Int. J. Mol. Sci.*, **24**, 12905 (2023)
266. J.Awaka, A.Takashima, K.Kataoka, N.Kijima, Y.Idemoto, J.Akimoto. *Chem. Lett.*, **40**, 60 (2011)
267. C.A.Geiger, E.Alekseev, B.Lazic, M.Fisch, T.Armbruster, R.Langner, M.Fechtelkord, N.Kim, T.Pettke, W.Weppner. *Inorg. Chem.*, **50**, 1089 (2011)
268. J.H.Ahn, S.-Y.Park, J.-M.Lee, Y.Park, J.-H.Lee. *J. Power Sources*, **254**, 287 (2014)
269. A.Karuthedath Parameswaran, S.Pazhaniswamy, L.Dekanovsky, N.Balakrishnan, C.S.Paneerselvam, M.V.Reddy, S.Adams, Z.Sofer. *J. Power Sources*, **565**, 232907 (2023)
270. L.J.Miara, W.D.Richards, Y.E.Wang, G.Ceder. *Chem. Mater.*, **27**, 4040 (2015)
271. T.Wang, X.Zhang, Z.Yao, J.Li, K.Zhu, J.Wang, K.Yan. *J. Electron. Mater.*, **49**, 4910 (2020)
272. S.Hu, Y.-F.Li, R.Yang, Z.Yang, L.Wang. *Ceram. Int.*, **44**, 6614 (2018)
273. Y.Jiang, X.Zhu, S.Qin, M.Ling, J.Zhu. *Solid State Ionics*, **300**, 73 (2017)
274. M.Kotobuki, M.Koishi. *J. Alloys Compd.*, **826**, 154213 (2020)
275. Y.Huang, Y.Huang, B.Liu, H.Cao, L.Zhao, A.Song, Y.Lin, M.Wang, X.Li, Z.Zhang. *Electrochim. Acta*, **286**, 242 (2018)
276. X.Wang, J.Liu, R.Yin, Y.Xu, Y.Cui, L.Zhao, X.Yu. *Mater. Lett.*, **231**, 43 (2018)
277. S.Ohta, T.Kobayashi, T.Asaoka. *J. Power Sources*, **196**, 3342 (2011)
278. T.Thompson, A.Sharafi, M.D.Johannes, A.Huq, J.L.Allen, J.Wolfenstine, J.Sakamoto. *Adv. Energy Mater.*, **5**, 1500096 (2015)
279. S.Ramakumar, C.Deviannapoorani, L.Dhivya, L.S.Shankar, R.Murugan. *Prog. Mater. Sci.*, **88**, 325 (2017)
280. Y.Zhang, J.Deng, D.Hu, F.Chen, Q.Shen, L.Zhang, S.Dong. *Electrochim. Acta*, **296**, 823 (2019)
281. E.A.Il'ina, E.D.Lyalin, B.D.Antonov, A.A.Pankratov. *Russ. J. Appl. Chem.*, **92**, 1657 (2019)
282. T.Zhang, T.D.Christopher, S.Huang, Y.Liu, W.Gao, T.Söhnel, P.Cao. *Ceram. Int.*, **45**, 20954 (2019)
283. Y.Gong, Z.-G.Liu, Y.-J.Jin, J.-H.Ouyang, L.Chen, Y.-J.Wang. *Ceram. Int.*, **45**, 18439 (2019)
284. E.Ilina, E.Lyalin, M.Vlasov, A.Kabanov, K.Okhotnikov, E.Sherstobitova, M.Zobel. *ACS Appl. Energy Mater.*, **5**, 2959 (2022)
285. S.Reis, R.Grosso, J.Kosctiuk, M.Franchetti, F.Oliveira, A.Souza, C.Gonin, H.Freitas, R.Monteiro, L.Parreira, M.Berton. *Batteries*, **9**, 137 (2023)
286. D.K.Schwanz, A.Villa, M.Balasubramanian, B.Helfrecht, E.E.Marinero. *AIP Adv.*, **10**, 035204 (2020)
287. X.Liang, S.Li, G.Yang, X.Wu, D.Huang, Y.Ning, J.Luo, Z.Fang. *Appl. Phys. A*, **128**, 4 (2022)
288. C.Deviannapoorani, L.Dhivya, S.Ramakumar, R.Murugan. *J. Power Sources*, **240**, 18 (2013)
289. Y.Li, Z.Wang, Y.Cao, F.Du, C.Chen, Z.Cui, X.Guo. *Electrochim. Acta*, **180**, 37 (2015)
290. Y.X.Gao, X.P.Wang, H.Lu, L.C.Zhang, L.Ma, Q.F.Fang. *Solid State Ionics*, **291**, 1 (2016)
291. Z.Xu, X.Hu, B.Fu, K.Khan, J.Wu, T.Li, H.Zhou, Z.Fang, M.Wu. *J. Mater.*, **9**, 651 (2023)
292. X.Tong, V.Thangadurai, E.D.Wachsman. *Inorg. Chem.*, **54**, 3600 (2015)
293. Y.Luo, Y.Zhang, Q.Zhang, Y.Zheng, H.Chen, L.Guo. *Ceram. Int.*, **45**, 17874 (2019)
294. J.Gai, E.Zhao, F.Ma, D.Sun, X.Ma, Y.Jin, Q.Wu, Y.Cui. *J. Eur. Ceram. Soc.*, **38**, 1673 (2018)
295. Q.Zhang, Y.Luo, S.Chen, J.Jiao, M.Shen, H.Chen, L.Guo. *J. Mater. Sci. Mater. Electron.*, **31**, 2650 (2020)
296. C.Wang, K.Fu, S.P.Kammampata, D.W.McOwen, A.J.Samson, L.Zhang, G.T.Hitz, A.M.Nolan, E.D.Wachsman, Y.Mo, V.Thangadurai, L.Hu. *Chem. Rev.*, **120**, 4257 (2020)
297. A.Wachter-Welzl, J.Kirowitz, R.Wagner, S.Smetaczek, G.C.Brunauer, M.Bonta, D.Rettenwander, S.Taibl, A.Limbeck, G.Amthauer, J.Fleig. *Solid State Ionics*, **319**, 203 (2018)
298. A.Castillo, T.Charpentier, O.Rapaud, N.Pradeilles, S.Yagoubi, E.Foy, M.Moskura, H.Khodja. *Ceram. Int.*, **44**, 18844 (2018)
299. M.R.Bonilla, F.A.García Daza, J.Carrasco, E.Akhmatskaya. *Acta Mater.*, **175**, 426 (2019)
300. L.Zhuang, X.Huang, Y.Lu, J.Tang, Y.Zhou, X.Ao, Y.Yang, B.Tian. *Ceram. Int.*, **47**, 22768 (2021)
301. M.Ashuri, M.Golmohammad, A.Soleimany Mehranjani, M.Faghihi Sani. *J. Mater. Sci. Mater. Electron.*, **32**, 6369 (2021)
302. D.Rettenwander, J.Langer, W.Schmidt, C.Arrer, K.J.Harris, V.Terskikh, G.R.Goward, M.Wilkening, G.Amthauer. *Chem. Mater.*, **27**, 3135 (2015)
303. R.Jalem, M.J.D.Rushton, W.Manalastas, M.Nakayama, T.Kasuga, J.A.Kilner, R.W.Grimes. *Chem. Mater.*, **27**, 2821 (2015)
304. Y.Matsuda, A.Sakaida, K.Sugimoto, D.Mori, Y.Takeda, O.Yamamoto, N.Imanishi. *Solid State Ionics*, **311**, 69 (2017)
305. S.Qin, X.Zhu, Y.Jiang, M.Ling, Z.Hu, J.Zhu. *Appl. Phys. Lett.*, **112**, (2018)
306. O.Sharifi, M.Golmohammad, M.Soozandeh, A.S.Mehranjani. *J. Solid State Electrochem.*, **27**, 2433 (2023)
307. C.Chen, Y.Sun, L.He, M.Kotobuki, E.Hanc, Y.Chen, K.Zeng, L.Lu. *ACS Appl. Energy Mater.*, **3**, 4708 (2020)
308. X.Huang, J.Su, Z.Song, T.Xiu, J.Jin, M.E.Badding, Z.Wen. *Ceram. Int.*, **47**, 2123 (2021)

309. R.Wagner, G.J.Redhammer, D.Rettenwander, A.Senyshyn, W.Schmidt, M.Wilkening, G.Amthauer. *Chem. Mater.*, **28**, 1861 (2016)
310. C.Fritsch, T.Zinkevich, S.Indris, M.Etter, V.Baran, T.Bergfeldt, M.Knapp, H.Ehrenberg, A.-L.Hansen. *RSC Adv.*, **11**, 30283 (2021)
311. D.Rettenwander, C.A.Geiger, M.Tribus, P.Tropper, R.Wagner, G.Tippelt, W.Lottermoser, G.Amthauer. *J. Solid State Chem.*, **230**, 266 (2015)
312. E.Hanc, W.Zając, J.Molenda. *Solid State Ionics*, **262**, 617 (2014)
313. C.Deviannapoorani, L.S.Shankar, S.Ramakumar, R.Murugan. *Ionics*, **22**, 1281 (2016)
314. M.Abdulai, K.B.Dermenci, S.Turan. *Ceram. Int.*, **47**, 17034 (2021)
315. Amardeep, S.Kobi, A.Mukhopadhyay. *Scr. Mater.*, **162**, 214 (2019)
316. R.H.Brugge, J.A.Kilner, A.Aguadero. *Solid State Ionics*, **337**, 154 (2019)
317. Y.Matsuda, Y.Itami, K.Hayamizu, T.Ishigaki, M.Matsui, Y.Takeda, O.Yamamoto, N.Imanishi. *RSC Adv.*, **6**, 78210 (2016)
318. A.sodhiya, R.Kumar, A.kumar Singh, S.Soni. *Appl. Phys. A*, **127**, 584 (2021)
319. E.Enkhbayar, J.Kim. *ACS Omega*, **7**, 47265 (2022)
320. T.Yang, Y.Li, W.Wu, Z.Cao, W.He, Y.Gao, J.Liu, G.Li. *Ceram. Int.*, **44**, 1538 (2018)
321. Y.Li, T.Yang, W.Wu, Z.Cao, W.He, Y.Gao, J.Liu, G.Li. *Ionics*, **24**, 3305 (2018)
322. J.Wu, Y.Lu, H.Wu, Q.Luo, Z.Bai, J.Li. *J. Solid State Electrochem.*, **27**, 2499 (2023)
323. X.Chen, T.Cao, M.Xue, H.Lv, B.Li, C.Zhang. *Solid State Ionics*, **314**, 92 (2018)
324. X.Liu, M.Gao, Y.Liu, L.Xiong, J.Chen. *Ceram. Int.*, **45**, 13488 (2019)
325. X.-Z.Liu, L.Ding, Y.-Z.Liu, L.-P.Xiong, J.Chen, X.-L.Luo. *Rare Met.*, **40**, 2301 (2021)
326. F.Han, Y.Zhu, X.He, Y.Mo, C.Wang. *Adv. Energy Mater.*, **6**, 1501590 (2016)
327. S.A.Pervez, G.Kim, B.P.Vinayan, M.A.Cambaz, M.Kuenzel, M.Hekmatfar, M.Fichtner, S.Passerini. *Small*, **16**, 2000279 (2020)
328. L.Yang, Z.Lu, Y.Qin, C.Wu, C.Fu, Y.Gao, J.Liu, L.Jiang, Z.Du, Z.Xie, Z.Li, F.Kong, G.Yin. *J. Mater. Chem. A*, **9**, 5952 (2021)
329. M.Golozar, A.Paolella, H.Demers, S.Savoie, G.Girard, N.Delaporte, R.Gauvin, A.Guerfi, H.Lorrmann, K.Zaghib. *Sci. Rep.*, **10**, 18410 (2020)
330. S.-K.Jung, H.Gwon, H.Kim, G.Yoon, D.Shin, J.Hong, C.Jung, J.-S.Kim. *Nat. Commun.*, **13**, 7638 (2022)
331. M.Müller, J.Schmieg, S.Dierickx, J.Joos, A.Weber, D.Gerthsen, E.Ivers-Tiffée. *ACS Appl. Mater. Interfaces*, **14**, 14739 (2022)
332. W.Jiang, L.Dong, S.Liu, B.Ai, S.Zhao, W.Zhang, K.Pan, L.Zhang. *Nanomaterials*, **12**, 2023 (2022)
333. C.Li, G.Liu, K.Wang, W.Dong, J.Han, Y.Yu, Z.Min, C.Yang, Z.Lu. *ACS Appl. Mater. Interfaces*, **13**, 39271 (2021)
334. J.Su, X.Huang, Z.Song, T.Xiu, M.E.Badding, J.Jin, Z.Wen. *Ceram. Int.*, **45**, 14991 (2019)
335. J.Li, H.Luo, K.Liu, J.Zhang, H.Zhai, X.Su, J.Wu, X.Tang, G.Tan. *ACS Appl. Mater. Interfaces*, **15**, 7165 (2023)
336. C.Tsai, N.T.Thuy Tran, R.Schierholz, Z.Liu, A.Windmüller, C.Lin, Q.Xu, X.Lu, S.Yu, H.Tempel, H.Kungl, S.Lin, R.-A.Eichel. *J. Mater. Chem. A*, **10**, 10998 (2022)
337. F.Shen, W.Guo, D.Zeng, Z.Sun, J.Gao, J.Li, B.Zhao, B.He, X.Han. *ACS Appl. Mater. Interfaces*, **12**, 30313 (2020)
338. M.Liu, W.Xie, B.Li, Y.Wang, G.Li, S.Zhang, Y.Wen, J.Qiu, J.Chen, P.Zhao. *ACS Appl. Mater. Interfaces*, **14**, 43116 (2022)
339. C.Wu, J.J.Lou, J.Zhang, Z.Chen, A.Kakar, B.Emley, Q.Ai, H.Guo, Y.Liang, J.J.Lou, Y.Yao, Z.Fan. *Nano Energy*, **87**, 106081 (2021)
340. T.Yu, B.Ke, H.Li, S.Guo, H.Zhou. *Mater. Chem. Front.*, **5**, 4892 (2021)
341. J.Lau, R.H.DeBlock, D.M.Butts, D.S.Ashby, C.S.Choi, B.S.Dunn. *Adv. Energy Mater.*, **8**, 1800933 (2018)
342. C.Wang, J.Liang, Y.Zhao, M.Zheng, X.Li, X.Sun. *Energy Environ. Sci.*, **14**, 2577 (2021)
343. W.G.Suci, H.K.(Kiwi) Aliwarga, Y.R.Azinuddin, R.B.Setyawati, K.N.R.Stulasti, A.Purwanto. *Open Eng.*, **12**, 409 (2022)
344. H.Choi, M.Kim, H.Lee, S.Jung, Y.-G.Lee, Y.M.Lee, K.Y.Cho. *Nano Energy*, **102**, 107679 (2022)
345. Y.Kato, S.Hori, T.Saito, K.Suzuki, M.Hirayama, A.Mitsui, M.Yonemura, H.Iba, R.Kanno. *Nat. Energy*, **1**, 16030 (2016)
346. Q.Su, X.Wang, C.Deng, Y.Yun, Y.Zhao, Y.Peng. *Insect Sci.*, **27**, 908 (2020)
347. C.Dietrich, D.A.Weber, S.J.Sedlmaier, S.Indris, S.P.Culver, D.Walter, J.Janek, W.G.Zeier. *J. Mater. Chem. A*, **5**, 18111 (2017)
348. Z.D.Hood, C.Kates, M.Kirkham, S.Adhikari, C.Liang, N.A.W.Holzwarth. *Solid State Ionics*, **284**, 61 (2016)
349. R.Mercier, J.P.Malugani, B.Fahys, J.Douglande, G.Robert. *J. Solid State Chem.*, **43**, 151 (1982)
350. Ö.U.Kudu, T.Famprikis, B.Fleutot, M.-D.Braida, T.Le Mercier, M.S.Islam, C.Masquelier. *J. Power Sources*, **407**, 31 (2018)
351. S.Lu, F.Kosaka, S.Shiotani, H.Tsukasaki, S.Mori, J.Otomo. *Solid State Ionics*, **362**, 115583 (2021)
352. K.Homma, M.Yonemura, T.Kobayashi, M.Nagao, M.Hirayama, R.Kanno. *Solid State Ionics*, **182**, 53 (2011)
353. Z.Liu, W.Fu, E.A.Payzant, X.Yu, Z.Wu, N.J.Dudney, J.Kiggans, K.Hong, A.J.Rondinone, C.Liang. *J. Am. Chem. Soc.*, **135**, 975 (2013)
354. K.Kaup, L.Zhou, A.Huq, L.F.Nazar. *J. Mater. Chem. A*, **8**, 12446 (2020)
355. C.Wei, D.Yu, X.Xu, R.Wang, J.Li, J.Lin, S.Chen, L.Zhang, C.Yu. *Chem. – An Asian J.*, **18**, e202300304 (2023)
356. H.Tsukasaki, S.Mori, S.Shiotani, H.Yamamura. *Solid State Ionics*, **317**, 122 (2018)
357. C.Dietrich, D.A.Weber, S.Culver, A.Senyshyn, S.J.Sedlmaier, S.Indris, J.Janek, W.G.Zeier. *Inorg. Chem.*, **56**, 6681 (2017)
358. C.Dietrich, M.Sadowski, S.Sicolo, D.A.Weber, S.J.Sedlmaier, K.S.Weldert, S.Indris, K.Albe, J.Janek, W.G.Zeier. *Chem. Mater.*, **28**, 8764 (2016)
359. Y.Seino, T.Ota, K.Takada, A.Hayashi, M.Tatsumisago. *Energy Environ. Sci.*, **7**, 627 (2014)
360. Y.Seino, M.Nakagawa, M.Senga, H.Higuchi, K.Takada, T.Sasaki. *J. Mater. Chem. A*, **3**, 2756 (2015)
361. I.-H.Chu, H.Nguyen, S.Hy, Y.-C.Lin, Z.Wang, Z.Xu, Z.Deng, Y.S.Meng, S.P.Ong. *ACS Appl. Mater. Interfaces*, **8**, 7843 (2018)
362. J.Zhou, P.Chen, W.Wang, X.Zhang. *Chem. Eng. J.*, **446**, 137041 (2022)
363. Y.Aoki, K.Ogawa, T.Nakagawa, Y.Hasegawa, Y.Sakiyama, T.Kojima, M.Tabuchi. *Solid State Ionics*, **310**, 50 (2017)
364. M.Khurram Tufail, N.Ahmad, L.Zhou, M.Faheem, L.Yang, R.Chen, W.Yang. *Chem. Eng. J.*, **425**, 130535 (2021)
365. Y.Zhu, X.He, Y.Mo. *Adv. Sci.*, **4**, 1600517 (2017)
366. S.Wang, W.Zhang, X.Chen, D.Das, R.Ruess, A.Gautam, F.Walther, S.Ohno, R.Koerver, Q.Zhang, W.G.Zeier, F.H.Richter, C.Nan, J.Janek. *Adv. Energy Mater.*, **11**, 2100654 (2021)
367. X.Fan, X.Ji, F.Han, J.Yue, J.Chen, L.Chen, T.Deng, J.Jiang, C.Wang. *Sci. Adv.*, **4**, 174 (2018)
368. A.L.Santhosha, L.Medenbach, J.R.Buchheim, P.Adelhelm. *Batter. Supercaps*, **2**, 524 (2019)
369. K.Lim, B.Fenk, K.Küster, T.Acartürk, J.Weiss, U.Starke, J.Popovic, J.Maier. *ACS Appl. Mater. Interfaces*, **14**, 16147 (2022)
370. J.Li, Y.Li, J.Cheng, Q.Sun, L.Dai, N.Ci, D.Li, L.Ci. *J. Power Sources*, **518**, 230739 (2022)

371. S.Yang, K.Yamamoto, X.Mei, A.Sakuda, T.Uchiyama, T.Watanabe, T.Takami, A.Hayashi, M.Tatsumisago, Y.Uchimoto. *ACS Appl. Energy Mater.*, **5**, 667 (2022)
372. G.H.Lee, S.G.Lee, S.H.Park, D.Jun, Y.J.Lee. *J. Mater. Chem. A*, **10**, 10662 (2022)
373. K.Kim, T.Kim, G.Song, S.Lee, M.S.Jung, S.Ha, A.R.Ha, K.T.Lee. *Adv. Sci.*, **10**, 2303308 (2023)
374. A.Gautam, M.Ghidiu, E.Suard, M.A.Kraft, W.G.Zeier. *ACS Appl. Energy Mater.*, **4**, 7309 (2021)
375. P.Lu, Y.Xia, Y.Huang, Z.Li, Y.Wu, X.Wang, G.Sun, S.Shi, Z.Sha, L.Chen, H.Li, F.Wu. *Adv. Funct. Mater.*, **33**, 2211211 (2023)
376. I.Hanghofer, B.Gadermaier, H.M.R.Wilkening. *Chem. Mater.*, **31**, 4591 (2019)
377. M.V.Reddy, C.M.Julien, A.Mauger, K.Zaghib. *Nanomaterials*, **10**, 1606 (2020)
378. A.Hayashi, S.Hama, H.Morimoto, M.Tatsumisago, T.Minami. *Chem. Lett.*, **30**, 872 (2001)
379. B.Tao, C.Ren, H.Li, B.Liu, X.Jia, X.Dong, S.Zhang, H.Chang. *Adv. Funct. Mater.*, **32**, 2203551 (2022)
380. D.A.Ziolkowska, W.Arnold, T.Druffel, M.Sunkara, H.Wang. *ACS Appl. Mater. Interfaces*, **11**, 6015 (2019)
381. R.P.Rao, S.Adams. *Phys. Status Solidi*, **208**, 1804 (2011)
382. C.Yu, S.Ganapathy, J.Hageman, L.van Eijck, E.R.H.van Eck, L.Zhang, T.Schwietert, S.Basak, E.M.Kelder, M.Wagemaker. *ACS Appl. Mater. Interfaces*, **10**, 33296 (2018)
383. L.Zhou, K.-H.Park, X.Sun, F.Lalère, T.Adermann, P.Hartmann, L.F.Nazar. *ACS Energy Lett.*, **4**, 265 (2019)
384. J.Xu, L.Liu, N.Yao, F.Wu, H.Li, L.Chen. *Mater. Today Nano*, **8**, 100048 (2019)
385. W.H.Smith, S.A.Vaselabadi, C.A.Wolden. *ACS Appl. Energy Mater.*, **5**, 4029 (2022)
386. H.Gamo, I.Kusaba, K.Hikima, A.Matsuda. *Inorg. Chem.*, **62**, 6076 (2023)
387. R.F.Indrawan, H.Gamo, A.Nagai, A.Matsuda. *Chem. Mater.*, **35**, 2549 (2023)
388. N.Minafra, S.P.Culver, T.Krauskopf, A.Senyshyn, W.G.Zeier. *J. Mater. Chem. A*, **6**, 645 (2018)
389. M.A.Kraft, S.Ohno, T.Zinkevich, R.Koerver, S.P.Culver, T.Fuchs, A.Senyshyn, S.Indris, B.J.Morgan, W.G.Zeier. *J. Am. Chem. Soc.*, **140**, 16330 (2018)
390. T.Bernges, S.P.Culver, N.Minafra, R.Koerver, W.G.Zeier. *Inorg. Chem.*, **57**, 13920 (2018)
391. Z.Ma, H.-G.Xue, S.-P.Guo. *J. Mater. Sci.*, **53**, 3927 (2018)
392. B.D.Dandena, D.-S.Tsai, S.-H.Wu, W.-N.Su, B.J.Hwang. *Energy Storage Mater.*, **69**, 103305 (2024)
393. L.Zhou, A.Assoud, Q.Zhang, X.Wu, L.F.Nazar. *J. Am. Chem. Soc.*, **141**, 19002 (2019)
394. K.Hogrefe, N.Minafra, I.Hanghofer, A.Banik, W.G.Zeier, H.M.R.Wilkening. *J. Am. Chem. Soc.*, **144**, 1795 (2022)
395. P.-H.Chien, B.Ouyang, X.Feng, L.Dong, D.Mitlin, J.Nanda, J.Liu. *Chem. Mater.*, **36**, 382 (2024)
396. X.Li, J.Liang, J.Luo, M.Norouzi Banis, C.Wang, W.Li, S.Deng, C.Yu, F.Zhao, Y.Hu, T.-K.Sham, L.Zhang, S.Zhao, S.Lu, H.Huang, R.Li, K.R.Adair, X.Sun. *Energy Environ. Sci.*, **12**, 2665 (2019)
397. X.Li, J.Liang, N.Chen, J.Luo, K.R.Adair, C.Wang, M.N.Banis, T.Sham, L.Zhang, S.Zhao, S.Lu, H.Huang, R.Li, X.Sun. *Angew. Chem., Int. Ed.*, **58**, 16427 (2019)
398. S.Wang, Q.Bai, A.M.Nolan, Y.Liu, S.Gong, Q.Sun, Y.Mo. *Angew. Chem., Int. Ed.*, **58**, 8039 (2019)
399. K.-H.Park, K.Kaup, A.Assoud, Q.Zhang, X.Wu, L.F.Nazar. *ACS Energy Lett.*, **5**, 533 (2020)
400. J.Liang, X.Li, S.Wang, K.R.Adair, W.Li, Y.Zhao, C.Wang, Y.Hu, L.Zhang, S.Zhao, S.Lu, H.Huang, R.Li, Y.Mo, X.Sun. *J. Am. Chem. Soc.*, **142**, 7012 (2020)
401. B.Tao, D.Zhong, H.Li, G.Wang, H.Chang. *Chem. Sci.*, **14**, 8693 (2023)
402. X.Li, J.Liang, J.T.Kim, J.Fu, H.Duan, N.Chen, R.Li, S.Zhao, J.Wang, H.Huang, X.Sun. *Adv. Mater.*, **34**, 2200856 (2022)
403. M.Chen, R.Prasada Rao, S.Adams. *Solid State Ionics*, **268**, 300 (2014)
404. M.Chen, X.Yin, M.V.Reddy, S.Adams. *J. Mater. Chem. A*, **3**, 10698 (2015)
405. J.Zhang, H.Zhong, C.Zheng, Y.Xia, C.Liang, H.Huang, Y.Gan, X.Tao, W.Zhang. *J. Power Sources*, **391**, 73 (2018)
406. X.Bai, Y.Duan, W.Zhuang, R.Yang, J.Wang. *J. Mater. Chem. A*, **8**, 25663 (2020)
407. W.Arnold, D.A.Buchberger, Y.Li, M.Sunkara, T.Druffel, H.Wang. *J. Power Sources*, **464**, 228158 (2020)
408. Y.Kato, K.Kawamoto, R.Kanno, M.Hirayama. *Electrochemistry*, **80**, 749 (2012)
409. S.Hori, M.Kato, K.Suzuki, M.Hirayama, Y.Kato, R.Kanno. *J. Am. Ceram. Soc.*, **98**, 3352 (2015)
410. O.Kwon, M.Hirayama, K.Suzuki, Y.Kato, T.Saito, M.Yonemura, T.Kamiyama, R.Kanno. *J. Mater. Chem. A*, **3**, 438 (2015)
411. J.Yin, X.Yao, G.Peng, J.Yang, Z.Huang, D.Liu, Y.Tao, X.Xu. *Solid State Ionics*, **274**, 8 (2015)
412. D.A.Weber, A.Senyshyn, K.S.Weldert, S.Wenzel, W.Zhang, R.Kaiser, S.Berendts, J.Janek, W.G.Zeier. *Chem. Mater.*, **28**, 5905 (2016)
413. Y.-G.Lee, S.Fujiki, C.Jung, N.Suzuki, N.Yashiro, R.Omoda, D.-S.Ko, T.Shiratsuchi, T.Sugimoto, S.Ryu, J.H.Ku, T.Watanabe, Y.Park, Y.Aihara, D.Im, I.T.Han. *Nat. Energy*, **5**, 299 (2020)
414. J.A.Dawson, M.S.Islam. *ACS Mater. Lett.*, **4**, 424 (2022)
415. T.Ito, S.Hori, M.Hirayama, R.Kanno. *J. Mater. Chem. A*, **10**, 14392 (2022)
416. R.Iwasaki, S.Hori, R.Kanno, T.Yajima, D.Hirai, Y.Kato, Z.Hiroi. *Chem. Mater.*, **31**, 3694 (2019)
417. L.Schweiger, K.Hogrefe, B.Gadermaier, J.L.M.Rupp, H.M.R.Wilkening. *J. Am. Chem. Soc.*, **144**, 9597 (2022)
418. C.Mi, S.R.Hall. *Solid State Ionics*, **389**, 116106 (2023)
419. Q.Zheng, Y.Song, W.Huang, J.Yang, T.Li, Y.Xu. *Energy Storage Mater.*, **63**, 103038 (2023)
420. A.Kuhn, O.Gerbig, C.Zhu, F.Falkenberg, J.Maier, B.V.Lotsch. *Phys. Chem. Chem. Phys.*, **16**, 14669 (2014)
421. Q.Wang, D.Liu, X.Ma, X.Zhou, Z.Lei. *ACS Appl. Mater. Interfaces*, **14**, 22225 (2022)
422. P.Dong, Q.Jiao, Z.Zhang, M.Jiang, C.Lin, X.Zhang, H.Ma, B.Ma, S.Dai, T.Xu. *J. Am. Ceram. Soc.*, **105**, 3252 (2022)
423. P.Bron, S.Johansson, K.Zick, J.Schmedt auf der Günne, S.Dehnen, B.Roling. *J. Am. Chem. Soc.*, **135**, 15694 (2013)
424. C.Vinado, S.Wang, Y.He, X.Xiao, Y.Li, C.Wang, J.Yang. *J. Power Sources*, **396**, 824 (2018)
425. I.Tarhouchi, V.Viallet, P.Vinatier, M.Ménétrier. *Solid State Ionics*, **296**, 18 (2016)
426. Y.Lin, J.Chen, J.Yan, Y.Zhuang, H.Lu, C.Zhao. *Front. Chem.*, **10**, (2022)
427. P.Bron, S.Dehnen, B.Roling. *J. Power Sources*, **329**, 530 (2016)
428. K.-H.Kim, S.W.Martin. *Chem. Mater.*, **31**, 3984 (2019)
429. A.K.Mishra, H.A.Chaliyawala, R.Patel, S.Paneliya, A.Vanpariya, P.Patel, A.Ray, R.Pati, I.Mukhopadhyay. *J. Electrochem. Soc.*, **168**, 080536 (2021)
430. Z.Zhang, X.Wang, X.Li, J.Zhao, G.Liu, W.Yu, X.Dong, J.Wang. *Mater. Today Sustain.*, **21**, 100316 (2023)
431. S.Zhou, S.Zhong, Y.Dong, Z.Liu, L.Dong, B.Yuan, H.Xie, Y.Liu, L.Qiao, J.Han, W.He. *Adv. Funct. Mater.*, **33**, 2214432 (2023)
432. D.Y.Voropaeva, S.A.Novikova, A.B.Yaroslavtsev. *Russ. Chem. Rev.*, **89**, 1132 (2020)
433. K.Deng, Q.Zeng, D.Wang, Z.Liu, Z.Qiu, Y.Zhang, M.Xiao, Y.Meng. *J. Mater. Chem. A*, **8**, 1557 (2020)
434. K.Liu, S.Jiang, T.L.Dzwiniel, H.-K.Kim, Z.Yu, N.L.Dietz Rago, J.J.Kim, T.T.Fister, J.Yang, Q.Liu, J.Gilbert, L.Cheng, V.Srinivasan, Z.Zhang, C.Liao. *ACS Appl. Mater. Interfaces*, **12**, 29162 (2020)
435. S.B.Aziz, T.J.Woo, M.F.Z.Kadir, H.M.Ahmed. *J. Sci. Adv. Mater. Devices*, **3**, 1 (2018)

436. X.Liu, W.Shi, S.Zhuang, Y.Liu, D.He, G.Feng, T.Ge, T.Wang. *ChemSusChem*, e202301896 (2024)
437. X.Yu, M.Xiao, S.Wang, Q.Zhao, Y.Meng. *J. Appl. Polym. Sci.*, **115**, 2718 (2010)
438. Y.Cui, J.Chai, H.Du, Y.Duan, G.Xie, Z.Liu, G.Cui. *ACS Appl. Mater. Interfaces*, **9**, 8737 (2017)
439. Z.Lin, O.Sheng, X.Cai, D.Duan, K.Yue, J.Nai, Y.Wang, T.Liu, X.Tao, Y.Liu. *J. Energy Chem.*, **81**, 358 (2023)
440. B.K.Money, J.Swenson. *Macromolecules*, **46**, 6949 (2013)
441. X.Judez, M.Martinez-Ibañez, A.Santiago, M.Armand, H.Zhang, C.Li. *J. Power Sources*, **438**, 226985 (2019)
442. J.Chattopadhyay, T.S.Pathak, D.M.F.Santos. *Polymers*, **15**, 3907 (2023)
443. Z.Xue, D.He, X.Xie. *J. Mater. Chem. A*, **3**, 19218 (2015)
444. T.Kobayashi, Y.Kobayashi, M.Tabuchi, K.Shono, Y.Ohno, Y.Mita, H.Miyashiro. *ACS Appl. Mater. Interfaces*, **5**, 12387 (2013)
445. L.Herbers, J.Minář, S.Stuckenberg, V.Küpers, D.Berghus, S.Nowak, M.Winter, P.Bieker. *Adv. Energy Sustain. Res.*, **4**, 2300153 (2023)
446. X.Yang, M.Jiang, X.Gao, D.Bao, Q.Sun, N.Holmes, H.Duan, S.Mukherjee, K.Adair, C.Zhao, J.Liang, W.Li, J.Li, Y.Liu, H.Huang, L.Zhang, S.Lu, Q.Lu, R.Li, C.V.Singh, X.Sun. *Energy Environ. Sci.*, **13**, 1318 (2020)
447. R.Huang, Y.Ding, F.Zhang, W.Jiang, C.Zhang, P.Yan, M.Ling, H.Pan. *J. Energy Chem.*, **75**, 504 (2022)
448. G.Homann, L.Stolz, J.Nair, I.C.Laskovic, M.Winter, J.Kasnatscheew. *Sci. Rep.*, **10**, 4390 (2020)
449. Y.Yusim, E.Trevisanello, R.Ruess, F.H.Richter, A.Mayer, D.Bresser, S.Passerini, J.Janek, A.Henss. *Angew. Chem., Int. Ed.*, **62**, e202218316 (2023)
450. G.Homann, L.Stolz, K.Neuhaus, M.Winter, J.Kasnatscheew. *Adv. Funct. Mater.*, **30**, 2006289 (2020)
451. G.M.Stone, S.A.Mullin, A.A.Teran, D.T.Hallinan, A.M.Minor, A.Hexemer, N.P.Balsara. *J. Electrochem. Soc.*, **159**, A222 (2012)
452. E.D.Gomez, A.Panday, E.H.Feng, V.Chen, G.M.Stone, A.M.Minor, C.Kisielowski, K.H.Downing, O.Borodin, G.D.Smith, N.P.Balsara. *Nano Lett.*, **9**, 1212 (2009)
453. A.J.Butzelaar, P.Röring, T.P.Mach, M.Hoffmann, F.Jeschull, M.Wilhelm, M.Winter, G.Brunklaus, P.Théato. *ACS Appl. Mater. Interfaces*, **13**, 39257 (2021)
454. Z.Song, F.Chen, M.Martinez-Ibañez, W.Feng, M.Forsyth, Z.Zhou, M.Armand, H.Zhang. *Nat. Commun.*, **14**, 4884 (2023)
455. A.J.Butzelaar, K.L.Liu, P.Röring, G.Brunklaus, M.Winter, P.Theato. *ACS Appl. Polym. Mater.*, **3**, 1573 (2021)
456. V.St-Onge, M.Cui, S.Rochon, J.-C.Daigle, J.P.Claverie. *Commun. Mater.*, **2**, 83 (2021)
457. Y.Sun, X.Zhang, C.Ma, N.Guo, Y.Liu, J.Liu, H.Xie. *J. Power Sources*, **516**, 230686 (2021)
458. R.Subramani, M.-N.Pham, Y.-H.Lin, C.-T.Hsieh, Y.-L.Lee, J.-S.Jan, C.-C.Chiu, H.Teng. *Chem. Eng. J.*, **431**, 133442 (2022)
459. R.Sahore, G.Yang, X.C.Chen, W.-Y.Tsai, J.Li, N.J.Dudney, A.Westover. *ACS Appl. Energy Mater.*, **5**, 1409 (2022)
460. L.Gao, H.Liang, J.Li, B.Cheng, N.Deng, W.Kang. *J. Power Sources*, **515**, 230622 (2021)
461. Q.Zeng, P.Chen, Z.Li, X.Wen, W.Wen, Y.Liu, H.Zhao, S.Zhang, H.Zhou, L.Zhang. *ACS Appl. Mater. Interfaces*, **13**, 48569 (2021)
462. Y.Xu, S.Zhang, T.Liang, Z.Yao, X.Wang, C.Gu, X.Xia, J.Tu. *ACS Appl. Mater. Interfaces*, **13**, 11018 (2021)
463. S.Wang, J.Li, T.Li, W.Huang, L.Wang, S.Tao. *Chem. Eng. J.*, **461**, 141995 (2023)
464. X.Zhu, Z.Fang, Q.Deng, Y.Zhou, X.Fu, L.Wu, W.Yan, Y.Yang. *ACS Sustain. Chem. Eng.*, **10**, 4173 (2022)
465. K.Shi, Z.Xu, M.Huang, L.Zou, D.Zheng, Z.Yang, W.Zhang. *J. Membr. Sci.*, **638**, 119713 (2021)
466. J.-Y.Lee, P.-H.Chung, S.-C.Yeh, T.-Y.Yu, W.-Y.Lee, N.-L.Wu, R.-J.Jeng. *J. Phys. Chem. C*, **125**, 26339 (2021)
467. Y.Sha, T.Yu, T.Dong, X.Wu, H.Tao, H.Zhang. *ACS Appl. Energy Mater.*, **4**, 14755 (2021)
468. Y.-F.Huang, T.Gu, G.Rui, P.Shi, W.Fu, L.Chen, X.Liu, J.Zeng, B.Kang, Z.Yan, F.J.Stadler, L.Zhu, F.Kang, Y.-B.He. *Energy Environ. Sci.*, **14**, 6021 (2021)
469. J.-P.Zeng, J.-F.Liu, H.-D.Huang, S.-C.Shi, B.-H.Kang, C.Dai, L.-W.Zhang, Z.-C.Yan, F.J.Stadler, Y.-B.He, Y.-F.Huang. *J. Mater. Chem. A*, **10**, 18061 (2022)
470. Z.Wang, Q.Guo, R.Jiang, S.Deng, J.Ma, P.Cui, X.Yao. *Chem. Eng. J.*, **435**, 135106 (2022)
471. T.Zheng, X.Cui, Y.Chu, H.Li, Q.Pan. *ACS Appl. Mater. Interfaces*, **14**, 5932 (2022)
472. C.Zuo, H.Li, G.Chen, J.Yang, Z.Xu, Z.Xue. *ACS Appl. Energy Mater.*, **4**, 9402 (2021)
473. X.Liu, J.Liu, B.Lin, F.Chu, Y.Ren. *ACS Appl. Energy Mater.*, **5**, 1031 (2022)
474. S.Chen, Y.Li, Y.Wang, Z.Li, C.Peng, Y.Feng, W.Feng. *Macromolecules*, **54**, 9135 (2021)
475. K.Wen, C.Xin, S.Guan, X.Wu, S.He, C.Xue, S.Liu, Y.Shen, L.Li, C.Nan. *Adv. Mater.*, **34**, 2202143 (2022)
476. J.Gou, W.Liu, A.Tang, H.Xie. *Eur. Polym. J.*, **158**, 110703 (2021)
477. Q.Wu, Y.Yang, Z.Chen, Q.Su, S.Huang, D.Song, C.Zhu, R.Ma, C.Li. *ACS Appl. Energy Mater.*, **4**, 9420 (2021)
478. Y.Wang, K.Huang, P.Zhang, H.Li, H.Mi. *Appl. Surf. Sci.*, **574**, 151593 (2022)
479. R.Poiana, E.Lufrano, A.Tsurumaki, C.Simari, I.Nicotera, M.A.Navarra. *Electrochim. Acta*, **401**, 139470 (2022)
480. B.Zhou, Y.Zhou, L.Lai, Z.Chen, J.Li, Y.Jiang, J.Liu, Z.Wang, Z.Xue. *ACS Appl. Energy Mater.*, **4**, 9582 (2021)
481. L.Zhou, H.Zhao, K.Liang, J.Chen, J.Li, X.Huang, Y.Qi, Y.Ren. *J. Colloid Interface Sci.*, **613**, 606 (2022)
482. R.Rohan, Y.Sun, W.Cai, Y.Zhang, K.Pareek, G.Xu, H.Cheng. *Solid State Ionics*, **268**, 294 (2014)
483. X.Guan, Q.Wu, X.Zhang, X.Guo, C.Li, J.Xu. *Chem. Eng. J.*, **382**, 122935 (2020)
484. J.Zhang, S.Wang, D.Han, M.Xiao, L.Sun, Y.Meng. *Energy Storage Mater.*, **24**, 579 (2020)
485. D.Voropaeva, S.Novikova, N.Trofimenko, A.Yaroslavtsev. *Processes*, **10**, 2509 (2022)
486. D.Voropaeva, E.Safronova, S.Novikova, A.Yaroslavtsev. *J. Phys. Chem. C*, **128**, 4143 (2024)
487. B.Jinisha, K.M.Anilkumar, M.Manoj, V.S.Pradeep, S.Jayalekshmi. *Electrochim. Acta*, **235**, 210 (2017)
488. J.Wan, J.Xie, X.Kong, Z.Liu, K.Liu, F.Shi, A.Pei, H.Chen, W.Chen, J.Chen, X.Zhang, L.Zong, J.Wang, L.-Q.Chen, J.Qin, Y.Cui. *Nat. Nanotechnol.*, **14**, 705 (2019)
489. Q.Yang, Z.Zhang, X.-G.Sun, Y.-S.Hu, H.Xing, S.Dai. *Chem. Soc. Rev.*, **47**, 2020 (2018)
490. K.Liu, Z.Wang, L.Shi, S.Jungsuttiwong, S.Yuan. *J. Energy Chem.*, **59**, 320 (2021)
491. G.Yang, Y.Song, Q.Wang, L.Zhang, L.Deng. *Mater. Des.*, **190**, 108563 (2020)
492. N.Nishimura, H.Ohno. *Polymer*, **55**, 3289 (2014)
493. W.Qian, J.Texter, F.Yan. *Chem. Soc. Rev.*, **46**, 1124 (2017)
494. J.Li, F.Li, L.Zhang, H.Zhang, U.Lassi, X.Ji. *Green Chem. Eng.*, **2**, 253 (2021)
495. Y.Wu, Y.Li, Y.Wang, Q.Liu, Q.Chen, M.Chen. *J. Energy Chem.*, **64**, 62 (2022)
496. X.Lu, Y.Wang, X.Xu, B.Yan, T.Wu, L.Lu. *Adv. Energy Mater.*, **13**, 2301746 (2023)
497. L.Mathies, D.Diddens, D.Dong, D.Bedrov, H.Leipner. *Solid State Ionics*, **357**, 115497 (2020)
498. M.M.Nasef, H.Saidi, K.Z.M.Dahlan. *Nucl. Instruments Methods Phys. Res. Sect. B: Beam Interact. with Mater. Atoms*, **265**, 168 (2007)
499. H.Xie, Z.Tang, Z.Li, Y.He, Y.Liu, H.Wang. *J. Solid State Electrochem.*, **12**, 1497 (2008)
500. K.S.Ngai, S.Ramesh, K.Ramesh, J.C.Juan. *Ionics*, **22**, 1259 (2016)

501. J.Mi, J.Ma, L.Chen, C.Lai, K.Yang, J.Biao, H.Xia, X.Song, W.Lv, G.Zhong, Y.-B.He. *Energy Storage Mater.*, **48**, 375 (2022)
502. L.Li, Y.Shan, F.Wang, X.Chen, Y.Zhao, D.Zhou, H.Wang, W.Cui. *ACS Appl. Mater. Interfaces*, **13**, 48525 (2021)
503. X.Zhang, J.Han, X.Niu, C.Xin, C.Xue, S.Wang, Y.Shen, L.Zhang, L.Li, C.Nan. *Batter. Supercaps*, **3**, 876 (2020)
504. P.Yao, B.Zhu, H.Zhai, X.Liao, Y.Zhu, W.Xu, Q.Cheng, C.Jayyosi, Z.Li, J.Zhu, K.M.Myers, X.Chen, Y.Yang. *Nano Lett.*, **18**, 6113 (2018)
505. M.A.S.Azizi Samir, A.M.Mateos, F.Alloin, J.-Y.Sanchez, A.Dufresne. *Electrochim. Acta*, **49**, 4667 (2004)
506. K.Xu. *Chem Rev.*, **114**, 11503 (2014)
507. K.Xu. *Chem Rev.*, **104**, 4303 (2004)
508. M.Marcinek, J.Syzdek, M.Marczewski, M.Piszcz, L.Niedzicki, M.Kalita, A.Plewa-Marczewska, A.Bitner, P.Wieczorek, T.Trzeciak, M.Kasprzyk, P.Łężak, Z.Zukowska, A.Zalewska, W.Wieczorek. *Solid State Ionics*, **276**, 107 (2015)
509. F.Boudin, X.Andrieu, C.Jehoulet, I.Olsen. *J. Power Sources*, **81**–**82**, 804 (1999)
510. D.Saikia, A.Kumar. *Electrochim. Acta*, **49**, 2581 (2004)
511. J.Kalhoff, G.G.Eshetu, D.Bresser, S.Passerini. *ChemSusChem*, **8**, 2154 (2015)
512. Q.Zhou, S.Dong, Z.Lv, G.Xu, L.Huang, Q.Wang, Z.Cui, G.Cui. *Adv. Energy Mater.*, **10**, 1903441 (2020)
513. P.Lyu, X.Liu, J.Qu, J.Zhao, Y.Huo, Z.Qu, Z.Rao. *Energy Storage Mater.*, **31**, 195 (2020)
514. X.Liu, C.Zhang, S.Gao, S.Cai, Q.Wang, J.Liu, Z.Liu. *Mater. Chem. Phys.*, **239**, 122014 (2020)
515. F.Liu, T.Lan, K.Chen, Q.Wang, Z.Huang, C.Shi, S.Zhang, S.Li, M.Wang, B.Hong, Z.Zhang, J.Li, Y.Lai. *ACS Appl. Mater. Interfaces*, **15**, 23136 (2023)
516. K.Deng, Z.Xu, S.Zhou, Z.Zhao, K.Zeng, M.Xiao, Y.Meng, Y.Xu. *J. Power Sources*, **510**, 230411 (2021)
517. L.Hu, Z.Zhang, K.Amine. *Electrochem. Commun.*, **35**, 76 (2013)
518. C.Brissot, M.Rosso, J.-N.Chazalviel, P.Baudry, S.Lascaud. *Electrochim. Acta*, **43**, 1569 (1998)
519. M.Alvarez-Tirado, G.Guzmán-González, S.Vauthier, S.Cotte, A.Guéguen, L.Castro, D.Mecerreyes. *Macromol. Chem. Phys.*, **223**, 2100407 (2022)
520. Y.Luo, L.Gao, W.Kang. *J. Energy Chem.*, **89**, 543 (2024)
521. D.Y.Voropaeva, S.A.Novikova, T.L.Kulova, A.B.Yaroslavtsev. *Ionics*, **24**, 1685 (2018)
522. D.Voropaeva, D.Golubenko, A.Merkel, A.Yaroslavtsev. *J. Membr. Sci.*, **601**, 117918 (2020)
523. J.Liu, P.D.Pickett, B.Park, S.P.Upadhyay, S.V.Orski, J.L.Schaefer. *Polym. Chem.*, **11**, 461 (2020)
524. F.Ahmed, I.Choi, M.M.Rahman, H.Jang, T.Ryu, S.Yoon, L.Jin, Y.Jin, W.Kim. *ACS Appl. Mater. Interfaces*, **11**, 34930 (2019)
525. J.Zhu, Z.Zhang, S.Zhao, A.S.Westover, I.Belharouak, P.Cao. *Adv. Energy Mater.*, **11**, 2003836 (2021)
526. C.Chen, Z.Li, X.Du, Q.Zhou, P.Han, G.Cui. *eTransportation*, **20**, 100318 (2024)
527. S.Feng, D.Shi, F.Liu, L.Zheng, J.Nie, W.Feng, X.Huang, M.Armand, Z.Zhou. *Electrochim. Acta*, **93**, 254 (2013)
528. A.E.Feiring, S.K.Choi, M.Doyle, E.R.Wonchoba. *Macromolecules*, **33**, 9262 (2000)
529. Q.Ma, H.Zhang, C.Zhou, L.Zheng, P.Cheng, J.Nie, W.Feng, Y.S.Hu, H.Li, X.Huang, L.Chen, M.Armand, Z.Zhou. *Angew. Chem., Int. Ed.*, **55**, 2521 (2016)
530. B.A.Paren, N.Nguyen, V.Ballance, D.T.Hallinan, J.G.Kennemur, K.I.Winey. *Macromolecules*, **55**, 4692 (2022)
531. R.Meziane, J.-P.Bonnet, M.Courty, K.Djellab, M.Armand. *Electrochim. Acta*, **57**, 14 (2011)
532. W.Zhang, S.Feng, M.Huang, B.Qiao, K.Shigenobu, L.Giordano, J.Lopez, R.Tatara, K.Ueno, K.Dokko, M. Watanabe, Y.Shao-Horn, J.A.Johnson. *Chem. Mater.*, **33**, 524 (2021)
533. Y.Zhong, L.Zhong, S.Wang, J.Qin, D.Han, S.Ren, M.Xiao, L.Sun, Y.Meng. *J. Mater. Chem. A*, **7**, 24251 (2019)
534. X.Yan, Z.Xu, S.Yuan, A.Han, Y.Shen, X.Cheng, Y.Liang, S.Shen, J.Zhang. *J. Power Sources*, **536**, 231523 (2022)
535. J.Gao, C.S.Sun, L.Xu, J.Chen, C.Wang, D.C.Guo, H.Chen. *J. Power Sources*, **382**, 179 (2018)
536. I.Nicotera, C.Simari, M.Agostini, A.Enotiadis, S.Brutti. *J. Phys. Chem. C*, **123**, 27406 (2019)
537. Z.Jin, K.Xie, X.Hong, Z.Hu, X.Liu. *J. Power Sources*, **218**, 163 (2012)
538. H.Y.Liang, X.P.Qiu, S.C.Zhang, W.T.Zhu, L.Q.Chen. *J. Appl. Electrochem.*, **34**, 1211 (2004)
539. J.Gao, Q.Shao, J.Chen. *J. Energy Chem.*, **46**, 237 (2020)
540. E.Y.Evshchik, E.A.Sanginov, R.R.Kayumov, V.D.Zhuravlev, O.V.Bushkova, Y.A.Dobrovolsky. *Int. J. Electrochem. Sci.*, 2216 (2020)
541. S.Wu, M.Wu, H.Zhang, H.Tang. *ACS Appl. Polym. Mater.*, **5**, 4266 (2023)
542. Ş.Dombaycıoğlu, H.Günsel, A.O.Aydın. *ChemistrySelect*, **7**, e202202910 (2022)
543. A.B.Yaroslavtsev, S.A.Novikova, D.Y.Voropaeva, S.A.Li, T.L.Kulova. *Batteries*, **8**, 162 (2022)
544. Z.Shen, Y.Cheng, S.Sun, X.Ke, L.Liu, Z.Shi. *Carbon Energy*, **3**, 482 (2021)
545. H.Chen, M.Zheng, S.Qian, H.Y.Ling, Z.Wu, X.Liu, C.Yan, S.Zhang. *Carbon Energy*, **3**, 929 (2021)
546. Q.Zhou, J.Ma, S.Dong, X.Li, G.Cui. *Adv. Mater.*, **31**, 1902029 (2019)
547. S.Tang, W.Guo, Y.Fu. *Adv. Energy Mater.*, **11**, 2000802 (2021)
548. S.Ferrari, J.R.Nair, Y.Zhou, C.Wan. In *Polymer-Based Nanocomposites for Energy and Environmental Applications* (Elsevier, 2018). P. 283
549. H.Liang, L.Wang, A.Wang, Y.Song, Y.Wu, Y.Yang, X.He. *Nano-Micro Lett.*, **15**, 42 (2023)
550. Y.Zheng, Y.Yao, J.Ou, M.Li, D.Luo, H.Dou, Z.Li, K.Amine, A.Yu, Z.Chen. *Chem. Soc. Rev.*, **49**, 8790 (2020)
551. S.-J.Tan, X.-X.Zeng, Q.Ma, X.-W.Wu, Y.-G.Guo. *Electrochem. Energy Rev.*, **1**, 113 (2018)
552. L.-Z.Fan, H.He, C.-W.Nan. *Nat. Rev. Mater.*, **6**, 1003 (2021)
553. Z.Chang, H.Yang, X.Zhu, P.He, H.Zhou. *Nat. Commun.*, **13**, 1510 (2022)
554. J.Pan, P.Zhao, N.Wang, F.Huang, S.Dou. *Energy Environ. Sci.*, **15**, 2753 (2022)
555. S.Su, J.Ma, L.Zhao, K.Lin, Q.Li, S.Lv, F.Kang, Y.He. *Carbon Energy*, **3**, 866 (2021)
556. X.Yu, A.Manthiram. *Energy Storage Mater.*, **34**, 282 (2021)
557. Z.Cheng, T.Liu, B.Zhao, F.Shen, H.Jin, X.Han. *Energy Storage Mater.*, **34**, 388 (2021)
558. S.Liu, W.Liu, D.Ba, Y.Zhao, Y.Ye, Y.Li, J.Liu. *Adv. Mater.*, **35**, 2110423 (2023)
559. B.Kumar, L.G.Scanlon. *J. Power Sources*, **52**, 261 (1994)
560. H.Yang, B.Zhang, M.Jing, X.Shen, L.Wang, H.Xu, X.Yan, X.He. *Adv. Energy Mater.*, **12**, 2201762 (2022)
561. W.Zhang, J.Nie, F.Li, Z.L.Wang, C.Sun. *Nano Energy*, **45**, 413 (2018)
562. B.Tang, Y.Zhao, Z.Wang, S.Chen, Y.Wu, Y.Tseng, L.Li, Y.Guo, Z.Zhou, S.-H.Bo. *eScience*, **1**, 194 (2021)
563. S.Liu, L.Zhou, J.Han, K.Wen, S.Guan, C.Xue, Z.Zhang, B.Xu, Y.Lin, Y.Shen, L.Li, C.Nan. *Adv. Energy Mater.*, **12**, 2200660 (2022)
564. F.Croce, L.Persi, B.Scrosati, F.Serraino-Fiory, E.Plichta, M.A.Hendrickson. *Electrochim. Acta*, **46**, 2457 (2001)
565. D.Xie, M.Zhang, Y.Wu, L.Xiang, Y.Tang. *Adv. Funct. Mater.*, **30**, 1906770 (2020)
566. S.Sen, E.Trevisanello, E.Niemöller, B.-X.Shi, F.J.Simon, F.H.Richter. *J. Mater. Chem. A*, **9**, 18701 (2021)
567. S.Ramesh, L.C.Wen. *Ionics*, **16**, 255 (2010)
568. D.Lin, W.Liu, Y.Liu, H.R.Lee, P.-C.Hsu, K.Liu, Y.Cui. *Nano Lett.*, **16**, 459 (2016)
569. P.Pal, A.Ghosh. *Electrochim. Acta*, **260**, 157 (2018)

570. F.Pignanelli, M.Romero, J.Castiglioni, R.Faccio, A.W.Mombrú. *J. Phys. Chem. Solids*, **135**, 109082 (2019)
571. T.Itoh. *Solid State Ionics*, **156**, 393 (2003)
572. N.T.Kalyana Sundaram, T.Vasudevan, A.Subramania. *J. Phys. Chem. Solids*, **68**, 264 (2007)
573. X.Yang, J.Liu, N.Pei, Z.Chen, R.Li, L.Fu, P.Zhang, J.Zhao. *Nano-Micro Lett.*, **15**, 74 (2023)
574. M.D.Tikekar, L.A.Archer, D.L.Koch. *J. Electrochem. Soc.*, **161**, A847 (2014)
575. R.Xu, X.-B.Cheng, C.Yan, X.-Q.Zhang, Y.Xiao, C.-Z.Zhao, J.-Q.Huang, Q.Zhang. *Matter*, **1**, 317 (2019)
576. H.Wang, L.Sheng, G.Yasin, L.Wang, H.Xu, X.He. *Energy Storage Mater.*, **33**, 188 (2020)
577. Y.Wang, X.Li, Y.Qin, D.Zhang, Z.Song, S.Ding. *Nano Energy*, **90**, 106490 (2021)
578. Y.Hu, N.Dunlap, S.Wan, S.Lu, S.Huang, I.Sellinger, M.Ortiz, Y.Jin, S.Lee, W.Zhang. *J. Am. Chem. Soc.*, **141**, 7518 (2019)
579. L.Chen, W.Li, L.Fan, C.Nan, Q.Zhang. *Adv. Funct. Mater.*, **29**, 1901047 (2019)
580. H.Jamal, F.Khan, H.-R.Si, J.H.Kim. *J. Mater. Chem. A*, **9**, 27304 (2021)
581. H.Jamal, F.Khan, S.Hyun, S.W.Min, J.H.Kim. *J. Mater. Chem. A*, **9**, 4126 (2021)
582. Z.Li, S.Wang, J.Shi, Y.Liu, S.Zheng, H.Zou, Y.Chen, W.Kuang, K.Ding, L.Chen, Y.Lan, Y.Cai, Q.Zheng. *Energy Storage Mater.*, **47**, 262 (2022)
583. Y.Shi, Z.Fan, B.Ding, Z.Li, Q.Lin, S.Chen, H.Dou, X.Zhang. *J. Electroanal. Chem.*, **881**, 114916 (2021)
584. P.N.Didwal, Y.N.Singhbabu, R.Verma, B.-J.Sung, G.-H.Lee, J.-S.Lee, D.R.Chang, C.-J.Park. *Energy Storage Mater.*, **37**, 476 (2021)
585. S.Hua, M.Jing, C.Han, H.Yang, H.Chen, F.Chen, L.Chen, B.Ju, F.Tu, X.Shen, S.Qin. *Int. J. Energy Res.*, **43**, 7296 (2019)
586. W.Xiao, Z.Wang, Y.Zhang, R.Fang, Z.Yuan, C.Miao, X.Yan, Y.Jiang. *J. Power Sources*, **382**, 128 (2018)
587. X.Ao, X.Wang, J.Tan, S.Zhang, C.Su, L.Dong, M.Tang, Z.Wang, B.Tian, H.Wang. *Nano Energy*, **79**, 105475 (2021)
588. Y.Li, Z.Sun, D.Liu, Y.Gao, Y.Wang, H.Bu, M.Li, Y.Zhang, G.Gao, S.Ding. *J. Mater. Chem. A*, **8**, 2021 (2020)
589. Y.Zhang, X.Wang, W.Feng, Y.Zhen, P.Zhao, L.Li, Z.Cai. *J. Solid State Electrochem.*, **23**, 749 (2019)
590. O.Sheng, C.Jin, J.Luo, H.Yuan, H.Huang, Y.Gan, J.Zhang, Y.Xia, C.Liang, W.Zhang, X.Tao. *Nano Lett.*, **18**, 3104 (2018)
591. Y.Lin, X.Wang, J.Liu, J.D.Miller. *Nano Energy*, **31**, 478 (2017)
592. Z.Lei, J.Shen, W.Zhang, Q.Wang, J.Wang, Y.Deng, C.Wang. *Nano Res.*, **13**, 2259 (2020)
593. K.Zhu, Y.Liu, J.Liu. *RSC Adv.*, **4**, 42278 (2014)
594. J.-F.Wu, X.Guo. *J. Mater. Chem. A*, **7**, 2653 (2019)
595. W.Jia, Z.Li, Z.Wu, L.Wang, B.Wu, Y.Wang, Y.Cao, J.Li. *Solid State Ionics*, **315**, 7 (2018)
596. Q.Zhu, X.Wang, J.D.Miller. *ACS Appl. Mater. Interfaces*, **11**, 8954 (2019)
597. T.Yang, J.Zheng, Q.Cheng, Y.-Y.Hu, C.K.Chan. *ACS Appl. Mater. Interfaces*, **9**, 21773 (2017)
598. Z.Wan, D.Lei, W.Yang, C.Liu, K.Shi, X.Hao, L.Shen, W.Lv, B.Li, Q.Yang, F.Kang, Y.He. *Adv. Funct. Mater.*, **29**, 1805301 (2019)
599. R.Li, S.Guo, L.Yu, L.Wang, D.Wu, Y.Li, X.Hu. *Adv. Mater. Interfaces*, **6**, 1900200 (2019)
600. M.Wu, D.Liu, D.Qu, Z.Xie, J.Li, J.Lei, H.Tang. *ACS Appl. Mater. Interfaces*, **12**, 52652 (2020)
601. Y.Zhao, J.Yan, W.Cai, Y.Lai, J.Song, J.Yu, B.Ding. *Energy Storage Mater.*, **23**, 306 (2019)
602. D.H.Kim, M.Y.Kim, S.H.Yang, H.M.Ryu, H.Y.Jung, H.-J.Ban, S.-J.Park, J.S.Lim, H.-S.Kim. *J. Ind. Eng. Chem.*, **71**, 445 (2019)
603. J.Sun, Y.Li, Q.Zhang, C.Hou, Q.Shi, H.Wang. *Chem. Eng. J.*, **375**, 121922 (2019)
604. C.-Z.Zhao, X.-Q.Zhang, X.-B.Cheng, R.Zhang, R.Xu, P.-Y.Chen, H.-J.Peng, J.-Q.Huang, Q.Zhang. *Proc. Natl. Acad. Sci.*, **114**, 11069 (2017)
605. J.Zhang, X.Zang, H.Wen, T.Dong, J.Chai, Y.Li, B.Chen, J.Zhao, S.Dong, J.Ma, L.Yue, Z.Liu, X.Guo, G.Cui, L.Chen. *J. Mater. Chem. A*, **5**, 4940 (2017)
606. A.Li, X.Liao, H.Zhang, L.Shi, P.Wang, Q.Cheng, J.Borovilas, Z.Li, W.Huang, Z.Fu, M.Dontigny, K.Zaghib, K.Myers, X.Chuan, X.Chen, Y.Yang. *Adv. Mater.*, **32**, 1905517 (2020)
607. G.Piana, F.Bella, F.Geobaldo, G.Meligrana, C.Gerbaldi. *J. Energy Storage*, **26**, 100947 (2019)
608. Z.Huang, J.Li, L.Li, H.Xu, C.Han, M.Liu, J.Xiang, X.Shen, M.Jing. *Ceram. Int.*, **48**, 25949 (2022)
609. G.Wang, H.Liu, Y.Liang, C.Wang, L.-Z.Fan. *Energy Storage Mater.*, **45**, 1212 (2022)
610. Y.Li, H.Wang. *Ind. Eng. Chem. Res.*, **60**, 1494 (2021)
611. Y.Jin, X.Zong, X.Zhang, C.Liu, D.Li, Z.Jia, G.Li, X.Zhou, J.Wei, Y.Xiong. *J. Power Sources*, **501**, 230027 (2021)
612. J.Bae, Y.Li, J.Zhang, X.Zhou, F.Zhao, Y.Shi, J.B.Goodenough, G.Yu. *Angew. Chem., Int. Ed.*, **57**, 2096 (2018)
613. K.Liu, M.Wu, L.Wei, Y.Lin, T.Zhao. *J. Membr. Sci.*, **610**, 118265 (2020)
614. K.Liu, R.Zhang, J.Sun, M.Wu, T.Zhao. *ACS Appl. Mater. Interfaces*, **11**, 46930 (2019)
615. P.Zhu, C.Yan, M.Dirican, J.Zhu, J.Zang, R.K.Selvan, C.-C.Chung, H.Jia, Y.Li, Y.Kiyak, N.Wu, X.Zhang. *J. Mater. Chem. A*, **6**, 4279 (2018)
616. J.Li, H.Chen, Y.Shen, C.Hu, Z.Cheng, W.Lu, Y.Qiu, L.Chen. *Energy Storage Mater.*, **23**, 277 (2019)
617. Y.Li, W.Arnold, A.Thapa, J.B.Jasinski, G.Sumanasekera, M.Sunkara, T.Druffel, H.Wang. *ACS Appl. Mater. Interfaces*, **12**, 42653 (2020)
618. H.Liu, P.He, G.Wang, Y.Liang, C.Wang, L.-Z.Fan. *Chem. Eng. J.*, **430**, 132991 (2022)
619. Y.Zhang, R.Chen, S.Wang, T.Liu, B.Xu, X.Zhang, X.Wang, Y.Shen, Y.-H.Lin, M.Li, L.-Z.Fan, L.Li, C.-W.Nan. *Energy Storage Mater.*, **25**, 145 (2020)
620. C.Lai, C.Shu, W.Li, L.Wang, X.Wang, T.Zhang, X.Yin, I.Ahmad, M.Li, X.Tian, P.Yang, W.Tang, N.Miao, G.W.Zheng. *Nano Lett.*, **20**, 8273 (2020)
621. S.Luo, Z.Wang, A.Fan, X.Liu, H.Wang, W.Ma, L.Zhu, X.Zhang. *J. Power Sources*, **485**, 229325 (2021)
622. J.Zhang, C.Zheng, J.Lou, Y.Xia, C.Liang, H.Huang, Y.Gan, X.Tao, W.Zhang. *J. Power Sources*, **412**, 78 (2019)
623. J.Yi, D.Zhou, Y.Liang, H.Liu, H.Ni, L.-Z.Fan. *J. Energy Chem.*, **58**, 17 (2021)
624. X.Li, D.Wang, H.Wang, H.Yan, Z.Gong, Y.Yang. *ACS Appl. Mater. Interfaces*, **11**, 22745 (2019)
625. J.Zheng, Y.-Y.Hu. *ACS Appl. Mater. Interfaces*, **10**, 4113 (2018)
626. L.Chen, Y.Li, S.-P.Li, L.-Z.Fan, C.-W.Nan, J.B.Goodenough. *Nano Energy*, **46**, 176 (2018)
627. X.Yu, J.Ma, C.Mou, G.Cui. *Acta Phys. Chim. Sin.*, **38**, 1912061 (2022)
628. Q.Wu, M.Fang, S.Jiao, S.Li, S.Zhang, Z.Shen, S.Mao, J.Mao, J.Zhang, Y.Tan, K.Shen, J.Lv, W.Hu, Y.He, Y.Lu. *Nat. Commun.*, **14**, 6296 (2023)
629. C.F.N.Marchiori, R.P.Carvalho, M.Ebadi, D.Brandell, C.M.Araujo. *Chem. Mater.*, **32**, 7237 (2020)
630. L.Yang, J.Zhang, W.Xue, J.Li, R.Chen, H.Pan, X.Yu, Y.Liu, H.Li, L.Chen, X.Huang. *Adv. Funct. Mater.*, **32**, 2200096 (2022)
631. S.Kaboli, H.Demers, A.Paolella, A.Darwiche, M.Dontigny, D.Clément, A.Guerfi, M.L.Trudeau, J.B.Goodenough, K.Zaghib. *Nano Lett.*, **20**, 1607 (2020)
632. Y.Wang, J.Ju, S.Dong, Y.Yan, F.Jiang, L.Cui, Q.Wang, X.Han, G.Cui. *Adv. Funct. Mater.*, **31**, 2101523 (2021)
633. M.A.Cabañero Martínez, N.Boaretto, A.J.Naylor, F.Alcaide, G.D.Salian, F.Palombarini, E.Ayerbe, M.Borras, M.Casas-Cabanas. *Adv. Energy Mater.*, **12**, 2201264 (2022)

634. F.He, Z.Hu, W.Tang, A.Wang, B.Wen, L.Zhang, J.Luo. *Adv. Funct. Mater.*, **32**, 2201465 (2022)
635. Y.Wang, C.J.Zanelotti, X.Wang, R.Kerr, L.Jin, W.H.Kan, T.J.Dingemans, M.Forsyth, L.A.Madsen. *Nat. Mater.*, **20**, 1255 (2021)
636. Z.Lu, L.Peng, Y.Rong, E.Wang, R.Shi, H.Yang, Y.Xu, R.Yang, C.Jin. *Energy Environ. Mater.*, **7**, e12498 (2024)
637. J.-H.Choi, C.-H.Lee, J.-H.Yu, C.-H.Doh, S.-M.Lee. *J. Power Sources*, **274**, 458 (2015)
638. M.Falco, L.Castro, J.R.Nair, F.Bella, F.Bardé, G.Meligrana, C.Gerbaldi. *ACS Appl. Energy Mater.*, **2**, 1600 (2019)
639. S.H.-S.Cheng, K.-Q.He, Y.Liu, J.-W.Zha, M.Kamruzzaman, R.L.-W.Ma, Z.-M.Dang, R.K.Y.Li, C.Y.Chung. *Electrochim. Acta*, **253**, 430 (2017)
640. J.H.Cha, P.N.Didwal, J.M.Kim, D.R.Chang, C.-J.Park. *J. Membr. Sci.*, **595**, 117538 (2020)
641. H.Huo, Y.Chen, J.Luo, X.Yang, X.Guo, X.Sun. *Adv. Energy Mater.*, **9**, 1804004 (2019)
642. W.Liu, S.W.Lee, D.Lin, F.Shi, S.Wang, A.D.Sendek, Y.Cui. *Nat. Energy*, **2**, 17035 (2017)
643. J.Dai, K.Fu, Y.Gong, J.Song, C.Chen, Y.Yao, G.Pastel, L.Zhang, E.Wachsman, L.Hu. *ACS Mater. Lett.*, **1**, 354 (2019)
644. X.Zhang, J.Xie, F.Shi, D.Lin, Y.Liu, W.Liu, A.Pei, Y.Gong, H.Wang, K.Liu, Y.Xiang, Y.Cui. *Nano Lett.*, **18**, 3829 (2018)
645. X.Wang, H.Zhai, B.Qie, Q.Cheng, A.Li, J.Borovilas, B.Xu, C.Shi, T.Jin, X.Liao, Y.Li, X.He, S.Du, Y.Fu, M.Dontigny, K.Zaghib, Y.Yang. *Nano Energy*, **60**, 205 (2019)
646. H.Zhai, P.Xu, M.Ning, Q.Cheng, J.Mandal, Y.Yang. *Nano Lett.*, **17**, 3182 (2017)
647. C.Wang, Y.Yang, X.Liu, H.Zhong, H.Xu, Z.Xu, H.Shao, F.Ding. *ACS Appl. Mater. Interfaces*, **9**, 13694 (2017)
648. J.M.Whiteley, P.Taynton, W.Zhang, S.Lee. *Adv. Mater.*, **27**, 6922 (2015)
649. Y.Zhao, C.Wu, G.Peng, X.Chen, X.Yao, Y.Bai, F.Wu, S.Chen, X.Xu. *J. Power Sources*, **301**, 47 (2016)
650. M.Li, J.E.Frerichs, M.Kolek, W.Sun, D.Zhou, C.J.Huang, B.J.Hwang, M.R.Hansen, M.Winter, P.Bieker. *Adv. Funct. Mater.*, **30**, 1910123 (2020)
651. L.Zhou, D.L.Danilov, F.Qiao, J.Wang, H.Li, R.Eichel, P.H.L.Notten. *Adv. Energy Mater.*, **12**, 2202094 (2022)
652. H.Zhang, U.Oteo, X.Judez, G.G.Eshetu, M.Martinez-Ibañez, J.Carrasco, C.Li, M.Armand. *Joule*, **3**, 1689 (2019)
653. Y.Liu, H.Liu, Y.Lin, Y.Zhao, H.Yuan, Y.Su, J.Zhang, S.Ren, H.Fan, Y.Zhang. *Adv. Funct. Mater.*, **31**, 2104863 (2021)
654. X.Tao, Y.Liu, W.Liu, G.Zhou, J.Zhao, D.Lin, C.Zu, O.Sheng, W.Zhang, H.-W.Lee, Y.Cui. *Nano Lett.*, **17**, 2967 (2017)
655. S.Li, S.Zhang, L.Shen, Q.Liu, J.Ma, W.Lv, Y.He, Q.Yang. *Adv. Sci.*, **7**, 1903088 (2020)
656. C.C.Liang. *J. Electrochem. Soc.*, **120**, 1289 (1973)
657. E.Rangasamy, G.Sahu, J.K.Keum, A.J.Rondinone, N.J.Dudney, C.Liang. *J. Mater. Chem. A*, **2**, 4111 (2014)
658. A.Unemoto, T.Ikeshoji, S.Yasaku, M.Matsuo, V.Stavila, T.J.Udovic, S.Orimo. *Chem. Mater.*, **27**, 5407 (2015)
659. D.Blanchard, A.Nale, D.Sveinbjörnsson, T.M.Eggenhuisen, M.H.W.Verkuijlen, Suwarno, T.Vegge, A.P.M.Kentgens, P.E.de Jongh. *Adv. Funct. Mater.*, **25**, 184 (2015)
660. A.Borgschulte, R.Gremaud, S.Kato, N.P.Stadie, A.Remhof, A.Züttel, M.Matsuo, S.-I.Orimo. *Appl. Phys. Lett.*, **97**, 031916 (2010)
661. A.Yamauchi, A.Sakuda, A.Hayashi, M.Tatsumisago. *J. Power Sources*, **244**, 707 (2013)